2013 CIG-QUEST-IRIS Workshop:

Seismic Imaging of Structure and Source

July 14-17, 2013

University of Alaska Fairbanks

Organizing Committee

Carl Tape, University of Alaska Fairbanks
Tim Ahern, IRIS
Alan Levander, Rice University
Tarje Nissen-Meyer, ETH Zurich
Arthur Rodgers, Lawrence Livermore National Laboratory

ABSTRACTS VOLUME

Support from Comutational Infrastrure for Geodynamics:
Ariel Shoresh, Gilda Garcia, Lorraine Hwang

Aagaard, B. T., Brocher, T. M., Jachens, R. C., and Simpson, R. W., USGS Bay Area Seismic Velocity Model: Construction and Earthquake Simulations (talk)

Aderhold, K., Abercrombie, R. E., and Antolik, M., Controls on seismic slip in the oceanic lithosphere: Oceanic strike-slip earthquakes near Sumatra and South Sandwich Islands (poster)

Ahern, T, Bahavar, M., Casey, R., Trabant, R., Casey, R., Clark, A., Hutko, A., Karstens, R., Suleiman, Y., and Weertman, B., IRIS Services, Products, Quality Assurance Efforts, and Potential Links to High Performance Computing in the Era of BIG DATA (talk)

Allam, A. A., Tape, C., and Ben-Zion, Y., Finite-frequency sensitivity of seismic waves to fault zone structures (poster)

Alvizuri, C, and Tape, C., Full moment tensor inversions with uncertainty estimates: examples from Uturuncu volcano, Bolivia (poster)

Aster, R., Kyle, P., and Oppenheimer, C., Imaging Structure and Source Processes at Erebus Volcano (poster)

Basini, P., Liu, Q., Tape, C., and Yang, Y., Ambient noise tomography of Southern California (poster)

Ben-Zion, Y., Multi-scale 4D imaging of fault zone environments (talk)

Bonnin, M., Nolet, G., Villaseñor, A., Gallart, J., and Thomas. C., Tomography of the upper mantle beneath the African/Iberian collision zone (poster)

Bostock, M. G., Royer, A. A., Matharu, G., and Nowack, R., Low Frequency Earthquakes: A New Seismic Source for Imaging Subduction Zone Structure (talk)

Bozdag, E., Lefebvre, M., Lei, W., Peter, D., Smith, J., Zhu, H., Komatitsch, D., and Tromp, J., Global Adjoint Tomography (poster)

Brown, J., On the utility of communication-avoiding and vectorization strategies in wave propagation analysis (poster)

Cakir, R., and Walsh, T. J., Practical and Cost-Effective Shallow and Deep Shear-Wave Velocity Surveys for 3D Earthquake Simulations in Sedimentary Basins (poster)

Campillo, M., Ambient noise imaging (talk)

Casarotti, C., Hexahedral meshing 101: seismic wave propagation and complex geological volumes (talk)

Chen, C., James, D. E., and Fouch, M. J., Uppermost mantle structure beneath the High Lava Plains, Oregon, USA, imaged by teleseismic scattered waves (poster)

Chen, M., Niu, F., Liu, Q., and Tromp, J., Adjoint tomography of the crustal and upper-mantle seismic structure beneath Continental China (poster)

Cottaar, S., and Romanowic, B., An exceptionally large ULVZ at the base of the mantle near Hawaii (poster)

Collis, S., Ober, C., Krebs, J., van Bloemen Waanders, B., Smith, T., Young, J., Overfelt, J., and Downey, N., Seismic Full-Wavefield Inversion Using Discontinuous Galerkin Methods (poster)

Fan, W., Shearer, P. M., and Gerstoft, P., Finite Slip Inversions from Near-Field Seismic Data: How to Quantify the Uncertainties? (poster)

Fichtner, A., Rickers, F., and Trampert, J., Towards a comprehensive multi-scale model of Europe and western Asia (talk)

French, S., Lekic, V., and Romanowicz, B., Oceanic low-velocity structure in SEMum2: Interpretations and synthetic validation (poster)

Freymueller, J., Active Tectonics of Alaska (talk)

Gerstoft, P., and Traer, J., Unified theory of microseisms and hum (poster)

Gill, D., Maechling, P., Jordan, T., Plesch, A., Taborda, R., and Callaghan, S., Small, P., SCEC Unified Community Velocity Model: Mesh Generation and Visualization (poster)

Hanasoge, .S, Source-Structure Tradeoff in Noise Tomography (poster)

Haney, M., Chouet, B., and Lyons, J., Long Period, Very Long Period, and Ultra Long Period Signals from the 2009 Redoubt Eruption (poster)

Harris, D. B., and Rodgers, A. J., Model-Based Subspace Detectors Constructed with SPECFEM3D (poster)

Harris, D. B., Building Subspace Detectors for Random Media (poster)

Hosseini, K., and Sigloch, K., obspyDMT: Parallel Retrieving, Processing and Management of Massive Seismological Datasets (poster)

Hosseini. K., Sigloh, K., Nissen-Meyer, and T., Stähler, S., Finite frequency measurements of diffracted P waves for waveform tomography (poster)

Hung, S.-H., Cheng, I.-H., Zhou, Y. , and Chang, Y.-H., 3-D Multi-scale Finite-frequency Rayleigh Wave Tomography of Crustal and Upper Mantle Structure beneath Central Tibet (poster)

Igel, H., Krischer, L., Simon, M., Mauerberger, S., Pelties, C., Wenk, S., and Hosseini, K., Challenges in computational seismology (talk)

Ilhan, I., and Coakley, B. J., Stratigraphy and multi-phase tectonic history of the Chukchi Borderland from multi-channel reflection seismic data (poster)

Inbal, A., Ampuero, J.-P., and Avouac, J.-P., Joint inversion of strain and aftershock data for the distribution of afterslip following moderate events on the San-Jacinto Fault (poster)

Ishii, M., Kiser, E., Rupture Properties of Intermediate-Depth Earthquakes Using Back-Projection Technique (talk)

Ji, C., Quickly Imaging Global Large Earthquakes Using Seismic Waveforms: A balance between quickness and accuracy (talk)

Kiser, E., Levander, A., Harder, S., Abers, G., Creager, K., Vidale, J. E., Moran, S., and Malonei, S., Mush: The design of the Mount St. Helens high-resolution active source seismic experiment (poster)

Krischer, L., Megies, T., Barsch, L., Beyreuther, M., and Wassermann, J., ObsPy: A Python Toolbox for Seismology (poster)

Larmat, C., Patton, H, J., Rowe, A. J., Rougier, E., and Yang, D., Towards validation of new explosion sources models: Properties of structure and source at the Source Physics Experiment (SPEs) (poster)

Lee, E., Chen, P., Jordan, T. J., Maechling, P. J., Denolle, M., and Beroza, G. C., Full-3D Waveform Inversions for Earthquake Source Parameters and Crustal Structure Model in Southern California (poster)

Lei, W., Bozdag, E., Smith, J., Lefebvre, M., and Tromp, J., Seismic Time Window Selection on Large Dataset (poster)

Li, D., Sun, D., and Helmberger, D., Notes on the Variability of reflected core-phases (poster)

Lin, F., Tsai, V., Clayton, R., and Schmandt, B., Seismic tomography and interferometry: from shallow to deep (poster)

Liu, Q.,Tong, P., and Basini, P. High-resolution array imaging based on numerical simulations (talk)

Luo, Y., and Ampuero, J-P, Numerical Study of Fault Zone Heterogeneity: Scaling and More (poster)

Maceira, M., Larmat, C., Porritt, R., Higdon, D. M., and Allen, R. M., Validation of 3D Seismic Models: finite-frequency or ray theory? (poster)

Maechling, P., Gill, D., Small, P., Ely, G., Taborda, R., and Jordan, T. , SCEC Unified Community Velocity Model: Development Goals and Current Status (talk)

Magnoni, F., Casarotti, E., Cirella, A., Michelini, A., Molinari, I., Morelli, A., Piersanti, A., and Tromp, J., Spectral-Element Simulations and Source Solutions for the May 20, 2012, Po Valley Main Shock (poster)

Masoni, I., Brossier, R., Virieuxm J., and Boelle, J. L., Alternative misfit functions for Full Waveform Inversion of surface waves (poster)

Matharu, G., Bostock, M., Christensen, N., Tromp, J., and Peter, D., Investigating Elastic Anisotropy of the Leech River Complex, Vancouver Island using Finite Frequency Kernels (poster)

Matzel, E., Investigating faults using seismic interferometry (poster)

Meng, L., Allen, R., and Ampuero, J-P. , Application of Seismic Array processing to Earthquake Early Warning (poster)

Mikesell, T. D., Mikesell, S., Voronin, G., Nolet, and Ritsema., J., Global finite-frequency surface-wave tomography (poster)

Molinari, I., Morelli, A., Berbellini, A., Argnani, A., Basini, P., and Danecek, P., SHAKE-IT: realistic earthquakes scenario simulations in Northern Italy (poster)

Nissen-Meyer, T., Driel, M. v., Staehler, S., Hosseini, K., Hempel, S., and Fournier, A., AxiSEM: High-frequency global wavefields for forward and inverse modeling (talk)

Padhy, S., Furumura, T., and Maeda, T., Anti-waveguide effects in Pacific slab: evidence from high-frequency waveform analysis and numerical modeling (poster)

Pelties, C, Smith, C., Heimisson, G., Wenk, S., and Gabriel, A., Rapid CAD and tetrahedral mesh generation for dynamic rupture problemsm (talk)

Pitarka, A., Mellors, R. J., Vorobiev, O. J., Rodgers, A. J., Walter, W. R., Antoun, T., Petersson, A., Sjogreen, B., Matzel, E., and Wagoner, J., Three Dimensional Simulation of Far-Field Ground Motion from Source Physics Experiment Using a Hydrodynamic-to-Elastic Coupling Technique (poster)

Morency, C., Peter, D., Covellone, B., Savage, B., Rodgers, A., and Tromp, J., Adjoint Waveform Tomography of the Middle East (poster)

Romanowicz, B., French, S., and Lekic, V., Low velocities in the oceanic upper mantle and their relation to plumes: insights from SEM-based waveform tomography (talk)

Rondenay, S., Imaging with the Generalized Radon Transform: a review of the theory and applications (talk)

Routh, P., McAdow, D., Lazaratos, S., Krebs, J., and Hinkley, D., Full Wavefield Inversion's Impact on the Upstream Business (talk)

Ruhl, C., Seaman, T., and Smith, K., Fault Structures and Stress Orientations from Moderate Earthquake Sequences and Relocated Seismicity in the Mina Deflection, Western Nevada-Eastern California (poster)

Sales de Andrade, E., and Liu, Q., Global Seismic Tomography Based on a Sensitivity Kernel Database (poster)

Schutt, D. L., Lowry, A. R., Buehler, J. S., and Blackwell, D. D., Lithosphere Temperatures within the western United States (poster)

Silwal, V., and Tape, C., Seismic moment tensor inversion: Sampling the posterior probability distribution (poster)

Sladen, A., Q.Blétery, Q., and Delouis, B., The 2011 M9.0 Tohoku-Oki earthquake: a new challenge for multi-data finite-fault slip inversions (poster)

Smith, J., Bozdag, E., Lefebvre, M., and Tromp, J., An Adapatable Seismic Data Format for High-Performance Computing (poster)

Somala, S. N., High-resolution Data in Seismic Source Imaging (poster)

Stähler, S. C., Sigloch, K., Zhang, R., Hosseini-zad, K., and Igel, H., Probabilistic Seismic Source Inversion from teleseismic Body-waves (poster)

Taborda, R., and Bielak, J., Comparative validation of a set of physics-based simulations of the 2008 Chino Hills earthquake using different velocity models of the 2008 Chino Hills earthquake using different velocity models (poster)

Tape, C., A three-dimensional seismic velocity reference model for Alaska (poster)

Tape, C., West, M., Silwal, V., and Ruppert, N., Earthquake nucleation and triggering on an optimally oriented fault (Sumatra to Alaska) (poster)

Tong, P., Chen, C. W., Basini, P., and Liu, Q., High-resolution seismic array imaging based on SEM-FK hybrid methods

Tromp, J., Bozdag, E., Lefebvre, M., Lei, W., Smith, J., Zhu, H., Imaging Earth's Interior based on Spectral-Element and Adjoint Methods (talk)

Vilotte, J. P., The Virtual Earthquake and Seismology Research e-science Community in Europe: lessons and some identified challenges (talk)

Asnaashari, A., Brossier, R., Dietrich, M., Garambois, S., Métivier, L., Operto, S., Ribodetti, A., and Virieux, J., Full waveform inversion: challenges (talk)

Wenk, S., Hadziioannou, C., Pelties, C., and Igel, H., Application of the ADER-DG method to simulate Love waves in the ocean generated noise wave field (poster)

Yao, H., Shearer, P., Gerstoft, P., and Yin, J., Compressive sensing of great earthquake ruptures (poster)

Ye, L., and Lay, T., Rupture Processes and Seismic Radiation Characteristics for Large Earthquakes (poster)

Yuan, Y., and Simons, F. J., Multiscale adjoint waveform-difference tomography using wavelets (poster)

USGS Bay Area Seismic Velocity Model: Construction and Earthquake Simulations

B. T. Aagaard[1], T. M. Brocher[2], R. C. Jachens[3], and R. W. Simpson[4]

[1]US Geological Survey, Menlo Park, CA, baagaard@usgs.gov
[2]US Geological Survey, Menlo Park, CA, brocher@usgs.gov
[3]US Geological Survey, Menlo Park, CA, jachens@usgs.gov
[4]US Geological Survey, Menlo Park, CA, simpson@usgs.gov

The USGS San Francisco Bay Area 3-D Seismic Velocity Model provides elastic material properties and frequency independent attenuation parameters over a large region of central California. A high resolution portion covering the San Francisco Bay urban area is surrounded by a coarser resolution portion extending along the San Andreas fault from Parkfield to Cape Mendocino and from the Pacific Ocean to the Sierra Nevada foothills. The model was constructed from a 3-D geologic block model that defines the geologic units and fault surfaces and a set of empirical rules for defining physical properties within each geologic unit as a function of depth. The model defines numerous sedimentary basins as well as sharp velocity contrasts across several major faults. The model is consistent with the much coarser resolution Thurber et al. regional tomographic Vp model. The model is distributed as an Etree database with a small software library for efficient querying on a laptop with limited memory and processing power as well as on Beowulf clusters.

Several ground-motion modeling studies have used the velocity model to characterize the 3-D effects on earthquake shaking for past earthquakes as well as hypothetical scenarios. The simulations show strong basin effects consistent with damage patterns in the M7.8 1906 San Francisco, 1969 M5.7 Santa Rosa, and M6.9 1989 Loma Prieta earthquakes. Modeling of hypothetical Hayward fault earthquakes demonstrate strong coupling between rupture directivity and basin effects in the San Jose and Livermore regions.

The accuracy of the seismic velocity model, as measured in comparisons of long period ($T > 2$ s) synthetic and observed body and surface waves, varies significantly. Extensively studied regions with detailed geologic structure, such as the Santa Clara Valley, reproduce observed waveforms quite well. Other regions, which have been subjected to extensive folding and deformation and not characterized in as much detail, such as the region between the Hayward fault and the Great Valley, are less accurate as evident in misfits in arrival times and amplitude of synthetic waveforms. Future work will focus on incorporating finer scale information on near-surface properties and using full waveform tomography to improve the accuracy of the model using a variety of data sources, including strong-motion data from moderate earthquakes.

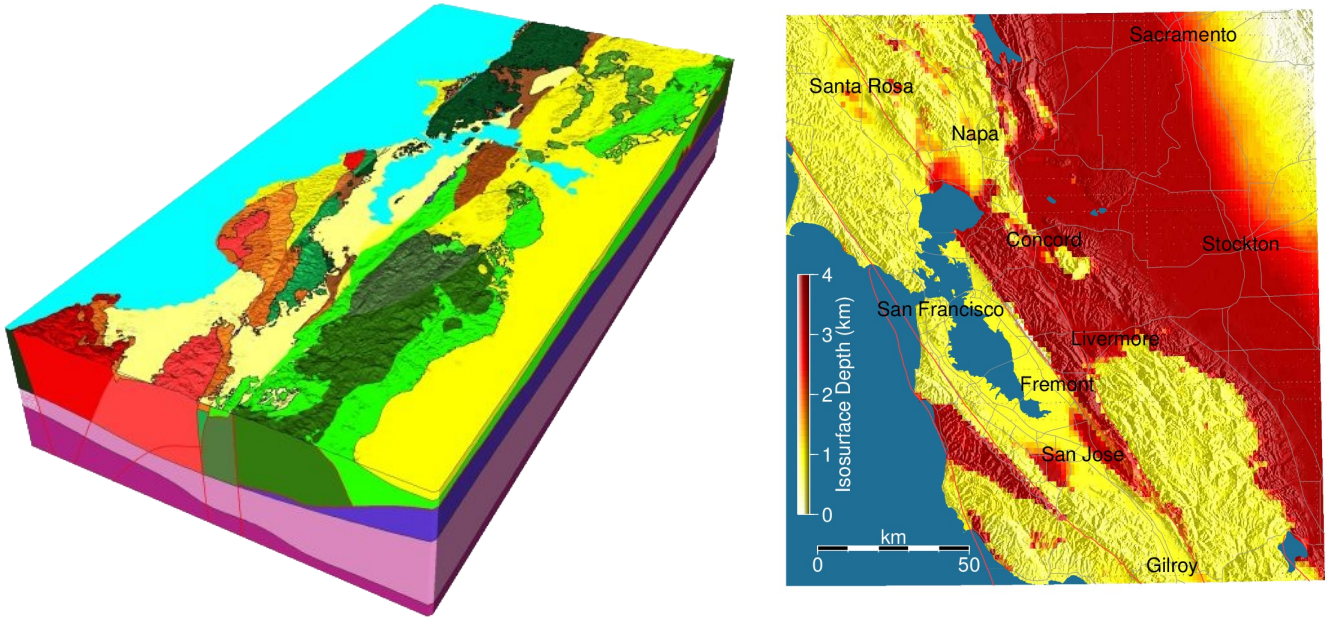

Perspective view of the San Francisco Bay Area 3-D geologic model (left) and a map of depth to the 2.5 km/s shear wave isosurface (right).

Controls on seismic slip in the oceanic lithosphere: Oceanic strike-slip earthquakes near Sumatra and South Sandwich Islands

K. Aderhold[1], R. E. Abercrombie[1], M. Antolik[2]

[1]Boston University, Department of Earth & Environment, kasey@bu.edu, rea@bu.edu
[2]Quantum Technology Sciences Inc., mantolik@qtsi.com

We investigate the controls on seismic slip in oceanic lithosphere through teleseismic body-wave modeling of oceanic strike-slip earthquakes to determine fault plane as well as the depth of slip. Determining the distribution of slip both along strike and with depth provides insight into the controls on seismic rupture and the seismogenic thickness of the oceanic lithosphere. Back projection, using large seismic arrays, implies that the April 11, 2012 Sumatra M_W 8.6 and 8.2 earthquakes displayed complex rupture patterns, however a consensus has not been reached as to whether East-West trending faults were ruptured in addition to North-South trending faults. The complexity of these events prevents details of depth and fault plane from being resolved. Modeling smaller earthquakes within the oceanic plate off the coast of Sumatra enables us to identify the fault planes ruptured as well as the depth extent of seismic slip near the April 2012 earthquakes, and in a comparision site near the South Sandwich Islands.

This study focuses on oceanic strike-slip earthquakes of magnitude $7.0 < M_W < 8.0$ since 1990 in two study sites: the Sumatra subduction zone and the South Sandwich Islands. We model three events at each site using a point source to fit teleseismic body-waves. We calculate slip inversions for the two conjugate fault planes associated with the best-fitting focal mechanism for each event. Emphasis is made on fitting the first arrival P wave polarities, and directivity effects are based on both P and SH waves. The three $M_W > 7.0$ events in Sumatra and the South Sandwich Islands ruptured oceanic lithosphere of 40-70 My and 0-40 My respectively (Müller et al, 2008). The seismograms of the Sumatra events were affected significantly by thick layers (1-3km) of low velocity sediments in the source region, while the South Sandwich Islands had less sediments (<1km). We examine smaller events ($6.0 < M_W < 7.0$) to determine point source focal mechanisms and constrain the event depth by fitting depth phases pP and sP. Two events along the 90º East Ridge have deep centroids similiar to those of April 2012 earthquakes. We compare all event depths to modeled temperature profiles to determine if temperature is the primary control on seismogenic depth, or if composition and geometry play an equal or greater role.

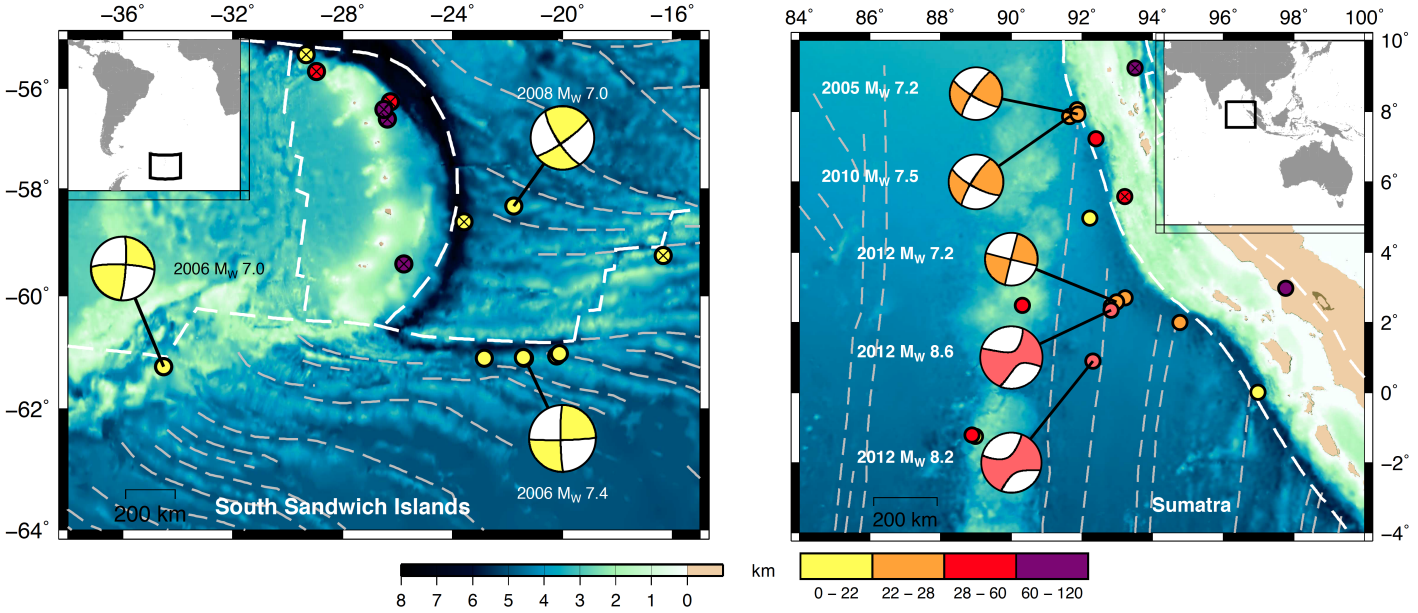

Figure 1. Bathymetry of the two sites with plate boundaries and fracture zones plotted as white and grey dashed lines respectively (Wessel & Smith, 1995; Mathews et al, 2011). Focal mechanisms for the six $7.0 < M_W < 8.0$ earthquakes are shown as well as the CMT mechanisms of the April 2012 events. Earthquakes of $6.0 < M_W < 7.0$ are indicated by dots of different colors for depth and crosses indicating CMT depths.

IRIS Services, Products, Quality Assurance Efforts, and Potential Links to High Performance Computing in the Era of BIG DATA

T. Ahern[1], M. Bahavar[1], R.Casey[1], C. Trabant[1], R.Casey[1], A. Clark[1], A. Hutko[1], R. Karstens[1], Y. Suleiman[1], B. Weertman[1]

[1]IRIS Data Management Center, 1408 NE 45th Street, Suite 201, Seattle, WA 98105

This keynote talk will focus on four fundamentally new areas currently being pursued by IRIS Data Services (DS). These include 1) the new but very significant web services, 2) development of higher level products, 3) improved Quality Assurance initiatives, and 4) links to high performance computing.

IRIS DS has traditionally been focussed upon ingesting, curating and distributing data to the research and monitoring communities through a variety of mechanisms. More recently the request services portfolio of IRIS DS has expanded to include a Service Oriented Architecture (SOA) design leveraging web services, that greatly enhances programmatic access to the waveform and metadata holdings managed at the IRIS DMC. This talk will discuss the availability of new web services available from the DMC. The DMC has also expanded the levels of products/information that it now supports and has expanded into a variety of DMC and/or research community developed products that serve as stepping-stones to further research.

As data volumes increase, it is clear that the manner in which the research community will interact with the data in the future must change and automation in the assessment of data quality must improve. A new QA system called MUSTANG, is now in beta-release and is a major development intended to improve the quality of seismic data world-wide. All data either provided by IRIS funded networks as well as networks that contribute data to the IRIS DMC for further distribution to the monitoring and research communities. Coupled with tighter connections to network operators, IRIS is optimistic that the automation of MUSTANG coupled with tighter connections to network operators will meet the objective of improved data quality.

IRIS is in the near final stages of deploying an Auxilliary Data Center near one of the nation's fastest computers at Lawrence Livermore National Labs. This architecture is an attempt to not only meet the IRIS DMC's needs for mitigation of any failure at the IRIS DMC in Seattle but also a step towards addressing the "cycles close to data" issue that currently limits seismologists' ability to perform massive computations over all or significant portions of the DMC data holdings. While this should be considered a first step in this direction it is nevertheless quite significant.

Finally this talk will mention a project to provide Digital Object Identifiers (DOIs) to provide a convenient way to provide attribution to data sets from permanent seismic networks, PI driven temporary seismic networks such as those facilitated by PASSCAL, as well as products managed at the IRIS DMC.

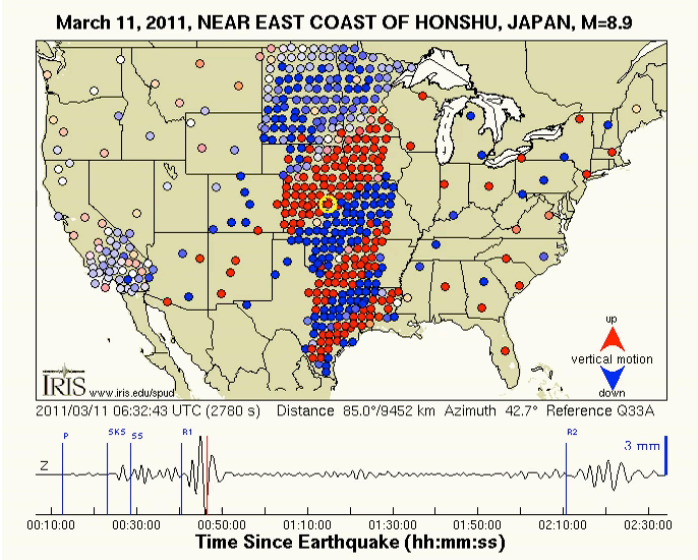

The Ground Motion Visualization Product produced after the March11, 2011 Tohoku earthquake showing the seismic phases as they move across USArray stations in the United States

Finite-frequency sensitivity of seismic waves to fault zone structures

A. A. Allam[1], C. Tape[2], Y. Ben-Zion[1]

[1]University of Southern California, Department of Earth Sciences, aallam@usc.edu
[2]University of Alaska Fairbanks, Geophysical Institute, carltape@gi.alaska.edu

We analyze the volumetric sensitivity of fault zone seismic head and trapped waves by constructing finite-frequency Fréchet kernels for these phases based on idealized models. We first validate numerical calculations by waveform comparisons with analytical results for a model with a bimaterial fault interface separating different elastic solids. After establishing numerical accuracy up to 10Hz, we construct sensitivity kernels for a 'vertical sandwich' model where a narrow low-velocity region is surrounded on either side by a higher velocity material. In contrast to P body waves, which have little or no sensitivity to fault zone structure, the sensitivity kernels for head waves have sharp peaks with high values near the fault in the faster medium. Surface wave kernels show the broadest spatial distribution of sensitivity, while trapped waves kernels are extremely narrow with sensitivity focused entirely inside the low-velocity fault zone layer. These results indicate that adjoint tomography based on high-frequency head and trapped waves kernels can constrain fault zone structure much more tightly than has previously been possible.

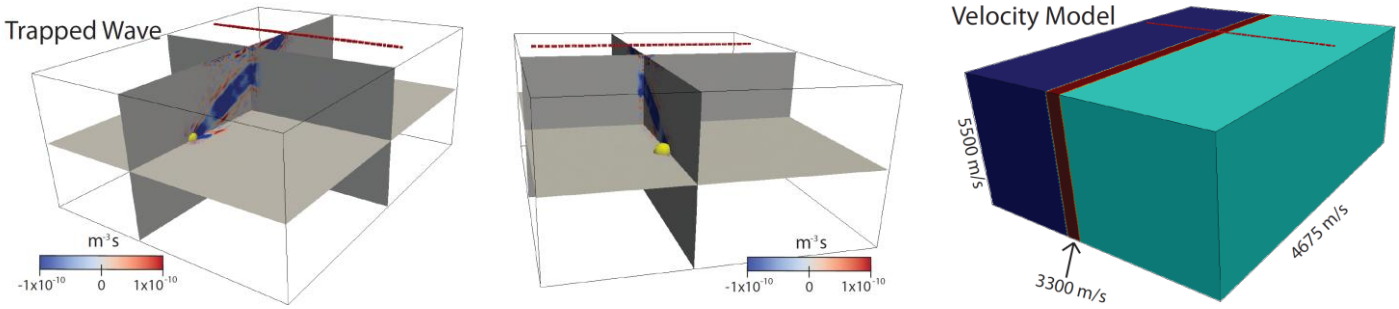

Figure 1. S-wave velocity sensitivity kernel for a trapped wave produced by the 'vertical sandwich' model shown. The trapped wave only has sensitivity to the vertical low-velocity zone and has no sensitivity to the material outside of this zone.

Full moment tensor inversions with uncertainty estimates: examples from Uturuncu volcano, Bolivia

C. Alvizuri, C. Tape

University of Alaska Fairbanks, alvizuri@gi.alaska.edu

A seismic moment tensor is a symmetric 3 x 3 matrix described by 6 parameters. These six parameters can either be thought of as the elements of the moment tensor or, more physically, as the magnitude (1), the isotropic component (1), the CLVD component (1), and the orientation (3). The ability to constrain all six parameters depends strongly on the station coverage and the signal-to-noise level within the seismic waveforms. Our goal is to determine full seismic moment tensors with data at different levels of quality or availability ranging from only polarity in p-wave first motions to full waveforms (body waves and surface waves). We apply the moment tensor inversion method of Zhu and Helmberger (1996) to both synthetic and real data sets. We search model parameter space using two techniques: (1) a complete grid search, (2) a neighborhood algorithm. Both approaches allow for the estimation of uncertainties of all six moment tensor parameters. We perform moment tensor inversions for a set of small shallow earthquakes below Uturuncu volcano in Bolivia. The majority of the events are small and only allow the use of P-wave polarity data, which are unable to adequately resolve the isotropic and CLVD components of the moment tensor. For the largest events ($M > 2$) we are able to include seismic waveforms in the inversion, which produce lower uncertainty estimates for the moment tensors. Our future efforts will involve testing the recoverability of randomly generated (full) moment tensors for known source-station geometries in both passive-source and active-source settings.

Imaging Structure and Source Processes at Erebus Volcano

R. Aster[1,2], P. Kyle[1], C. Oppenheimer[3]

[1]New Mexico Institute of Mining and Technology, aster@ees.nmt.edu
[2]Colorado State University
[2]Cambridge University

Mount Erebus is a large polygenetic volcano within the West Antarctic Rift System, and is the only active volcano on Ross Island, Antarctica. The volcano has hosted a persistent phonolite lava lake for over 40 years, which has remained remarkably stable in geochemical and mineralogical composition. The lava lake is also the site of persistent Strombolian eruptions and shallow glacial icequakes that provide repeating time-lapse natural seismic illumination of the upper volcano. New seismological imaging results are summarized that jointly utilize strong seismic scattering and active source tomography obtained with a dense (>100 station) three-component seismograph deployment. Detailed analysis of eruptive seismograms from near-repeating lava lake eruptions show systematic days-to-weeks long variations in the delay between short-period explosion and conduit system-associated very-long-period signal components that indicate variable response/communication times between the surface and the deeper conduit system. This variation may arise from changes in the uppermost conduit system geometry that affect elastodynamic communication within the system, and that these changes may be observable with seismic coda interferometric imagery. This work further suggests that background images obtained from dense temporary seismographic experiments can subsequently be leveraged for longer-term monitoring for temporal conduit system changes made at a smaller number of long-term stations. We present a conceptual model of the Erebus magmatic system from mantle to the surface that is based on an integration of geochemical, geophysical and petrological observations.

Mount Erebus Summit Crater and Plateau, aerial view.

Ambient noise tomography of Southern California

P. Basini[1], Q. Liu[1], C. Tape[2], Y. Yang[3]

[1]University of Toronto, Department of Physics.
[2]University of Alaska Fairbanks, Geophysical Institute and Department of Geology & Geophysics
[3]ARC Centre of Excellence for Core to Crust Fluid System and GEMOC ARC National Key Centre, Earth and Planetary Sciences, Macquarie University

We improve the 3-D crustal model m16 of Tape et al. (2009,2010) of Southern California based on stacked ambient noise cross-correlation functions (NCF) for regional stations. Under the assumption of diffuse wavefield, NCFs closely approximate the Greens functions between pairs of seismic stations. Owning to the dense instrumental coverage in south California and the depth sensitivity of NCFs, they provide a complementary dataset to earthquake data for the imaging of the lower crust and uppermost mantle.

Model updates are computed based on the adjoint tomography technique, where misfit between NCFs and 3D synthetic Greens functions, both filtered between 10-50 seconds, is iteratively reduced. The forward wavefields for 3D velocity models are computed fully numerically by the spectral-element methods (SEM). Similarly, Frechet derivatives (sensitivity kernels) are constructed by adjoint methods with adjoint sources given by differences between NCFs and 3D Greens functions, measured as multi-taper traveltime misfits.
At each iteration, model update is assumed to be a linear combination of shear wave-speed sensitivity kernels (i.e., source subspace method) and the coefficients are obtained by solving a linear system. However, its hessian matrix requires damping due to the uneven spatial distribution of seismic stations. The optimal damping parameter is obtained through an L-curve between misfit values and model norm for 20 selected master stations. The quality of inverted models will be assessed based on the data from an independent set of earthquakes.

Multi-scale 4D imaging of fault zone environments

Y. Ben-Zion

University of Southern California, Department of Earth Sciences, benzion@usc.edu <http://earth.usc.edu/~ybz/>

I review multi-signal multi-scale seismic imaging studies of fault zones with information on bimaterial interfaces and hierarchical damage structures that become reactivated at shallow depth during earthquakes. The studies use earthquake data to image the seismogenic sections and ambient noise to image the shallower structures. The fault damage zones follow a flower-type structure with pronounced damage generally limited to the sections above the seismicity. In places with across-fault velocity contrast, the damage zones are offset to the side with higher velocity at depth. These features are evident in earthquake traveltime and noise tomography of the San Jacinto fault zone with low velocity zones at scales of 3-6 km [1], and waveform modeling of trapped and diffracted waves within internal damage zones at a scale of 100 m [2] A similar sense of damage asymmetry is observed at various locations with multiple geological signals [3]. At sections of the San Andreas, Hayward and North Anatolian faults there are bimaterial interfaces with considerable along-strike and depth extent. These are seen most clearly with fault zone head waves [4], and are also indicated by teleseismic data and local tomographic images [1]. Synthetic adjoint calculations demonstrate the superior sensitivity of head and trapped waves to the fault zone structure [5]. Anisotropy signals provide evidence for low velocity zones at scales from several km to 100 m with predominance of fault-parallel cracks [6]. Polarization analysis at near fault stations also indicates predominance of fault-parallel cracks in fault damage zones [7]. Various monitoring techniques reveal co- and post-seismic temporal changes of seismic properties. Analyses based on ambient noise use relatively long time scales (>day) and indicate typically <1% temporal changes [8]. Analyses based on earthquake waveforms resolve time scales of seconds and show considerably larger changes. Results associated with local network around the North Anatolian fault indicate clear regional changes of seismic velocities produced by the M7.1 Duzce earthquake, with 20-50% reduction of S velocity at the top 100-500 m of the fault-zone followed by log(t) recovery [9]. These observations are consistent with laboratory experiments with different materials [10] and recent observations following the 2011 M9.0 Tohoku earthquake in Japan [11].

References

[1] Allam, A. A. and Y. Ben-Zion, *GJI*., 2012; Hillers, G. Y. Ben-Zion, M. Landès and M. Campillo, *G*^{3}, 2013; Zigone, D. Y. Ben-Zion, M. Campillo and P. Roux, 2013.

[2] Lewis, M.A, Z. Peng, Y. Ben-Zion and F. Vernon, *GJI*, 2005; Yang, H. and Zhu, L., *GJI*, 2010.

[3] Dor O., T. K. Rockwell and Y. Ben-Zion, *PAGEOPH*, 2006, Dor O. *et al.*, *GJI*, 2008; Wechsler, N. *et al*., *Geomorphology*, 2009; Mitchell, T. M., Y. Ben-Zion and T. Shimamoto, *EPSL*, 2011.

[4] Ben-Zion, Y. and P. Malin, *Science*, 1991; McGuire, J. and Y. Ben-Zion, *GJI*, 2005; Bulut *et al. EPSL*, 2012; Allam A.A., Y. Ben-Zion and Z. Peng., in preparation, 2013.

[5] Allam, A. A., C. Tape and Y. Ben-Zion, in preparation 2013.

[6] Peng, Z. and Y. Ben-Zion, *GJI*, 2004; Liu, Y., T. L. Teng and Y. Ben-Zion, *BSSA*, 2004; Durand, S., J. P. Montagner, P. Roux, F. Brenguier, R. M. Nadeau, and Y. Ricard, *GRL*, 2011.

[7] Pischiutta, M. *et al. GJI*, 2012, 2013.

[8] Brenguier, F., M. Campillo, C. Hadziioannou, N.M. Shapiro, R. M. Nadeau, and E. Larose, *Science*, 2008

[9] Peng, Z. and Y. Ben-Zion, *PAGEOPH*, 2006; Wu, C. Z. Peng and Y. Ben-Zion, *GJI*, 2009.

[10] Johnson J.A. & X. Jia *Nature*, 2005; Pasqualini, D. *et al.*, *JGR*, 2007; TenCate, J.A., *PAGEOPH*, 2011.

[11] Sawazaki, K. and R. Snieder, *GJI*, 2013.

Tomography of the upper mantle beneath the African/Iberian collision zone

M. Bonnin[1], G. Nolet[1], A. Villaseñor[2], J. Gallart[2] and C. Thomas[3]

[1] Géoazur, université de Nice Sophia-Antipolis, France, mbonnin@geoazur.unice.fr, nolet@geoazur.unice.fr
[2] Institute of Earth sciences "*Jaume Almera*", CSIC, Barcelona, Spain
[3] Institute für geophysik, Universität Müster, Germany

In this study we take advantage of the dense broadband-station networks available in western Mediterranean region (IberArray and MOROCCO-MUENSTER networks) to develop a high-resolution 3D tomographic *P* velocity model of the upper mantle beneath the African/Iberian collision zone. This model is based on teleseismic arrival times recorded between 2008 and 2012 for which cross-correlation delays are measured with a new technique in different frequency bands centred between 0.03 and 1.0 Hz, and interpreted using multiple frequency tomography.
Our preliminary results evidence the presence, beneath Alboran Sea, of a strong fast vertical anomaly observed to at least 650 km depth. The arched shape of the anomaly and its extent at depth are coherent with a lithospheric slab – probably remnants of the former westernmost arm o the Tethys ocean.

Slow anomalies are also widely observed at upper mantle depths especially beneath Morocco. These anomalies are correlated at surface with the position of the orogens (Rif and Atlas) and with volcanic fields. Our study seems thus to confirm the presence, beneath Morocco, of an anomalous (hot) upper mantle. These slow anomalies moreover present evidence of lateral connection with the Canary volcanic islands, likely indicating a lateral spreading to the east of the Canary plume.

Low Frequency Earthquakes: A New Seismic Source for Imaging Subduction Zone Structure

M.G. Bostock[1], A.A. Royer[1,] G. Matharu[1], R. Nowack[2]

[1]University of British Columbia, Department of Earth, Ocean and Atmospheric Sciences, bostock@eos.ubc.ca
[1]University of British Columbia, Department of Earth, Ocean and Atmospheric Sciences, alexandra.royer@gmail.com
[1]University of British Columbia, Department of Earth, Ocean and Atmospheric Sciences, gian.matharu@yahoo.com
[2]Purdue University, Department of Earth and Atmospheric Sciences, nowack@purdue.edu

Tectonic tremor is a recently documented phenomenon that occurs primarily at subduction zones and deep in the Earth's crust in tectonically active regions. It is often associated with slow slip on plate boundary faults where the two processes are collectively termed Episodic-Tremor-and-Slip or ETS. Tremor comprises a band-limited (1-10 Hz) signal with an envelope that rises and ebbs over periods of minutes to hours. Studies in Japan have shown tremor to be composed, in major part, of many repeating low frequency earthquakes (LFEs) with equivalent magnitudes ≤ M2. We have assembled a set of ~300 LFE waveform templates for Vancouver Island and Washington state through the application of an iterative correlation/detection/stacking procedure to tremor data for major ETS episodes since 2003. This procedure removes variability in source signature across individual repeating LFEs to produce what is effectively a record of empirical Green's functions. The corresponding locations are spatially complementary to sparse and infrequent intraplate events and so LFE templates afford a potentially useful source for imaging purposes. More specifically, the LFE locations are confined to a zone that coincides closely with the 25-40 km depth contours of the subducting plate and are demonstrably shallower in depth than intraplate events occurring in the same epicentral region.

The simplicity of the source-time dependence renders the LFE templates well suited to the analysis of source mechanism and as structural probes of the subduction zone. Direct P and S waves exhibit band-limited, zero-phase pulses once corrected for instrument response and moment tensor source. Clear and pronounced splitting of S-waves is observed for a selection of stations situated on and near the Leech River Terrane, a major schist belt with lab-measured anisotropy approaching 30%. Prominent signals within the coda of P and S are S-to-P conversions and S-S reflections that scatter from the boundaries of a pronounced low-velocity zone at the top of the subducting plate and thus harbour key information concerning the nature of the plate boundary in the realm of ETS. We have constructed 3-D models of the subduction zone employing results from previous tomographic studies and plate boundary models, and are currently engaged in forward and inverse modelling these signals. We will present results from linear inversions for LFE moment tensor sources, adjoint tomographic inversion for regional anisotropy, and grid searches employing 3-D dynamic raytracing to model plate boundary structure.

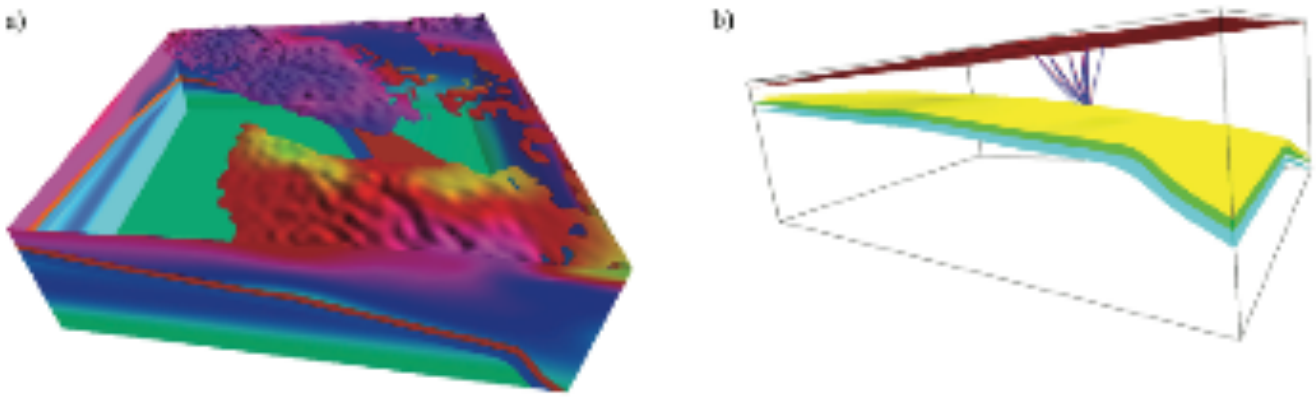

Cutaway view (a) of velocity model used for ray theoretical simulations of wave propagation in northern Cascadia, and (b) perspective from southeast of rays scattered from an LFE within a 2-layer low velocity zone.

Global Adjoint Tomography

E.Bozdag[1], M.Lefebvre[1], W. Lei[1], D. Peter[2], J. Smith[1], H. Zhu[1], D. Komatitsch[3], J. Tromp[1,4]

[1]Princeton University, Department of Geosciences, bozdag@princeton.edu
[2]ETH Zurich, Institute of Geophysics
[3]CNRS/University of Aix-Marseille, Laboratory of Mechanics and Acoustics
[4]Princeton University, Program in Applied and Computational Mathematics

Adjoint methods provide an efficient way for incorporating the full nonlinearity of wave propagation and 3D Fréchet kernels in iterative seismic inversions. Our goal is to take adjoint tomography forward to image the entire planet using the opportunities offered by advances in numerical wave propagation solvers and high-performance computing.

Using an iterative pre-conditioned conjugate gradient scheme, we initially set the aim to obtain a global crustal and mantle model with confined transverse isotropy in the upper mantle. Our strategy is to invert crustal and mantle structure together to avoid any bias introduced into upper-mantle images due to "crustal corrections", which are commonly used in classical tomography. We have started with 255 global CMT events ($5.8 \leq Mw \leq 7$) and used GSN stations as well as some local networks such as USArray, European stations, etc. We have demonstrated the feasibility of global scale inversions by performing two iterations based on numerical simulations accurate down to ~27 s. To simplify the problem, we primarily focus on elastic structure, and therefore our measurements are based on multitaper traveltime differences between observed and synthetic seismograms. We compute 3D sensitivity kernels for the selected events combining long-period surface waves (initially $T > 60$ s), where it is easier to handle nonlinearities due to the crust, with shorter-period body waves (initially $T > 27$ s), which are more sensitive to deeper parts of the mantle. 3D simulations dramatically increase the usable amount of data so that, with the current earthquake-station setup, we perform each iteration with more than two million measurements. Our initial results are promising to improve images from the upper mantle all the way down to the core-mantle boundary.

Recent improvements in our 3D solvers (e.g., a GPU version) and access to highperformance computational centers (e.g., ORNL's Cray XK7 "Titan" system) now enable us to perform iterations with higher-resolution ($T > 9$ s) and longer-duration (180 min) simulations to accommodate high-frequency body waves and major-arc surface waves, respectively, which help improve data coverage. Our ultimate aim is to use data from all available networks and earthquakes within the magnitude range of our interest which requires a solid framework to manage big data sets during pre-processing (i.e., data requests and quality checks, processing data, window selections etc.) and postprocessing (i.e., pre-conditioning and smoothing kernels). We discuss the current status and future of global adjoint tomography based on our initial results as well as practical issues such as handling big data in inversions and on high-performance computing systems.

On the utility of communication-avoiding and vectorization strategies in wave propagation analysis

Jed Brown[1]

[1] Mathematics and Computer Science Division, Argonne National Lab, jedbrown@mcs.anl.gov

Several approaches to reducing the cost of communication, improving memory locality, and providing opportunity for vectorization in PDE simulations and analysis have been receiving attention recently. For example, communication costs may be ameliorated via parallel-in-time integration, pipelining, and s-step methods, all of which focus on the space-time domain, as well as various forms of aggregation in stochastic and ensemble space. These approaches have varying costs and benefits, as well as far-reaching consequences on programming tools, software design, and the suitability of emerging hardware architectures. This poster will provide performance models and lower bounds to compare these methods in terms of work, memory bandwidth, network latency, network bandwidth, and opportunities for reuse.

Practical and Cost-Effective Shallow and Deep Shear-Wave Velocity Surveys for 3D Earthquake Simulations in Sedimentary Basins

Recep Cakir and Timothy J. Walsh

Division of Geology and Earth Resources, Washington State Department of Natural Resources
recep.cakir@dnr.wa.gov and tim.walsh@dnr.wa.gov

Understanding 3D wave propagation or simulation for basin areas in Washington is important to generate better seismic hazard maps, thus improving building codes specifically for the urban areas such as Seattle and Tacoma. Construction of the seismic model parameters (shear-wave velocity and density and geometry) of the earth model for a basin area is essential for any seismic wave simulation purposes. The shear-wave velocity (Vs) information is the main model parameter to construct a simulation model. Due to its limited availability, model parameters of a basin have been constructed using indirect subsurface information (boreholes, seismic reflection/refraction (Vp), and gravity-magnetic modeling) (Frankel, 2009). In addition, shallow soil information (a couple of hundred meters to one kilometer) have often been assigned to a constant Vs value (i.e., 600 m/sec).

Washington State Department of Natural Resources – Division of Geology and Earth Resources (WADNR-DGER) has been conducting active and passive seismic surveys to estimate shallow and deep shear-wave velocities (Vs) in Washington. We have used SH-refraction, Multichannel Analysis of Surface Waves (MASW) (Rayleigh and Love waves) and downhole seismic methods to estimate shallow Vs-profiles. Recently, we tested passive single-station and multi-sensor microtremor measurements to estimate Vs at depths (from 10 to 3000 meters) in Seattle and Olympia. Single-station (3-comp broadband) Horizontal-to-Vertical Spectral Ratio (HVSR), and multi-sensor and 2-station (broadband) microtremor arrays were used to estimate deep Vs layered models. These cost-effective and practical shallow and deep seismic survey methods can be directly used to construct or verify complete 3D model parameters used or to be used in the seismic wave propagation simulations for basin areas in Washington. Finally, rapid shallow Vs measurements in correlation with shallow borehole information can be directly used to account for shallow soil layer effects in the 3D simulations.

Ambient noise imaging

M. Campillo

ISTerre, Université Joseph Fourier and CNRS, Grenoble, France

I present a few mathematical results to justify the use of the correlations of ambient noise records for imaging purposes. I discuss the limit of this approach and give some quantification of the errors induced by the actual properties of ambient noise. The first application of ambient noise correlations concerned surface wave imaging. Since the first applications, ambient noise surface wave tomography emerged as a powerful tool to image the crust and upper mantle and to provide reliable S wave velocity models. I describe some of the improvements recently proposed. Indeed body waves are key ingredients for imaging of the Earth. I discuss the retrieval of reflected crustal body waves and show that the retrieved signals have kinematics and polarization similar to the expected Green functions. In the last part of my talk, I present the teleseismic correlations for period between 5 and 100 s. Most of the teleseismic deep phases appear in the correlation section. I present applications showing that the signature of the structural heterogeneity is preserved in the correlations, opening the way to the use of this new type of data for global imaging, including deep mantle and core. As for the surface waves, a critical analysis of the use of correlation is necessary and I present a preliminary discussion of the possible drawbacks as well as of the specific requirements in the processing of the raw data.

Hexahedral meshing 101: seismic wave propagation and complex geological volumes

E. Casarotti[1]

[1]Istituto Nazionale di Geofisica e Vulcanologia, emanuele.casarotti@ingv.it

Unstructured hexahedral mesh generation is a critical part of the modeling process in the Spectral-Element Method (SEM). We present some examples of seismic wave propagation in complex geological models, meshed using CUBIT (Sandia Laboratory,cubit.sandia.gov), an advanced 3D unstructured hexahedral mesh generator, and GEOCUBIT, a python library that exploits the power of CUBIT in a multicore parallel environment. The main goal of this presentation is to provide tools and information useful to unburden the discouraging steep learning curve of the mesh generation phase. I will provide some examples from Italy, Southern California, Alaska, and Chile.

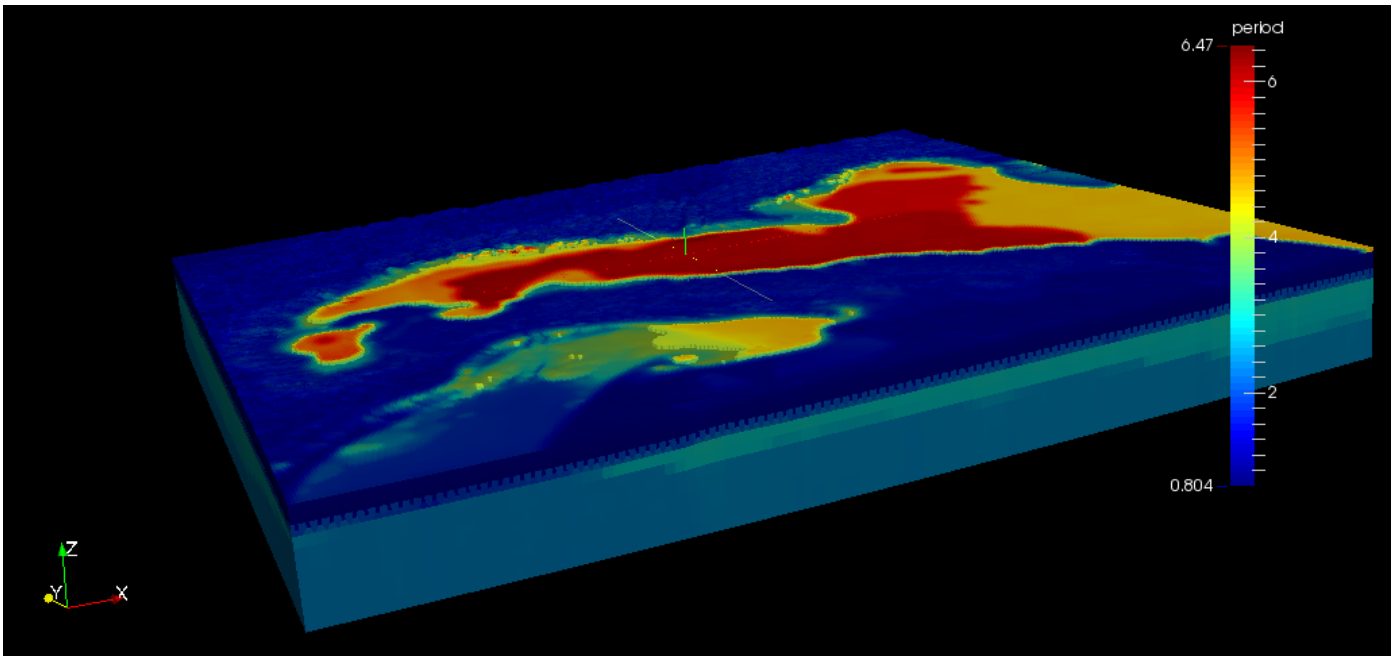

Caption: Mesh of Northern Italy composed of 5 Millions of hexahedral elements, colors enlights the minimun resolved period for seismic wave simulations of the 20 May 2012 M 5.9 Northern Italy earthquake. The geological model includes a 3D representation of sedimentary layers of the Po Valley and the Moho discontinuity.

Uppermost mantle structure beneath the High Lava Plains, Oregon, USA, imaged by teleseismic scattered waves

Chin-Wu Chen[1], David E. James[2], and Matthew J. Fouch[2]

[1]Institute of Oceanography, National Taiwan University, chinwuchen@ntu.edu.tw
[2]Department of Terrestrial Magnetism, Carnegie Institution of Washington, james@dtm.ciw.edu; fouch@dtm.ciw.edu

The High Lava Plains (HLP) in central and eastern Oregon represents one of the most active intraplate magmatic provinces on Earth. This region's recent tectonic history is dominated by voluminous mid-Miocene outpourings of Steens and Columbia River flood basalts, followed by a period of volcanic activitiy that generated two time-progressive rhyolitic tracks: the northeast-trending Snake River Plain / Yellowstone track, and the northwest-trending High Lava Plains hotspot "wave." The cause of this complex tectonomagmatic evolution is still not well understood; end-member source models include one driven by a mantle plume and one driven by subduction. Here, we compute high-resolution seismic images using a scattered wavefield technique to detect seismic discontinuities in the crust and uppermost mantle beneath the HLP, using data recorded by a temporary dense array. We process over 70 high-quality teleseismic events with good azimuthal coverage using a 2-D teleseismic migration algorithm based on the Generalized Radon Transform. Our migration images reveal complex structures beneath the HLP, including (1) a prominent Moho discontinuity with varying depth, with the thinnest crust of 35 km present beneath the volcanic track, and thicker crust of up to 45 km beneath the Owyhee Plateau; and (2) several zones of low-velocity anomalies confined to the uppermost mantle beneath regions of Holocene volcanism in southeastern Oregon (including areas of the Owyhee Plateau), as well as beneath volcanic centers near Steens Mountain and Newberry volcano. These low-velocity features exhibit remarkable similarity with those seen in complementary surface wave tomography and receiver function images. In conjunction with petrological constraints on the equilibration depth of primitive basaltic melts, our results suggest that the HLP mantle lithosphere is either thin or perhaps completely removed, likely as a consequence of episodes of extensive mantle upwelling and melting induced by slab rollback. Our image provides important constraints regarding the complexity of mantle dynamics in the Cascadian back-arc and the close casual link between subduction-related processes and the origin of HLP volcanism.

Adjoint tomography of the crustal and upper-mantle seismic structure beneath Continental China

Min Chen[1], Fenglin Niu[1], Qinya Liu[2], Jeroen Tromp[3]

[1]Rice University, Department of Earth Science, Houston, TX, United States, min.chen@rice.edu
[2]University of Toronto, Department of Physics, Toronto, ON, Canada
[3]Princeton University, Department of Geosciences, Princeton, NJ, United States

Four years of regional earthquake recordings from 1,869 seismic stations is used for high-resolution and high-fidelity seismic imaging of the crustal and upper-mantle structure beneath Continental China. This unprecedented high-density dataset is comprised of data recorded by the China Earthquake Administration (CEA) Array, NorthEast China Extended SeiSmic (NECESS) Array, the INDEPTH-IV Array, F-net and other global and regional seismic networks. Adjoint tomography is applied on this unprecedented dataset, aiming to solve detailed 3D maps of compressional and shear wavespeeds, and radial anisotropy. Contrary to traditional ray-theory based tomography, adjoint tomography takes into account full 3D wave propagation effects and off-ray-path sensitivity. In our implementation, it utilizes a spectral-element method for precise wave propagation simulations. The tomographic method starts with a 3D initial model which combines smooth radially anisotropic mantle model S362ANI and 3D crustal model Crust2.0. Traveltime and amplitude misfits are minimized iteratively based on a conjugate gradient method, harnessing 3D finite-frequency kernels computed for each updated 3D model. Our preliminary results already show strong correlations of 3D wavespeed heterogeneities in the crust and upper mantle with the surface tectonic units, such as the Himalaya Block, the Tibetan Plateau, the Tarim Basin, the Ordos Block, and the South China Block. Narrow slab features emerge from the smooth initial model above the transition zone. Our preliminary models also reveal 3D wavespeed variations comparable to or much sharper than the high-frequency P-and S-wave tomography models from previous studies. Additional iterations will be carried out to refine the 3D radially anisotropic model. The final model with resolution test will allow us to closely examine the seismic structures beneath the different tectonic units of China, and to better understand how the sub-surface processes shaped the surface geology and tectonic features.

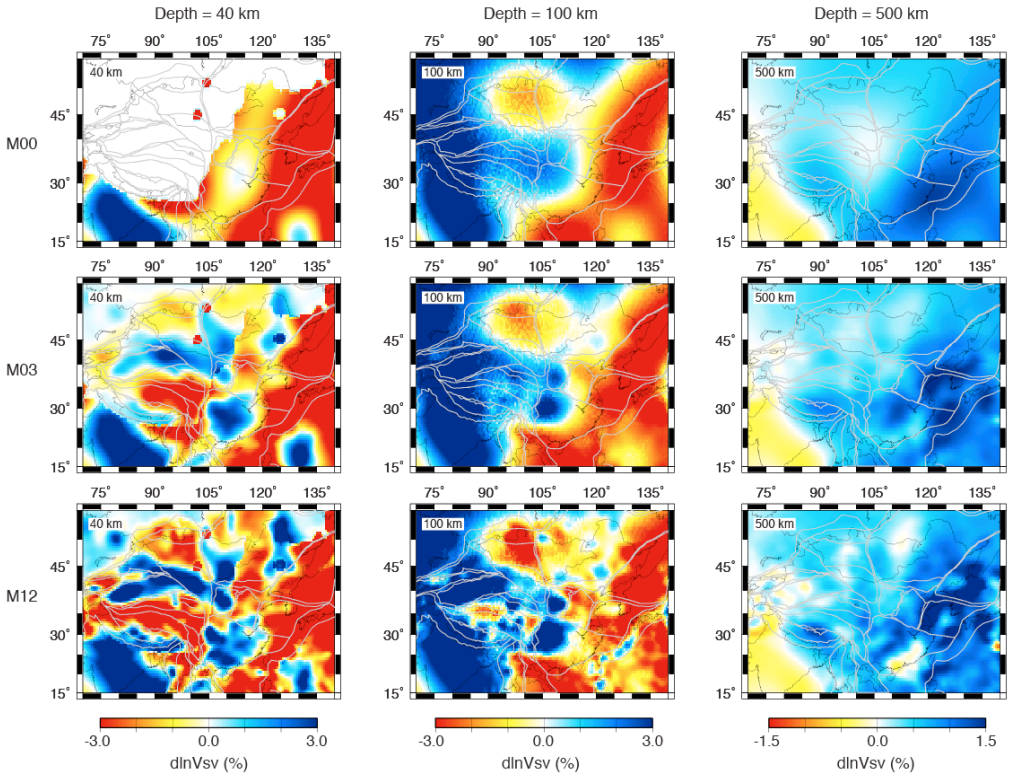

Constant depth map views of the initial model M00, the 3rd iteration model M03, and the 12th iteration model M12 at 40, 100 and 500 km depth. Note that at 40 km depth, 3D crustal model (Crust2.0) is masked out. Tomographic images sharpen with increasing number of iterations.

An exceptionally large ULVZ at the base of the mantle near Hawaii

S. Cottaar[1], B. Romanowicz[2]

[1]UC Berkeley, sanne@berkeley.edu
[2]IPGP, France, College de France, France

We present remarkable features in the waveforms of S, ScS and Sdiff phases of western Pacific events observed at stations in North America that indicate the presence of a very large ultra-low-velocity-zone (ULVZ) at the base of the mantle, centered roughly 11 deg to the southwest of Hawaii, within and near the northern border of the Pacific LLSVP (large low shear velocity province).

Previous studies have documented the presence of ULVZs at the base of the mantle, through observations of body wave complexities. Geometrically their heights are in the range of ~5-30 kilometers, while little is known about their lateral extent beyond > 100 km, due to limitations in sampling. Our data set allows us to forward model the full 3D, though simplified, geometry of this ULVZ, including its horizontal extent. Waveform complexities in the data mainly consist of strongly delayed (> 30 seconds) postcursors.

Ray theoretical analysis of travel times and beamforming analysis of out-of plane energy, lead us to consider a simplified cylindrical shape. Full 3D numerical forward modeling further constrains its parameters with a large aspect ratio of ~910 km in diameter and ~20 km in height. The shear wave velocity reduction is ~20%. We also illustrate the various trade-offs and uncertainties. Including one event from the Fiji towards stations in Alaska, provides azimuthal coverage and reduces the uncertainty in location.

This is to our knowledge the largest ULVZ mapped to date. Its location suggests that it may be the root of a long-lived, stable plume responsible for the Hawaiian volcanic chain, the hotspot track with the largest buoyancy flux.

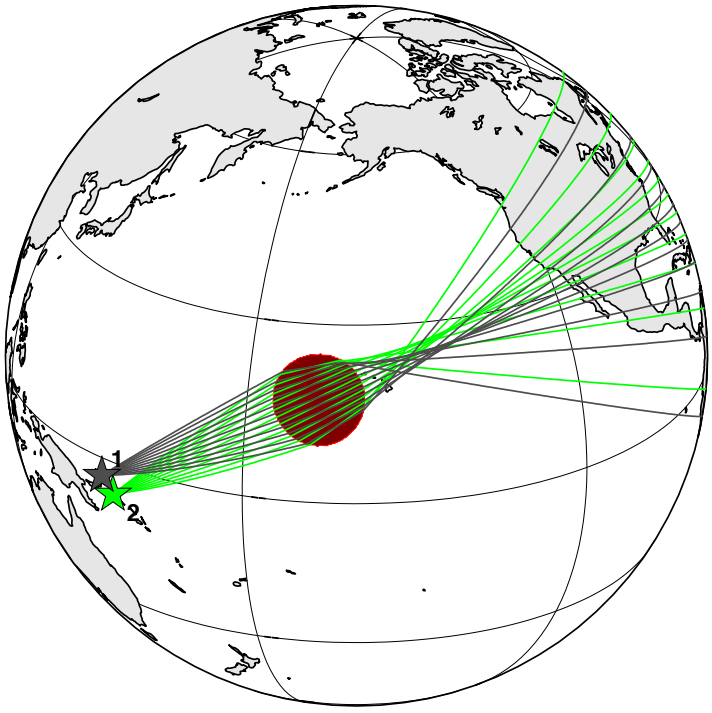

Ray-theoretical illustration of the focusing caused by the ULVZ. The resulting postcursors allow us to map its dimensions.

Seismic Full-Wavefield Inversion Using Discontinuous Galerkin Methods

S. Collis[1], C. Ober[1], J. Krebs[2], B. van Bloemen Waanders[1], T. Smith[1], J. Young[1], J. Overfelt[1] and N. Downey[2]

[1]Computer Science Research Institute, Sandia National Laboratory, Albuquerque, NM.
[2]ExxonMobil Upstream Research Company, Houston, TX.

Industry seismic wavefield simulators have traditionally been based on the finite difference (FD) method due to its efficiency and straightforward implementation. However, adapting FD methods to irregular computational domains, required in regions of complex topography or bathymetry, reduces their efficiency to the point where alternative computational methods become competitive. Furthermore it is difficult to adjust the resolution of the FD computational grid to increase computational efficiency in regions of relatively high seismic velocity and the accurate simulation of interface waves (ie. Rayleigh waves, Scholte waves) is difficult using FD methods.

We are developing a seismic wavefield simulator based on the discontinuous Galerkin (DG) method. DG methods provide all the mesh complexity associated with finite elements, including mesh refinement, hanging nodes and conformability to irregular surfaces. However, DG methods also include some of the efficiency associated with FD methods by not requiring global matrix inversion. Our objective is to use this DG simulator to develop a framework by which inversion of seismic data for elastic, attenuation and source parameters can be achieved. Here we present results achieved by this effort including inversion of acoustic and elastic datasets and source inversion. We also demonstrate the ability of the DG-based simulator to model surface waves and waves in regions of complex anisotropy and discuss the contrast between the behaviour of the DG-based simulator and inversion engines to those based on FD methods.

Finite Slip Inversions from Near-Field Seismic Data: How to Quantify the Uncertainties?

W. Fan[1], P. M. Shearer[1], P. Gerstoft[1]

[1]Scripps Institution of Oceanography, University of California, San Diego,
w3fan@ucsd.edu, pshearer@ucsd.edu, pgerstoft@ucsd.edu

Earthquake finite-slip inversions are subject to many limitations, such as poorly known velocity structures, generally ill-conditioned inversion problems, and unevenly collected data. Substantial model variations often exist between different groups even with the same data and similar approaches. In order to provide guidelines for interpretation, it is important to quantify the uncertainties of the problem. Ideally source inversion model parameterization should be informed by the likely resolution that can be achieved. To probe the robustness and resolution limits of near-field source inversion, we have used Inversion Exercise #1 of the Source Inversion Validation (SIV) initiative as a test case. In this synthetic modeling exercise, a layered velocity structure, fault geometry and recordings at different stations are provided. Inverted slip functions can then be compared to the starting model, which is also provided. We are analyzing this problem from the following perspectives: (1) To examine the stability of the inversion alone, we generate synthetic data using the provided velocity structure and source-time function, then perform inversions with our synthetic data. We experiment with different regularizations, including L1-norm model damping to identify the best approach and quantify the resolution that can be achieved. (2) To understand the effect of inaccuracies in the forward problem (Green's function), we implement the best approach we found in (1) to perform inversions with the model provided data, as well as data contaminated by noise or computed for a different velocity structure. Our overall goal is to quantify the model influence on the source inversion problem and propose the best regularization strategies for specific fault and station geometries.

Towards a comprehensive multi-scale model of Europe and western Asia

A. Fichtner[1], F. Rickers[2] and J. Trampert[3]

[1]Department of Earth Sciences, ETH Zurich. andreas.fichtner@erdw.ethz.ch
[2]Institut the Physique du Globe, Paris, France.
[3]Department of Earth Sciences, Utrecht University, The Netherlands.

We present a tomographic model of the crust and upper mantle beneath Europe and western Asia, constrained by the full waveform inversion of complete teleseismic and regional seismograms in a broad period range (8-200 s). Our method combines the spectral-element modelling of seismic wave propagation, adjoint techniques and the quantification of waveform differences via time-frequency phase misfits. To resolve both crustal and mantle structure, we simultaneously solve multiple regional- and continental-scale inverse problems. The inverse problems on different scales are coupled via 3D non-periodic homogenisation which induces apparent anisotropy that needs to be accounted for in the forward modelling. We assess tomographic resolution using curvature information obtained via second-order adjoints. Regions where resolution is particularly high compared to previous studies include the North Atlantic, the western Mediterranean and Anatolia, where lateral resolution length drops below 30 km within the lithosphere. The multitude of geologically interpretable features include the Iceland plume which clearly extends into the lower mantle. Furthermore, we observe two low-velocity fingers that extend from the Iceland plume into the North Atlantic asthenosphere, where they correlate with regions of Neogene uplift. Western Anatolia is characterised by the extension-related updoming of lower-crustal material. The deep expressions of volcanic provinces in central Anatolia and the North Anatolian Fault Zone are clearly imaged.

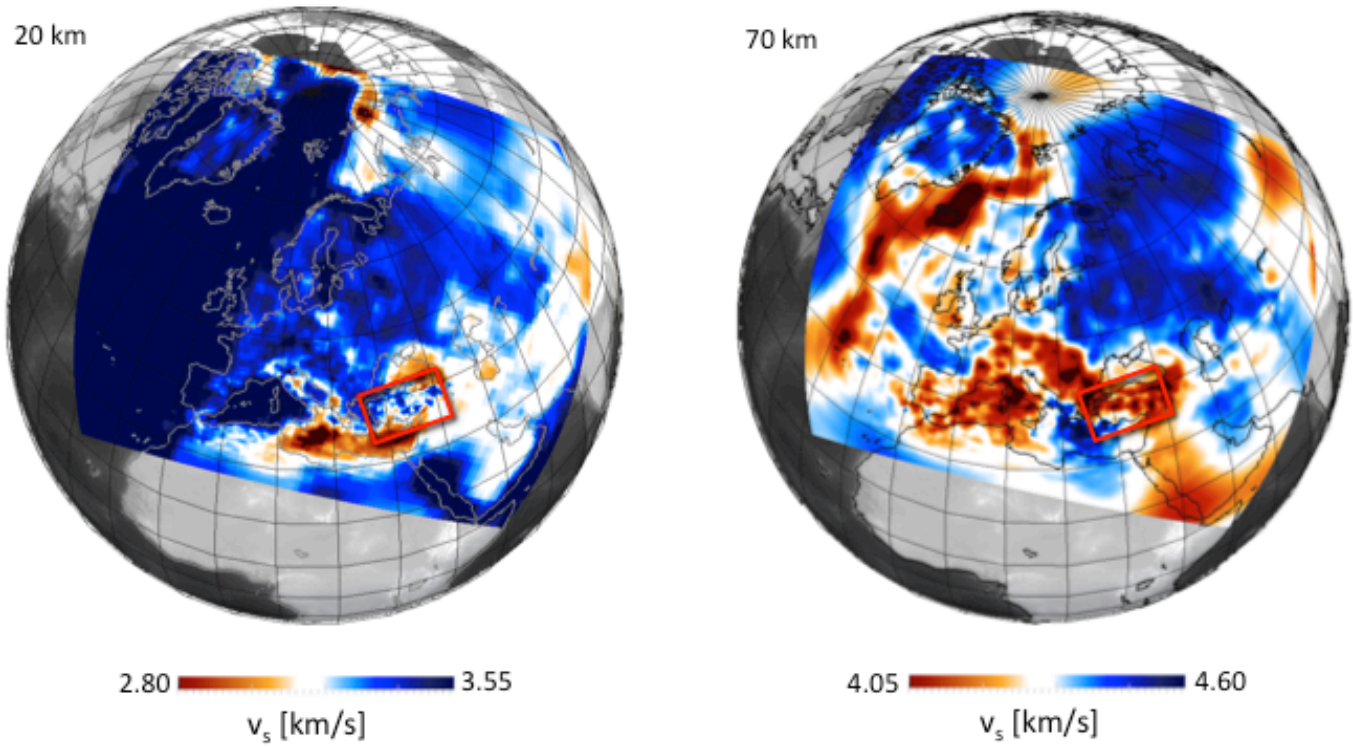

Isotropic shear velocity in our current model (52 iterations) at 20 and 70 km depth.

Oceanic low-velocity structure in SEMum2: Interpretations and synthetic validation

Scott French[1], Vedran Lekic[2], and Barbara Romanowicz[1,3,4]

[1]Berkeley Seismological Laboratory, UC Berkeley, Berkeley, CA, USA
[2]Department of Geology, University of Maryland, College Park, MD, USA
[3]Collège de France, Paris, France
[4]Institut de Physique du Globe de Paris, Paris, France

The SEMum model [Lekic & Romanowicz 2011a, GJI] was the first global upper-mantle Vs model developed using long-period waveform inversion based on spectral-element [Komatitsch & Vilotte 1998] forward modeling. As a result, SEMum exhibits stronger, more-realistic amplitudes of lateral heterogeneity, particularly above ~250km depth, than previous global models based on asymptotic modeling techniques [Lekic & Romanowicz 2011b, EPSL]. Our next-generation model obtained using this approach, SEMum2, reflects a range of improvements including a new treatment of crustal structure and refined lateral resolution. Here, we first present the SEMum2 model, focusing on a never-before-seen pattern of finger-like low-velocities in the 200-350km depth range beneath the oceans that orient sub-parallel to absolute plate motion. These low-velocity fingers (LVFs) interact with both the oceanic low-velocity zone above and a number of sub-vertical conduit-like low-velocity features below that extend to the lower mantle. We present possible interpretations of these features, corroborated by independent geophysical observations, as well as tests that validate SEMum2 model structure. Second, motivated by the observed interactions between LVFs and plume-like "conduit" features in SEMum2, which readily evoke channelization of upwellings in a low-viscosity asthenosphere, we seek to assess how well our waveform inversion scheme should recover such structures. Given the well-known limits of linear resolution analysis [Lévêque et al. 1993], we instead embark on a series of synthetic inversions, similar to Rickers et al. [2012], to examine whether hypothetical plume-like features may be imaged successfully using our "hybrid" technique, which combines the SEM for forward modeling with finite-frequency sensitivity kernels from non-linear asymptotic coupling theory [Li & Romanowicz 1995]. We present the results of these tests, with the goal of establishing model recovery consistent with the features seen in SEMum2.

Active Tectonics of Alaska

J. Freymueller

University of Alaska Fairbanks, Geophyical Institute, jeff.freymueller@gi.alaska.edu

Alaska is by far the most tectonically active part of North America, and one of the most tectonically active areas in the world. It hosts a combination of subduction, arc volcanism, continental terrane collision and accretion, and large-scale deformation of the continental lithosphere. The general outline of Alaska tectonics was sketched extremely well by George Plafker and others by the 1980s, but many important details, and particularly rates of motion, are now known primarily through modern space geodetic measurements. In addition to steady tectonic deformation of the continent, the observed crustal deformation includes significant components due to earthquake cycle deformation, transient postseismic deformation, volcanic inflation and eruption, and glacial isostatic adjustment. Geodetic data and the combination of plate configuration and geography have allowed us to study a wide variety of problems in the kinematics and dynamics of the lithosphere in one single area.

Most of the crust in Alaska and the surrounding area is moving relative to the North American plate, and the location of the edge of the geologically stable North American continent in the region is not yet clearly defined. Even the Arctic coast of Alaska appears to move relative to the North American plate, although quite slowly. Typical permanent crustal motions are of the order of a few to several mm/yr, and GPS observations across the region define a broad plate boundary zone that comprises not only Alaska, but also most or all of the Pacific coast of Canada. Likewise, there is no well-defined boundary between Alaska and northeast Asia. It is better to think of the entire north Pacific region as a broad plate boundary zone between the North American, Pacific, and Eurasian plates; a collage of tectonic blocks of various sizes that forms a single, large, diffuse deforming belt.

These large-scale tectonic motions are overprinted by deformation related to earthquake cycle processes, which often cause ground deformation that is larger than the long-term and large-scale motions. Separating these effects requires exploiting features in the data that constrain a single part of the overall model, or a single process. I will illustrate this process for the examples of postseismic deformation following the 1964 earthquake and elastic deformation from the subduction zone of the Aleutian arc.

Unified theory of microseisms and hum

Peter Gerstoft and James Traer
University of California, San Diego

Interaction of ocean surface-waves forces water-column pressure fluctuations that generate both double-frequency (DF) microseisms and hum. Prior treatment of non-linear ocean wave interactions has focused on the special case of opposing waves, which generate DF pressure fluctuations that do not decay with depth. Such fluctuations interact with the seabed at any depth. We consider arbitrary 2D surface-wave spectra and integrate over all possible pairings of wavevectors, directions and frequencies to obtain a full second-order spectrum for a perturbation expansion of pressure. Obliquely interacting waves generate evanescent pressure fluctuations, at frequencies corresponding to observations of both DF microseisms and the Earth's hum. Such fluctuations will only interact with the seabed in shallow water. They are generated both by arbitrary pairs of interacting wave trains and by a single wave train containing a spread of directions. As their generation does not require precise wave states, they are likely ubiquitous in shallow water.

SCEC Unified Community Velocity Model: Mesh Generation and Visualization

D. Gill[1], P. Maechling[1], T. Jordan[1], A. Plesch[2], R. Taborda[3], S. Callaghan[1], P. Small[1]

[1] University of Southern California ([davidgil,maechlin,tjordan,scottcal,patrices]@usc.edu)
[2] Harvard University (andreas_plesch@harvard.edu)
[3] Carnegie Mellon University, Department of Civil and Environmental Engineering (rtaborda@cmu.edu)

Three-dimensional (3D) material models, also called seismic velocity models, provide fundamental input data to ground motion simulations. One of their primary uses is in generating discrete representations of the crustal structure and sedimentary deposits in a region of interest for visualization and wave propagation simulations. Typical discrete representations of material models are in the form of structured and unstructured meshes or grids. Building these modes model is a critical step in running many large-scale ground motion simulations. The Unified Community Velocity Model (UCVM) software bundle developed by the Southern California Earthquake Center (SCEC) is a cohesive computer application framework to integrate and query independent velocity models. In this poster, we describe three examples that illustrate various capabilities of UCVM as used with two velocity models available for Southern California, namely CVM-S4 (the SCEC community velocity model) and CVM-H (the Harvard community velocity model). Although these two models for illustration, UCVM has also been configured to use velocity models outside of California, such as the Wasatch Front, Utah 3D velocity model.

In our first example, we show how UCVM can be used to extract a mesh covering the Los Angeles basin containing Vp, Vs, and density. This is a simple example that shows how UCVM can be used in a powerful manner without needing expensive hardware. Indeed, this first example can be run on any standard Linux machine without the need for much configuration or set up. This example makes use of the ucvm2mesh utility.

In our second example, we show how to create a 4-Hz Chino Hills octree-based database (*etree*) fed with the model's information, using a supercomputer such as Kraken. The final etree is approximately 250 GB in size. The etree is first built with an automated unstructured configuration and then compressed for optimized memory usage using two utilities, ecompact and ecoalesce—both of which are bundled with UCVM. The specific utilities involved are ucvm2etree-extract-MPI, ucvm2etree-merge-MPI, ucvm2etree-sort-MPI, ecompact and ecoalesce.

Finally, in our third example, we show how the UCVM software can integrate NetCDF utility code to produce 3D velocity model files compatible with NetCDF data viewers. UCVM includes the capability to generate a 3D velocity mesh in NetCDF format, which can then be viewed by IDV (UCAR Integrated Data Viewer). Using the IDV, users can view the Vp, Vs, or density properties of the model. This demonstrates that UCVM can generate meshes from any compatible community velocity model and that the resulting models can be visualized without the need for complex secondary tools, and it shows how developers can easily write tools that can convert from one data format to another using the UCVM API.

Source-Structure Tradeoff in Noise Tomography

Shravan Hanasoge[1,2]

[1]Department of Geosciences, Princeton University, USA
[2]Max-Planck-Institute for Solar System Research, Germany
hanasoge@princeton.edu

Cross correlations of microseismic oscillations excited by oceanic activity, recorded by seismometers, are used to infer structural properties of Earth. The sources of these oscillations are typically localized, resulting in anisotropic illumination of the crust. Here, we attempt to characterize the impact of the tradeoff between source and structure by posing a 2-D inverse problem where an arbitrary distribution of sources illuminates the heterogeneous medium. We use the adjoint method to compute noise cross correlation kernels (e.g., Gizon & Birch 2002, Tromp et al. 2010, Hanasoge et al. 2011, Hanasoge 2013) for travel-time, amplitude, and waveform-difference measurements. We also compute classical structure kernels for these measurements and compare them with the corresponding noise kernels.

Long Period, Very Long Period, and Ultra Long Period Signals from the 2009 Redoubt Eruption

M. Haney[1], B. Chouet[2], and J. Lyons[1]

[1]U.S. Geological Survey, Alaska Volcano Observatory, mhaney@usgs.gov, jlyons@usgs.gov
[2]U.S. Geological Survey, chouet@usgs.gov

The 2009 eruption of Redoubt Volcano, Alaska, produced as many as 4 lava domes and over 19 explosions between March 23 and April 4. Following the explosive phase, the volcano began a dome-building phase that continued until mid-summer. A network of 5 broadband seismometers located on the Redoubt edifice captured these two phases of the eruption in their entirety, in addition to recording the end of the precursory phase. We present the analysis of swarms of small, repetitive, long-period (LP, 0.5-2 s period) events that occurred during both the explosive and dome-building phases of the eruption. The results complement previous research conducted on the source of very-long-period (VLP, 2-30 s period) signals observed to accompany several of the explosions. In addition to the LPs and VLPs, ultra-long-period (ULP > 300 s) signals exist on the seismometers due to atmospheric coupling of gravity waves generated by the explosions.

We apply waveform inversion to locate the LPs and find their source mechanism. We focus on two prolific LP swarms from the eruption: a swarm of 5500+ similar events that occurred from April 2-4 (the April swarm) and a swarm of 30,000+ similar events that took place in early May (the May swarm). The April swarm ended with the final explosion of the eruption, a dome-collapse on April 4. The May swarm, in contrast, was not associated with an explosion, although a small dome-failure and steam and ash emission occurred approximately midway through the swarm. A challenge in the analysis of the swarms is that the individual LPs are relatively small in amplitude. We exploit the similarity in waveforms among the individual LPs and improve the signal-to-noise ratio substantially by stacking over all events on each station. An additional challenge is that the LPs, being higher frequency than the VLPs, suffer more from path effects. This limits the maximum range for stations to be included in the inversion. From waveform inversion using the 5 broadband seismometers on the Redoubt edifice within 4.5 km of the summit crater, we find a source depth of 1.5 km ASL. This places the LPs between the VLP source at Redoubt (0.8 km ASL) and the summit crater (2.3 km ASL). Based on our previous study of VLPs at Redoubt, we consider a moment-only inversion since the local network is not dense enough to uniquely resolve both moments and forces. The obtained moment tensor indicates the LPs are dominantly volumetric with consistently shaped source-time functions. Typical moments are on the order of 10^10 Nm.

By comparing data recorded on the broadband seismometers and a local infrasound microphone, we find evidence for gravity waves in the ULP band (> 300 s) following several of the Redoubt explosions. We model the propagation of internal gravity waves with finite differences and speculate on the extension of the waveform inversion approach to the analysis of gravity wave sources.

Model-Based Subspace Detectors Constructed with SPECFEM3D

D. B. Harris[1], A. J. Rodgers[2]

[1]Deschutes Signal Processing LLC, oregondsp@gmail.com
[2]Lawrence Livermore National Laboratory, rodgers7@llnl.gov

Waveform correlators enable sensitive detection of weak signals in situations of recurrent seismicity. The empirical approaches being widely studied use well-recorded signals from higher magnitude events as templates to search for signals from much smaller events. Detection thresholds an order of magnitude lower than those achievable with conventional power detectors (STA/LTA on array beams) have been reported with empirically-derived array correlators. However, empirical correlation detectors are, of course, limited to those areas with historical archives of observations and to detecting events with mechanisms consistent with past seismicity.

In this study, we attempt to circumvent these limitations at long periods by constructing waveform correlation-type templates for detection from the best available 3D models using SPECFEM3D GLOBE. We construct waveform basis functions for matching a variety of mechanisms using subspace detectors, a generalization of correlation detectors. Subspace detectors permit a degree of uncertainty about the waveforms being detected by projecting the observed data onto a subspace defined by a collection of basis functions rather than a single template waveform. The basis functions we construct with SPECFEM3D span Greens functions corresponding to the six independent components of the moment tensor.

We examine the potential for detecting aftershocks of the April 2012 Sumatra earthquakes using synthetic templates derived from the S29EA model for stations at regional and near-teleseismic distances. This choice allows us to perform the forward calculation of templates using a single chunk. We build a single multichannel subspace template for several aftershocks and test a subspace detector operating coherently over the observing network. Since our goal is coherent detection over a network, we modify the classical subspace detector (which assumes uniform noise levels on all observing channels) to estimate noise levels on all channels independently while computing the correlation statistic.

We also examine a strategy for ameliorating model error by constructing templates using several models (in addition to S29EA). We expand the dimension of the subspace used by the detector by aligning the waveform templates from a collection of models in a data matrix, then perform a singular value decomposition to obtain a low-rank basis for the synthetics.

Our eventual goal is to cover the aftershock region with a grid of subspace detectors with synthetically-generated templates, pending successful tests of detection of several selected aftershocks. This approach would allow detection and mapping of seismicity throughout the aftershock region. If model-based processing proves to be feasible by producing templates with adequate fidelity to observed waveforms, then the collection of templates could be constructed in a series of reciprocal calculations for each station.

Building Subspace Detectors for Random Media

D. B. Harris[1]

[1]Deschutes Signal Processing LLC, oregondsp@gmail.com

Correlation detectors use an empirical model of the full seismic waveform to perform sensitive detection, often achieving detection thresholds a full magnitude unit lower than power (STA/LTA) detectors at a given false alarm rate. They are applicable in situations of recurrent seismicity where prior observations provide templates for detecting future occurrences of a waveform pattern. It is desirable to extend correlation-type detection capabilities to regions without prior observations. Correlation templates might be constructed by solving the forward problem through the best available model for the medium. This approach may work well at long periods, but at sufficiently high periods, deterministic models will be insufficiently detailed to provide good waveform matches.

One approach to extending model-based templates to shorter periods is to replace a single-dimension template with a subspace (multi-dimension) representation [Rodgers et al., 2006], allowing a degree of uncertainty in the waveform representation corresponding to uncertainty in the model. In Rodgers et al. the subspace was constructed by solving forward problems through many realizations of a stochastic model, then performing a singular value decomposition of the resulting waveform set to obtain a representative basis. This approach produced some success in extending correlation detection across a network of stations to shorter periods (~10 sec). However, one problem with this technique is the lack of any theoretical estimate of the number of realizations required to obtain an adequate basis even assuming the stochastic model correctly represents the medium.

This problem is solved here for weakly stochastic media using the Born approximation to calculate perturbations to the reference wavefield propagating in a heterogeneous mean model. Medium perturbations are assumed to be normally distributed with a known (possibly nonstationary) spatial covariance structure. The Kahunen-Loeve (K-L) expansion is used to obtain a series representation for the medium perturbations with independent coefficients. The subspace representation for the signal can be calculated in a finite number (one per K-L series term) of forward perturbation simulations under the Born approximation with the number bounded by the effective dimension of the K-L expansion.

This process is illustrated with a 2-D membrane wavefield propagation problem using a specially-constructed pseudo-spectral propagation code. Simulations are performed to examine the dependence of subspace dimension on the temporal bandwidth of the wavefield. If the subspace dimension does not grow too quickly with bandwidth, then a subspace detector may provide processing gain over a simple power detector. If successful, this procedure might be generalized to extend the best elastic 3D tomographic models to predict wavefields at shorter periods by superimposing stochastic model perturbations. The "prediction" in this case would be a subspace prediction, in the sense that the observed wavefield could be constructed as a linear combination of basis waveforms spanning the subspace. Such predictions would be useful for detection providing the dimension of the subspace is not too large.

Rodgers, A., D. Harris, M. Pasyanos (2006), A model-based signal processing approach to seismic monitoring, AGU Fall Meeting abstract S32A-06.

obspyDMT: Parallel Retrieving, Processing and Management of Massive Seismological Datasets

K. Hosseini[1] and K. Sigloch[1]

[1]Department of Earth and Environmental Sciences (Geophysics), Ludwig-Maximilians-Universität München, Munich
hosseini@geophysik.uni-muenchen.de

We are living in the era of 'Big Data'. Larger datasets potentially mean more information; however, access, storage, identification, analysis and visualization of massive datasets have become a big challenge. In this study, we introduce a newly developed software that addresses these issues by presenting effective and fully automatic methods.

obspyDMT (ObsPy Data Management Tool) is a command line tool built upon Python and ObsPy tools for retrieving, processing and management of massive seismological data. It has several advantages over the current downloading tools. Since it uses the direct method and performs all the required steps automatically, the user's time decreases significantly compared to email-based request tools or web interfaces. Additionally, obspyDMT is able to retrieve seismological data (waveforms, response files and metadata) from multiple data centers and to homogenize to a common format. This functionality will become more powerful to the degree that more data-centers will implement direct access options. ObsPy supports both event-based requests (similar to SOD and WILBER) and continuous requests (similar to BREQ-FAST and NetDC). Data from several different events may be retrieved in parallel, further speeding up the process.

obspyDMT also implements map plots of events, stations, and ray paths, as well as record sections of waveform data.

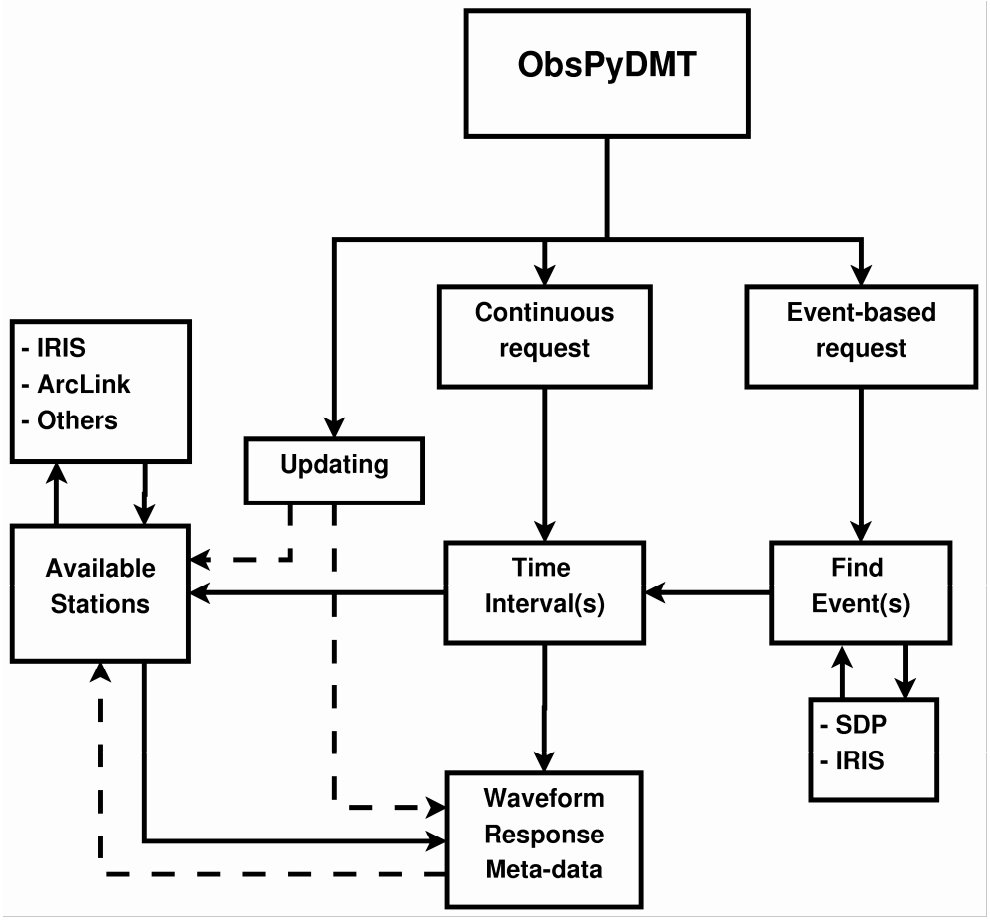

EVENT-BASED, CONTINUOUS AND UPDATING MODES.

Finite frequency measurements of diffracted P waves for waveform tomography

K. Hosseini[1], K. Sigloch[1], T. Nissen-Meyer[2] and S. Stähler[1]

[1]Department of Earth and Environmental Sciences (Geophysics), Ludwig-Maximilians-Universität München, Munich
hosseini@geophysik.uni-muenchen.de
[2]Institude of Geophysics, ETH Zurich, Zurich

Core-diffracted P-waves (Pdiff) graze the core and therefore sample the deepest part of the mantle extensively. The aim of this study is to extract maximum information from broadband data in order to gain a better understanding of lower-mantle structure and processes (heat flow across the CMB and mantle up/down-wellings). For this reason, finite frequency measurements for 8 frequency bands are made by comparing the predicted and observed waveforms in a cross-correlation sense.

To the maximum extent possible, we want to replace human quality check and intervention by robust automated quality diagnosis, based on the temporal, spectral, and spatial similarity of predictions and observations. First, the real data for one event are loaded from the archive and based on a priori criteria (epicentral distance and basic quality control), some of the seismograms are rejected. In the next step, the synthetic seismograms are either loaded (in case that they already exist in the synthetic archive) or generated by YSPEC [Al-Attar & Woodhouse (2008)] or AXISEM [Nissen-Meyer et al. (2007)] and are convolved with the source time function(s). Finally, 8 band-pass filters are applied and the finite frequency measurements (travel time and amplitude) are taken for each frequency band.

This method is applied to ~1900 events and the ray coverage of 97683 station-event pairs with cross-correlation coefficient exceeding 0.85 (mean cross-correlation coefficient: 0.93) is plotted in the following figure. In our experience, waveform fits of this quality produce phase shift data suitable for finite-frequency waveform tomography. In the figure, all segments where ray paths nominally graze the CMB are shown (but for tomography we will model fully numerical sensitivity kernels, not rays). Red color means that more than 10 rays sample the CMB at the location in question.

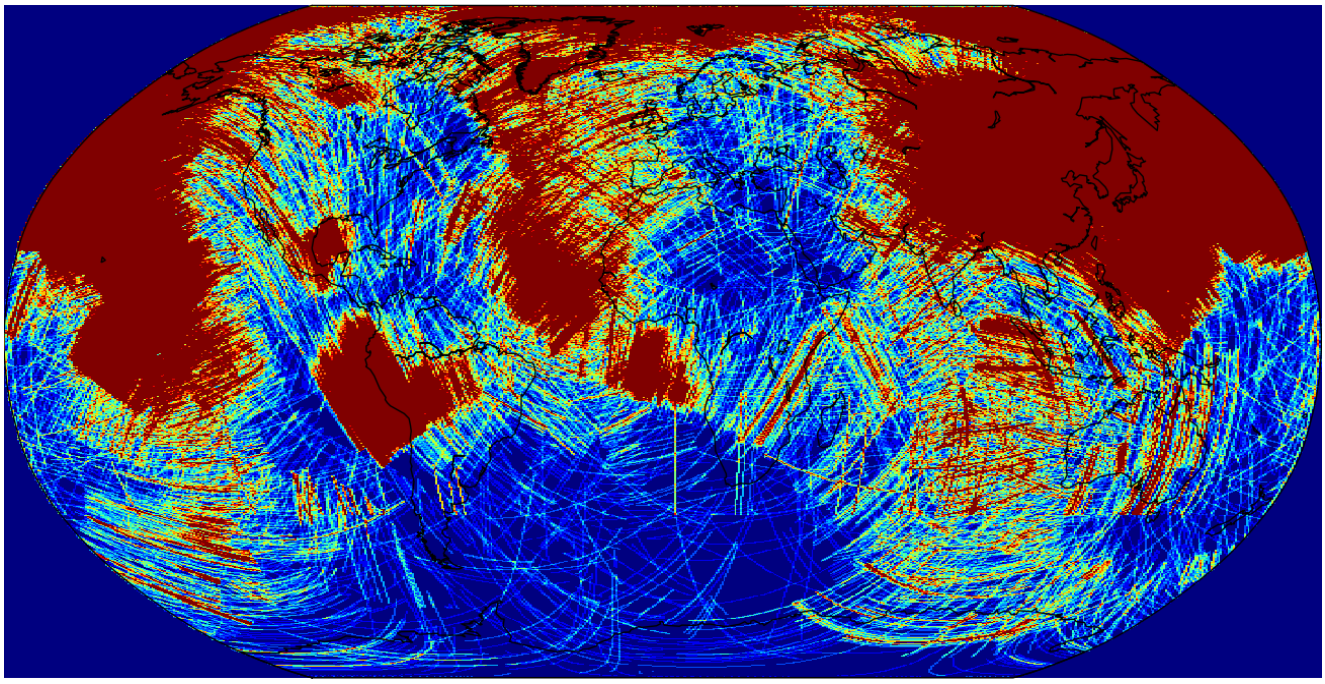

Pdiff COVERAGE FOR THE PROCESSED EVENTS IN OUR ARCHIVE.

3-D Multi-scale Finite-frequency Rayleigh Wave Tomography of Crustal and Upper Mantle Structure beneath Central Tibet

S.-H. Hung[1], I.-H. Cheng[1], Y. Zhou[2], Y.-H. Chang[1]

[1]Geosciences Department, National Taiwan University, shung@ntu.edu.tw
[2] Geosciences Department, Virginia Tech, yzhou@vt.edu

We present a surface-wave tomography method that combines a fully 3-D finite-frequency theory and wavelet-based multi-scale parameterization to deal with two major concerns in tomographic inverse problems: frequency-dependent off-path sensitivity resulting from intrinsic wave diffraction and nonstationary model resolution from uneven data coverage. To properly account for finite-frequency wave propagation, we adopt 3-D Born-Fréchet kernels formulated in the framework of surface-wave mode summation to construct the partial derivatives of dispersive phase anomalies to elastic wavespeed perturbations. To achieve both spectral resolution for long-wavelength structure in regions of sparse data and spatial resolution in densely-sampled regions, we employ multi-scale parameterization by means of the hierarchical wavelet decomposition. We apply this strategy to imaging shear wave velocity structure beneath central Tibet.

Our data were collected from a L-shaped Hi-CLIMB array through the Himalayan-Tibetan collison zone during 2004-2005. Following a standard procedure to obtain empirical Green's functions of fundamental-mode Rayleigh waves from ambient noise cross correlation functions (CCFs) between station pairs, the phase differences between the CCFs and their synthetic impulse responses are measured by a multi-taper cross-spectral method. For the multiresolution inversion, we introduce a biorthogonal wavelet system which comprises the wavelet expansion of the model in a primary space and of the data sensitivity kernel in a dual space. A parallelized singular value decomposition algorithm is utilized to directly solve for the expansion coefficients of the model under the minimum norm constraint in the wavelet space and further to assess the model resolution. Fractional perturbations in shear wave velocity are then reconstituted by the inverse transformation of the resulting wavelet coefficients.

The resulting model indicates that the shear wave velocities of the crust and lithospheric mantle beneath the Lhasa terrane are much higher than the Qiangtang terrane to the north and Tethyan Himalaya to the south. The strongest positive anomaly occurs in the core of Lhasa and gradually terminates northward across the Bangong-Nujian Suture (BNS) at about 32^{o}N. In contrast, anomalously low wave speeds stand out north of the BNS. There are two disconnected low velocity zones in the upper crust (< 30 km) observed at the east and west ends of our model along the Indus-Yarlung Suture (IYS). The absence of pervasive low velocity anomalies in the mid-to-lower crust indicates that the ductile channel flow of the lower crust may be inactive beneath southern Tibet.

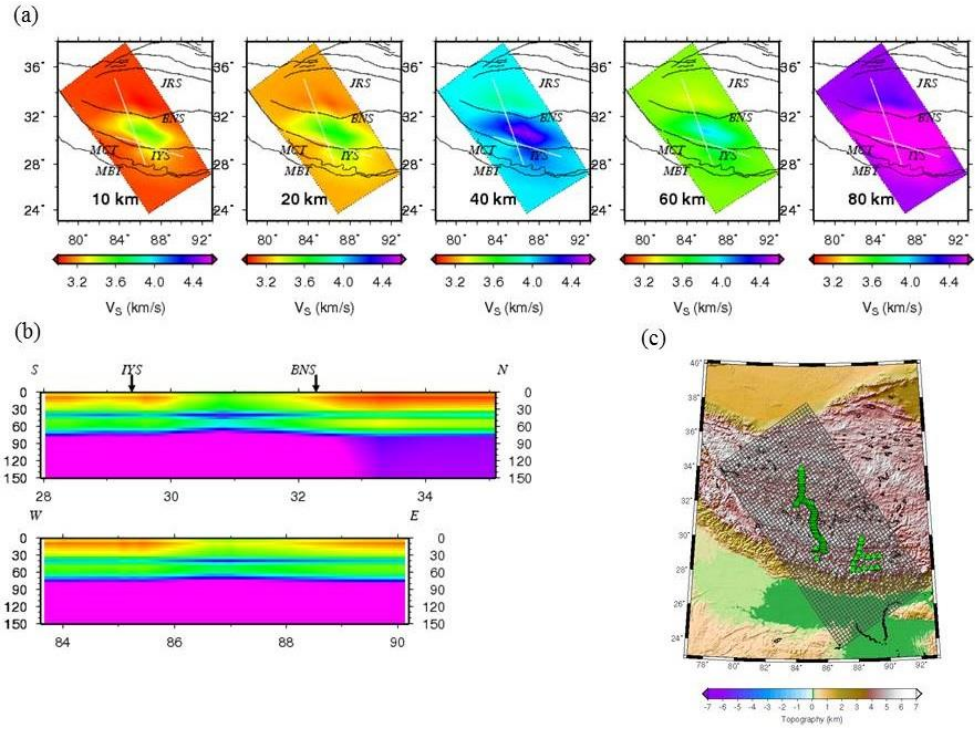

Fig. 1. (a) Cross-section views of the resulting 3-D shear velocity model: (a) the lateral variations at six depths; (b) the variations along the N-S and E-W vertical profiles as denoted by the white lines shown on (a). (c) the study region and station distribution from HiCLIMB Project.

Challenges in computational seismology

Heiner Igel, Lion Krischer, Marek Simon, Stefan Mauerberger, Christian Pelties, Stefan Wenk, Kasra Hosseini[1]

[1]all at Ludwig-Maximilians-University, Munich, Germany

The numerical solution of seismic wave and rupture propagation in 3-D Earth structures is today at the heart of many problems in Earth sciences. These include 1) the forecasting of strong ground motion for earthquake scenarios; 2) the simulation of wave propagation through complex reservoir models; 3) global wave propagation through mantle flow structures; 4) the inverse modelling by fitting complete wave forms on all scales. Due to the short spatial scales involved in seismic wave fields and structures, the simulation problem has always – and will for some time – be a tremendous challenge even on the largest supercomputers. We will show examples of large scale simulations for earthquake scenarios using spectral element and discontinuous Galerkin methods. We point out some benefits of using unstructured grids to mesh complex geological structure and the corresponding computational difficulties associated with load balancing. We also show results on kernel optimization of the Galerkin method and the meshing procedure. In addition, concepts will be discussed using python (ObsPy) as a work-flow tool on supercomputers to solve the complete inverse problem on industrial and regional scale problems. We point out necessary (e-) infrastructure for domain (e.g., Earth) scientists to be able to efficiently cope with simulation tools. This involves portability vs performance by increasing complexity of the available hardware (GPU, MIC, BlueGene, Intel CPUs, hyperthreading, multithreading, etc.).

Stratigraphy and multi-phase tectonic history of the Chukchi Borderland from multi-channel reflection seismic data

I. Ilhan[1] and B. J. Coakley[1]

[1]University of Alaska Fairbanks, Geophysical Institute, iilhan@alaska.edu, bernard.coakley@gi.alaska.edu

The Chukchi Edges project was designed to establish the relationship between the Chukchi Shelf and Borderland and indirectly test theories of opening for the Canada Basin. During this cruise, ~5300 km of 2D multi-channel seismic reflection profiles and other geophysical data (swath bathymetry, gravity, magnetics, sonobuoy refraction seismic) were collected from the RV Marcus G. Langseth across the transition between the Chukchi Shelf and Chukchi Borderland.

These profiles reveal extended basins separated by high-standing fault blocks. Basin stratigraphy can be subdivided on the basis of gross stratal geometry, reflection terminations and inferred unconformities. The wedge-shaped synrift sequences terminate against the basement highs and/or major faults, burying the basement topography. The inferred postrift seismic units are more nearly tabular, but thicken locally due to compaction of underlying synrift sediments.

Reflection character is dominated by alternating high and low amplitude continuous reflectors which would be consistent with pelagic or turbidite sediments. Chaotic units are also observed, which may indicate mass-flow deposits. At least two distinct packages of truncated reflectors are observed on the basement highs of the Chukchi Shelf, Chukchi Plateau and Northwind Ridge documenting major erosion due both to glacial planation and earlier erosional events perhaps associated with basement uplift prior to or during rifting. It is believed that the bulk of the synrift sediments are Mesozoic in age. Certainly Cenozoic sediments are also preserved in these basins, but the position of the boundary is unknown.

Locally, continuous reflectors are observed underlying the rift basin fill. Processed seismic sections reveal coherent parallel reflectors below the rift basin fill. These are a pre-rift sediments and, possibly volcanic rocks or, conceivably layer igneous or metamorphic rocks. Samples dredged from the steep exposed flanks of the rift basins are foliated metamorphic rocks of Paleozoic age. These older units, of very uncertain age, would, if sampled, provide constraint on the history and affinities of the Chukchi Borderland.

From the bathymetry, we can identify East and West sub-basins, separated by bathymetric highs. These two sub-basins contain distinct sedimentary sequences, raising questions about the relative timing of deformation and/or source of sediments delivered to the two basins. A time-structure map of top of the acoustic basement reveals basement structure and major sedimentary depocenters. The basement faults are oriented South-North nearly parallel to the regional trend of the area suggesting West-East extension. However, narrowing of the faults in the South and widening in the North complicates this simple interpretation. Time-structure map of top of the syn- rift (green) reveals NW-SE orientation of the major depocenters: Asymmetry and orientation of the sub-basins may, in part, be due to a second phase of tectonism (strike-slip) in the area.

In addition to the extensional basins, a number of small symmetric basins are observed on the flanks of the Chukchi Plateau. These basins may be transtensional and provide further support for a 2nd phase of tectonism, which overprinted the obvious extensional fabric of the Borderland. This is supported by the observation of uplifted post-rift sediments on the flanks of some of the basement highs.

Joint inversion of strain and aftershock data for the distribution of afterslip following moderate events on the San-Jacinto Fault

A. Inbal, J.-P. Ampuero and J.-P. Avouac

Seismological Laboratory, California Institute of Technology, Pasadena, California, USA

The San-Jacinto Fault (SJF) is one of the most active faults in southern California, which together with the southern San-Andreas Fault accommodates a large fraction of the total accumulated strain within the plate boundary. Seismicity along the SJF is distributed over several fault segments with distinct spatio-temporal characteristics. One of these segments, also known as the Anza seismic gap, is a 20 km long strand of the fault almost devoid of seismicity. Several M>6 events occurred along the SJF over the past 100 years, none of which is thought to had ruptured the gap (*Sanders and Kanamori*, 1984). In recent years four M4-5 events occurred south of the gap. Despite their moderate magnitudes, these earthquakes triggered rich aftershock sequences and pronounced post-seismic slip. This complex pattern of seismic and aseismic deformation along the SJF has important implications for seismic hazard estimation, and may also entail clues about the physical processes that govern fault slip at depth. Here we perform a joint inversion of the aftershock and geodetic data sets in order to recover the evolution of post-seismic slip on the SJF. We analyse continuous strain records from PBO borehole instruments installed within a few kilometres from the trace of the SJF. These sites recorded an abrupt, several weeks long increase in strain rate following three M4-5 events that occurred in 2010 and 2013. A similar, yet shorter response was observed following the 2010 M7.2 El Mayor-Cucapah earthquake. These episodes were accompanied by increased seismicity rates that decayed to the background level according to the modified Omori law.

The limited sensitivity of geodetic data sets to deep fault slip is a well known problem common to many source inversions. It is therefore instructive to incorporate additional data sets to better constrain slip on deep fault patches. This study utilizes Dieterich's aftershock model, which predicts the response of a fault governed by rate-and-state friction to a stress perturbation. Based on this formulation, we are able to infer the stress time-histories of individual fault patches from the observed changes in seismicity rates. This new approach provides resolution power at depths inaccessible to the surface geodetic network. Moreover, it allows us to gain important insights onto the fault mechanic properties. We apply this inversion scheme to a M4.7 that occurred on March 11, 2013. Remarkably, we find that the cumulative moment released post-seismically was comparable or larger than the co-seismic moment release. Most of the post-seismic slip occurred between 8-14 km depth, and is primarily concentrated SE of the Anza seismic gap.

References

Sanders, C. O., and H. Kanamori (1984), A Seismotectonic Analysis of the Anza Seismic Gap, San Jacinto Fault Zone, Southern California, *J. Geophy. Res., 89* (B7), 5873–5890.

Rupture Properties of Intermediate-Depth Earthquakes Using Back-Projection Technique

Miaki Ishii[1] & Eric Kiser[2]

[1]Harvard University, Department of Earth & Planetary Sciences, ishii@eps.harvard.edu
[2]Rice University, Department of Earth Science, edk2@rice.edu

Application of the back-projection technique to image the rupture properties of earthquakes is often performed using the first-arriving *P* waves recorded by a dense network of seismic stations at teleseismic distances. This approach works well to capture complexities in horizontal propagation, but because the ray paths are nearly vertical at the source, there is no depth resolution. This problem of poor depth resolution can be overcome for deep earthquakes by combining the direct *P* arrivals with depth phases such as *pP* and *sP*. We apply this method to examine the rupture characteristics of large, intermediate-depth earthquakes (depths between 100 and 400 km) that occurred between 2000 and 2008 using data from a dense network of stations in Japan. Most of these events show slip that is confined in depth, i.e., sub-horizontal rupture. Furthermore, a significant fraction of the events consists of multiple subevents that are well-separated in depth. For example, a Mw 7.4 event in Hindu Kush region has two sub-horizontal rupture planes that are separated by about 70 km in depth and by about 10 seconds in time. These events suggest that dynamic triggering is common for large earthquakes between 100- and 400-km depth.

The prevalence of sub-horizontal rupture propagation can be explained if they occur on pre-existing fabric generated prior to slab subduction. At the outer rise, complementary sets of faults are generated, and they are rotated as the plate descends into the mantle. Below 100-km depth, these outer-rise faults become nearly horizontal and vertical. The sub-horizontal faults develop into weak zones by focusing of water that has been released from the slab by dehydration. Serpentinization of fault material is expected to occur, and results in the reduction in the strength within the horizontal faults relative to the surrounding material. This difference in strength initiates shear instability within the weak zone, and the temperature increase from frictional heating enhances further slip through dehydration embrittlement. The runaway nature of slip and availability of many sub-horizontal weak zones, together with the presence of water to lower the normal stress, make the condition nearly ideal for dynamic triggering.

iMush: The design of the Mount St. Helens high-resolution active source seismic experiment

E. Kiser[1], A. Levander[1], S. Harder[2], G. Abers[3], K. Creager[4], J.E. Vidale[4], S. Moran[5], S. Malone[4]

[1]Rice University, Department of Earth Science, edk2@rice.edu
[2]University of Texas at El Paso, Department of Geological Sciences
[3]Lamont-Doherty Earth Observatory
[4]University of Washington, Department of Earth and Space Sciences
[5]USGS Cascades Volcano Observatory

Mount St. Helens is one of the most societally relevant and geologically interesting volcanoes in the United States. Although much has been learned about the shallow structure of this volcano since its eruption in 1980, important questions still remain regarding its magmatic system and connectivity to the rest of the Cascadia arc. For example, the structure of the magma plumbing system below the shallowest magma chamber under the volcano is still only poorly known. This information will be useful for hazard assessment for the southwest Washington area, and also for gaining insight into fundamental scientific questions such as the assimilation and differentiation processes that lead to the formation of continental crust.

As part of the multi-disciplinary imaging of Magma Under St. Helens (iMUSH) experiment, funded by NSF GeoPRISMS and EarthScope, an active source seismic experiment will be conducted in late summer 2014. The experiment will utilize all of the 2600 IRIS/PASSCAL/USArray Texan instruments. The instruments will be deployed as two 1000-instrument consecutive refraction profiles (one N/S and one WNW/ESE). Each of these profiles will be accompanied by two 1600-instrument arrays at varying distances from Mount St. Helens. Finally, one 2600-instrument array will be centered on Mount St. Helens. These instruments will record a total of twenty-four 500-1000 kg shots. Each refraction profile will have an average station spacing of 150 m, and a total length of 150 km. The stations in the arrays will be separated by ~1 km.

A critical step in the success of this project is to develop an experimental setup that can resolve the most interesting aspects of the magmatic system. In particular, we want to determine the distribution of shot locations that will provide good coverage throughout the entire model parameter space, while still allowing us to focus on regions likely to contain the magmatic plumbing system. In this study, we approach this problem by calculating Fréchet kernels with dynamic ray tracing.

An initial observation from these kernels is that waves traveling across the largest offsets of the experiment (~150km) have sensitivity below depths of 30km. This means that we may be able to image the magmatic system down to the Moho, estimated at ~40 km. Additional work is focusing on searching for the shot locations that provide the most information about very shallow features beneath Mount St. Helens, such as the first magmatic reservoir at about 3 km depth, and the associated Mount St. Helens seismic zone. One way in which we are guiding this search is to find the shot locations that maximize different measures of the eigenvalue spectra of the approximate Hessian that is formed from the Fréchet kernels from each shot/station pair.

ObsPy: A Python Toolbox for Seismology

Lion Krischer[1], Tobias Megies[2], Robert Barsch[3], Moritz Beyreuther, and Joachim Wassermann[4]

[1] Department of Earth and Environmental Sciences, Ludwig-Maximilians-Universität München, krischer@geophysik.uni-muenchen.de
[2] Department of Earth and Environmental Sciences, Ludwig-Maximilians-Universität München, megies@geophysik.uni-muenchen.de
[3] EGU Office, barsch@egu.eu
[4] Department of Earth and Environmental Sciences, Ludwig-Maximilians-Universität München, jowa@geophysik.uni-muenchen.de

Python combines the power of a full-blown programming language with the flexibility and accessibility of an interactive scripting language. Its extensive standard library and large variety of freely available high quality scientific modules cover most needs in developing scientific processing workflows.

ObsPy extends Python's capabilities to fit the specific needs that arise when working with seismological data. It a) comes with a continuously growing signal processing toolbox that covers most tasks common in seismological analysis, b) provides read and write support for many common waveform, station and event metadata formats and c) enables access to various data centers, webservices and databases to retrieve waveform data and station/event metadata.

In combination with mature and free Python packages like NumPy, SciPy, Matplotlib, Pandas, IPython and PyQt, ObsPy makes it possible to develop complete workflows in Python, ranging from reading locally stored data or requesting data from one or more different data centers via signal analysis and data processing to visualization in GUI and web applications, output of modified/derived data and the creation of publication-quality figures.

All functionality is extensively documented and the ObsPy Tutorial and Gallery give a good impression of the wide range of possible use cases. ObsPy is well tested and running on Linux, OS X and Windows and comes with installation routines for these systems. ObsPy is developed in a test-driven approach and is available under the LGPLv3 open source licence.

Users are welcome to request help, report bugs, propose enhancements or contribute code via either the user mailing list or the project page on GitHub.

Towards validation of new explosion source models: Properties of structure and source at the Source Physics Experiment (SPEs)

Carene Larmat, Howard J. Patton, Charlotte A. Rowe, Esteban Rougier, David Yang, LANL

How do explosions produce S-waves? In order to gain a better understanding of the generation and propagation of seismic energy from underground explosions for hard rock media, the U. S. Department of Energy has funded a series of chemical tests on the National Nuclear Security Site (NNSS) as part of the Source Physics Experiment (SPE). To date, three such tests of yields 100, 1000, and ~900 kg have been conducted in the same borehole. Waveforms have been recorded on five linear geophone lines extending radially from ground zero and having offsets from 100 to 2000 m with station spacing of 100 m. Our team at LANL is working on developing models of the velocity structure and the source to explain the azimuthal variations of P-wave arrival times, and phase velocity, geometrical spreading and attenuation properties of high-frequency Rg waves. Attenuation of Rg waves has been measured with a spectral domain method, and the results are consistent from one test to the next along all five lines. 1D velocity models were derived from combined analyses of P-wave travel times and Rg dispersion curves. 2D ray-tracing was performed to fit arrival times when 1D models failed to match observations. We find that a near-surface, thin, weathered layer of varying thickness and low wave speeds plays a major role on the observed waveforms. For example, travel time analysis indicates a general thickening of low wave speed layers north of the shot point with higher topography. This basin-like structure is consistent with amplification of Rg waves and the observation of weak Rg amplitude decay. Full waveform modeling will be performed to validate this interpretation. Scalar moments of the source have been estimated from Rg amplitudes and show (1) consistent results despite very different path attenuation properties along five different azimuths; (2) agreement with RDP measurements and moment tensor inversion results; and- (3) agreement with the source volume scaling of Denny & Johnson (1991; AGU Monograph, #65).

Full-3D Waveform Inversions for Earthquake Source Parameters and Crustal Structure Model in Southern California

[1]En-Jui Lee, [1]Po Chen, [2]Thomas H. Jordan, [2]Philip J. Maechling, [3]Marine Denolle,

[3]Gregory C. Beroza

[1]Department of Geology and Geophysics, University of Wyoming

[2]Department of Earth Sciences, University of Southern California

[3]Department of Geophysics, Stanford University

We apply a unified methodology for seismic waveform analysis and inversions to Southern California. To automate the waveform selection processes, we developed a semi-automatic seismic waveform analysis algorithm for full-wave earthquake source parameters and tomographic inversions. The algorithm is based on continuous wavelet transforms, a topological watershed method, and a set of user-adjustable criteria to select usable waveform windows for full-wave inversions. The algorithm takes advantages of time–frequency representations of seismograms and is able to separate seismic phases in both time and frequency domains. The selected wave packet pairs between observed and synthetic waveforms are then used for extracting frequency-dependent phase and amplitude misfit measurements, which are used in our seismic source and structural inversions.

To reduce source errors in our full-wave tomographic inversion, we developed a full-wave earthquake source inversion algorithm and applied it to earthquakes in Southern California. The procedure relies on the use of receiver-side Green's tensors (RGTs), which comprise the spatial-temporal displacements produced by the three orthogonal unit impulsive point forces acting at the receivers. Synthetic seismograms for earthquakes in our study area can be simply and rapidly calculated by extracting a small, source-centred volume from the RGT database and applying the reciprocity principle. We have developed a multiple grid-search method based on Bayesian inference for finding optimal focal mechanisms and locations. Preliminary comparison with the CMT solutions provided by the Southern California Seismic Network (SCSN) shows that our solutions generally provide better fit to the observed waveforms.

Our full-wave waveform tomography uses the 3D SCEC Community Velocity Model Version 4.0 as initial model, a staggered-grid finite-difference code to simulate seismic wave propagations. The sensitivity (Fréchet) kernels are calculated based on the scattering integral and adjoint methods to iteratively improve the model. We use both earthquake recordings and ambient noise Green's function data, stacking of station-to-station correlations of ambient seismic noise, in our waveform tomographic inversions. To reduce errors of earthquake sources, the epicenters and source parameters of earthquakes used in our tomographic inversion are inverted by our full-wave CMT inversion method. Our current model shows many features that relate to the geological structures at shallow depth and contrasting velocity values across faults. The velocity perturbations could up to 40% with respect to the initial model in some regions and relate to some structures that do not exist in the initial model, such as southern Great Valley.

The earthquake waveform misfits reduce over 65% and the ambient noise Green's function group velocity delay time variance reduce over 80% when compared with those at the initial stage.

Seismic Window Selection on Large Dataset

W. Lei[1], E. Bozdag[2], J. Smith[3], M. Lefebvre[4], J. Tromp[5]

[1]Princeton University, lei@princeton.edu
[2]Princeton Univeristy, bozdag@princeton.edu
[3]Princeton Univeristy, jas11@princeton.edu
[4]Princeton Univeristy, ml15@princeton.edu
[5]Princeton Univeristy, jtromp@princeton.edu

FLEXWIN, which works on a pair of simulated and observed seismograms, is a time window selection tool for making seismological measurements, such as cross-correlation traveltime delays or frequency-dependent phase and amplitude anomalies. To use this powerful tool for adjoint tomography on a global scale, we need a new preprocessing strategy due to the volume of the dataset. The new version of FLEXWIN, which utilizes the Adaptive Seismic Data Format (ASDF) instead of the traditional SAC format, meets I/O challenges on large high-performance computing platforms and is suitable for fast parallel processing. In addition, FLEXWIN is tuned to select windows for different types of earthquakes. To capture their distinct features, we categorize earthquakes by their depths and frequency bands. Moreover, instead of only picking phases between the first P arrival and the surface-wave arrivals, the new version of FLEXWIN is capable of incorporating many other later prominent phases. For example, in the body-wave band (17 s - 60 s), we include SKS, sSKS and their multiples in our measurements, while in the surface-wave band (60 s - 120 s) we add major-arc surface waves.

Seismic tomography and interferometry: from shallow to deep

F. Lin[1], V. Tsai[1], R. Clayton[1], and B. Schmandt[2]

[1] California Institute of Technology, Seismological Laboratory, linf@caltech.edu, tsai@caltech.edu, clay@gps.caltech.edu,
[2]University of New Mexico, Department of Earth & Planetary Sciences, bschmandt@unm.edu

Seismic waves propagating through the earth's interior provide important constraints for studying earth structure. Recently, large-scale seismic array deployments have promoted the development of new data analysis methods. Surface-wave tomography, which uses surface waves to determine crustal and upper mantle structure, and seismic interferometry, which extracts waves traveling between two stations by cross-correlating long duration noise signals, are among the many exciting research areas. In this presentation, two major forefronts of seismic tomography and interferometry research based on USArray data will be discussed. On the shallow end, I will present recent developments in using surface-wave phase velocity and Rayleigh-wave particle motion to determine shallow earth velocity and density structure. By including Rayleigh-wave particle motion, upper crustal structure, which is traditionally not resolvable, can now be constrained and shows clear correlation with known surface geological features. On the deep end, I will show how deep-propagating body waves, particularly core phases, traveling between stations can be extracted using seismic interferometry. These new developments are likely going to provide new opportunities to improve our understanding of earth structure.

High-resolution array imaging based on numerical simulations

Q. Liu, P. Tong and P. Basini

Department of Physics, University of Toronto, Toronto M5S1A7, Canada

With the proliferation of both permanent and transportable seismic arrays, high-resolution and robust regional images have been generated based on unique array processing techniques, including the noise-correlation functions (NCFs) and the stacking/inversion of scattered/converted waves of teleseismic phases. In this study, adjoint tomography methods, which rely on optimization techniques and numerical computation of forward and adjoint wavefields, are adapted to take advantage seismic array recordings.

We first show the improved models of southern California crust based on NCFs of regional seismic stations, utilizing an exisiting 3D crustal model as the starting model. Sensitivity kernels for Greens functions are computed fully numerically by the spectral-element methods (SEM), and model update is sought as a linear combination of `event kernels'. The preliminary inversion reveals a even slower lower-crust in the Mojave desert region, thanks to the depth sensitivity of NCFs.

For seismic coda waves, A hybrid method that interfaces frequency-wavenumber (FK) calculations for 1D background models, with an SEM numerical solver, is developed to calculate synthetic responses of 2D/3D local media to plane-wave incidence. This hybrid method accurately deals with local heterogeneities and discontinuity undulations, and presents an efficient tool for the forward modelling of teleseismic coda waves. Sensitivity kernels for teleseismic coda waves are then computed by interacting the forward teleseismic waves with an adjoint wavefield, produced by injecting coda waves as adjoint sources. We illustrate various synthetic tests, designed for discontinuity characterization and volumetric structural inversion in the crust or subduction zones. It is shown that using preconditioners based upon the scaled product of sensitivity kernels for different phases, combining finite-frequency traveltime inversion and waveform inversion, and adopting hierarchical inversions from long- to short-period waveforms can reduce the non-linearity of seismic inversion and speed up the recovery of heterogeneities.

Notes on the Variability of reflected core-phases

Dunzhu Li[1], Daoyuan Sun[2,1], Don Helmberger[1]

1 California Institute of Technology, Seismological Laboratory 252-21, Caltech, Pasadena, CA 91125
2 University of Southern California, Department of Earth Sciences, Los Angeles, CA 90089

Recent events beneath central America have produced excellent sets of core phases recorded by USArray ranging from 18 to 30 degrees. However variation in core-phase amplitudes displays considerable scatter with factors of 6 or more, which is well known from other studies. Here, we process both data and simulations attempting to establish the relationship between travel-time variation, waveform complexity, and amplitude using a Multi-path detector analysis. The scatters may exist at different depths, such as crust, upper mantle, Core Mantle Boundary (CMB), and Inner Core Boundary (ICB). If we want to obtain information about the CMB and ICB, the contribution of scatters in the crust and upper mantle must be removed. By analyses on the synthetics for the models with random heterogeneities in the upper mantle, we found that stacking over 2 °bins smoothed out the upper mantle contribution and recovered the deep structure. Another way to minimize the upper mantle effect is to compare the amplitude ratio between the same stations for the neighboring events. The large variations across the array directly reflect the variations at ICB or CMB. We applied these two approaches to the PcP and PKiKP data and identified candidate for anomalies at CMB and ICB.

Numerical Study of Fault Zone Heterogeneity: Scaling and More

Yingdi Luo[1], Jean-Paul Ampuero[1]

[1]California Institute of Technology, luoyd@gps.caltech.edu

Following Hillers et al (2006, 2007), we considered vertical strike-slip faults with non-uniform spatial distribution of critical slip distance (Dc), although larger (500 km long, 20 km deep seismogenic zone) and adopting a realistic value of the radiation damping coefficient. Our initial models were dominated by characteristic earthquake behavior, instead of producing events with a broad range of magnitudes. We note that previous simulations by Hillers et al were over-damped to save computational resources, at the expense of blurring the distinction between aseismic transients and seismic slip events. We hence carried out a systematic parametric study in order to determine the ranges of Dc values that lead to non-characteristic behavior. For different combinations of minimum and maximum Dc values on a fault we simulated multiple earthquake cycles with a total duration long enough to characterize the general behavior of the fault: characteristic (regularly repeating events that break the whole fault), non-characteristic (events with a range of magnitudes, in most cases with a complex but repeating pattern), aseismic transients and steady slip. We found that non-characteristic behavior in this model occurs only over a narrow range of Dc distribution. Guided by these results, we successfully adjusted the 3D model to generate complex sequences of seismic events with magnitudes ranging from M6 to M8.2. Our current synthetic catalog contains over 10,000 events, mostly M7 and larger. We will also show results of scaling relations of the synthetic events.

Validation of 3D Seismic Models: finite-frequency or ray theory?

M. Maceira[1], C. Larmat[2], R. Porritt[3], D. M. Higdon[4], R. M. Allen[5]

[1]Los Alamos National Laboratory, Earth and Environmental Sciences, mmaceira@lanl.gov
[2]Los Alamos National Laboratory, Earth and Environmental Sciences, carene@lanl.gov
[3]UC Berkeley, Department of Earth & Planetary Science, rob@seismo.berkeley.edu
[4]Los Alamos National Laboratory, Statistical Sciences, dhigdon@lanl.gov
[5]UC Berkeley, Department of Earth & Planetary Science, rallen@seismo.berkeley.edu

Since the beginning of tomography studies in the 1970s, geoscientists have mastered the art of inferring an image of the underground solid Earth from a collection of observables recorded at the surface. In particular and for the last years, the National Nuclear Security Administration (NNSA) has been focusing on addressing the Earth's 3D heterogeneities and complexities toward high-resolution 3D seismic models in programmatic areas. The goal is to improve the accuracy of event location, which is critical to detection of evasive nuclear tests at regional scale. However it is difficult to assess how reliable seismic source parameters estimates are when using these velocity models. Resolution tests are typically used to assess uncertainty but they intrinsically assume that the imaging theory used is accurate and thus only provide information on the data coverage. In the last years, new horizons have opened up in earth structure imaging, with the advent of new numerical and mathematical methods in computational seismology and statistical sciences. We are combining the high-performance computing resources at Los Alamos National Laboratory with these newly applied to seismology methods to start tackling the question of geophysical model validation and uncertainty quantification.

We present results from a study focused on validating 3D models for the Western USA - Dynamic North America (DNA) models - generated using both ray-theoretical and finite-frequency methods. We evaluate model performances by comparing observed and synthetic seismograms generated using the Spectral Element Method, which is emerging as the primary method for high-accuracy modeling of the full waveform propagation. Initial results based on statistical tests upon the misfits, show that both, finite-frequency and ray-theoretical DNA09 models, predict the observations well. Waveform cross-correlation coefficients show a difference in performance between models obtained with the finite-frequency or ray-theory limited to smallest periods (<15s), with no perceptible difference at longer periods (50-200s). At those shortest periods, and based on statistical analyses on S-wave phase delay measurements, finite-frequency shows an improvement over ray theory. We use random sampling to identify regions where synthetic seismograms computed with the ray theory and finite frequency models are most different. We also investigate the resolution of the imaging techniques in terms of the model parameterization.

SCEC Unified Community Velocity Model: Development Goals and Current Status

P. Maechling[1], D. Gill[1], P. Small[1], G. Ely[2], R. Taborda[3], and T. Jordan[1]

[1]University of Southern California ([maechlin,davidgil,patrices,tjordan]@usc.edu)
[2]Argonne National Laboratory (gely@anl.gov)
[3] Carnegie Mellon University, Civil and Environmental Engineering (rtaborda@cmu.edu)

The SCEC Unified Community Velocity Model (UCVM) is a software framework designed to help researchers use 3D velocity models in ground motion simulations. The UCVM software enables researchers to perform consistent comparisons between alternative velocity models for the same region, such as the two southern California 3D velocity models CVM-S and CVM-H. The UCVM software provides two significant new capabilities: (1) the ability to query Vp, Vs, and density from any standard regional California velocity model through a uniform interface, and (2) the ability to combine multiple velocity models into a single state-wide model. These features are crucial in order to support large-scale ground motion simulations and to facilitate improvements in the underlying velocity models.

UCVM supports several existing California velocity models including SCEC CVM-H, SCEC CVM-S and the CVM-SI variant, USGS Bay Area (cencalvm), Lin-Thurber Statewide, and other smaller regional models. New models may be easily incorporated as they become available. UCVM provides two query interfaces: (1) a Linux command line program, and (2) a C application programming interface (API). The C API query interface is simple, fully independent of any specific model, and MPI-friendly. Input coordinates are geographic longitude/latitude and the vertical coordinate may be either depth or elevation. Output parameters include Vp, Vs, and density along with the identity of the model from which these material properties were obtained.

In addition to access to the standard velocity models, UCVM also includes a high-resolution statewide digital elevation model, Vs30 map, and an optional near-surface geo-technical layer (GTL) based on Ely's Vs30-derived GTL. The elevation and Vs30 information is bundled along with the returned Vp,Vs velocities and density, so that all relevant information is retrieved with a single query. When the GTL is enabled, it is blended with the underlying crustal velocity models along a configurable transition depth range with an interpolation function.

Multiple, possibly overlapping, regional velocity models may be combined together into a single state-wide model. This is accomplished by tiling the regional models on top of one another in three dimensions in a researcher-specified order. A post-processing tool is provided to perform a simple numerical smoothing.

Spectral-Element Simulations and Source Solutions for the May 20, 2012, Po Valley Main Shock

F. Magnoni[1], E. Casarotti[1], A. Cirella[1], A. Michelini[1], I. Molinari[1], A. Morelli[1], A. Piersanti[1], J. Tromp[2]

[1]Istituto Nazionale di Geofisica e Vulcanologia, federica.magnoni@ingv.it
[2] Princeton University, Department of Geosciences and Program in Applied & Computational Mathematics

On May 20, 2012, an M_w 5.9 earthquake shook the Po Valley region (North Italy) and started a seismic sequence of several M5+ events. The zone is characterized by a large sedimentary basin, a significant presence of fluid and strong heterogeneities, leading to remarkable site effects and liquefaction phenomena. Recent studies in literature present different values of M_w and M_0 for the May 20 main shock, ranging within [5.6;6.2] and [0.31;2.23]x10^{25} dyne*cm, respectively. These different solutions have been obtained from seismic source inversions that are based upon different layered wave speed models and that use observed waveforms recorded by different set of stations.

Here we present both synthetic tests and source inversions with recorded seismograms, using a moment tensor inversion technique presented by Liu et al. (2004) and based upon a Spectral-Element Method (SEM). We analyze the variability of the moment tensor solutions depending on the wave speed models and the dataset adopted in the inversion procedure. The considered seismic stations include receivers of the Italian National Seismic Network (INSN), the Italian national accelerometric network (RAN) and the OGS (North Italy) network. The SEM simulations take into account the main structural discontinuities, high-resolution topography, different laterally homogeneous layered wave speed models or a detailed 3D regional model that has been derived from both seismological and geological information in the region.

FIGURE CAPTION
Snapshot of the propagation of seismic waves generated by the May 20, 2012, earthquake in North Italy. The simulation has been performed using the SEM code SPECFEM3D_Cartesian with a 3D wave speed model and a kinematic seismic source from geodetic and seismological data inversion. Red and blue colors denote positive and negative values of the vertical-component velocity wavefield. The view is from the NE.

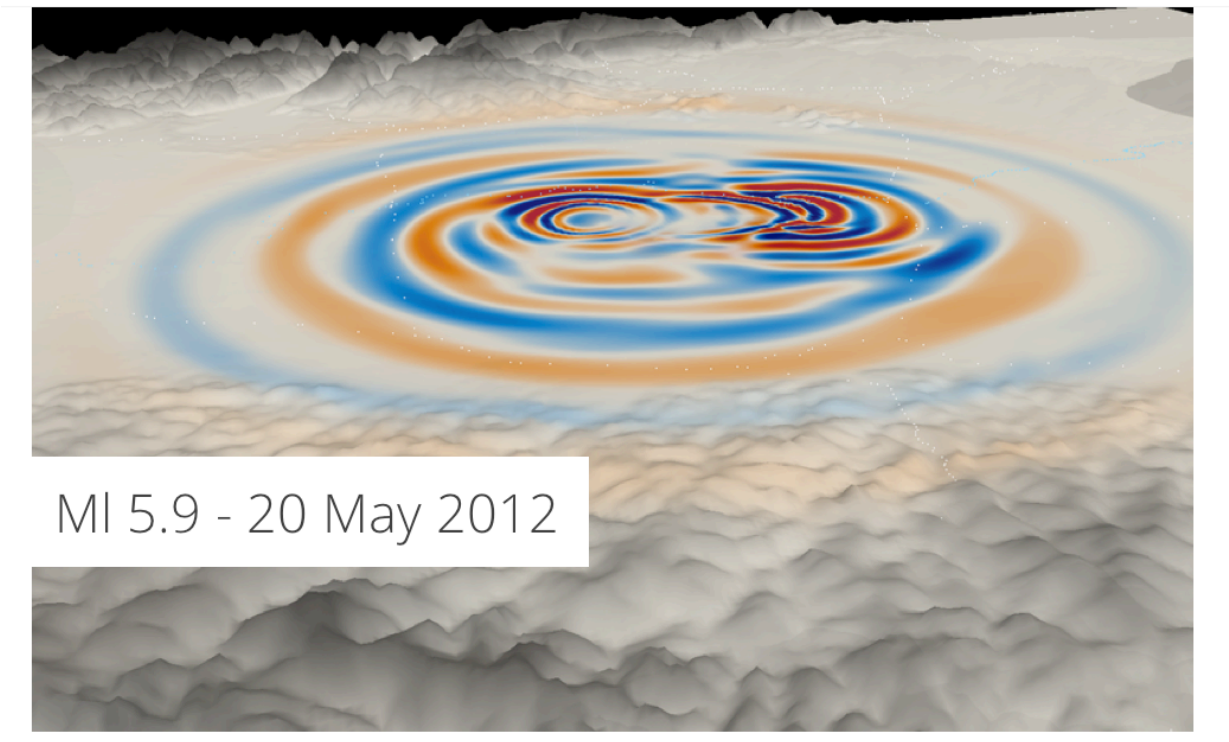

Alternative misfit functions for Full Waveform Inversion of surface waves

I. Masoni*(1,2), R. Brossier(1), J. Virieux(1), & J.L. Boelle(2)

[1]Université Joseph Fourier, Grenoble
[2]TOTAL S.A. Exploration & Production, Pau
*isabella.masoni@ujf-grenoble.fr

Surface waves are often the dominant signal in a seismic record, and can contain information on the geological properties of the medium through which it propagates. Applications considering 1D models have taken advantage of the dispersive property of surface waves to obtain velocity profiles of the subsurface from the inversion of dispersion curves. Surface waves are used at the near surface scale, down to a few tens of meters, such as in civil engineering, as well as on a much larger scale in global seismology to provide information on the Earth's eigenmodes and internal structure.

However for oil and gas exploration, a more intermediary scale of subsurface imaging, surface waves are traditionally treated as noise, too complex to analyse and not containing information about the target reservoir depth. Over the years sophisticated techniques have been developed to eliminate them from seismic data, both during acquisition and processing steps. Yet for land and shallow marine acquisitions, topography and weathered or unconsolidated top layers can lead to a very complex near surface. In such environments the presence of surface waves superimposed on the P and S waves coming from target depth, can make classical seismic processing very challenging, and knowing near surface velocity properties to correct for heterogeneities may be critical to successfully image the deeper lying targets.

This study aims to explore the use of surface waves using a Full Waveform Inversion (FWI) approach as an alternative to overcome the 1D limitations of conventional surface wave analysis. FWI is a high-resolution technique, used to derive quantitative models of the subsurface by matching the full observed seismogram with a synthetic seismogram calculated from an estimated velocity model. The misfit between the observed and calculated datasets is minimized as the model is updated, until a minimum is reached. The difference-based L2 norm, classically used in FWI and sensitive to both amplitude and phase information, suffers from cycle-skipping and local minima. For slow surface waves travelling in the near surface, the problem of cycle-skipping is even greater due to their small wavelengths. In the absence of low frequencies, convergence may not be possible when starting from a smooth initial model.

This study aims to investigate the advantages and limitations of alternative misfit functions to overcome this problem and improve the convexity of the inverse problem, allowing the use of less accurate initial models. Taking the difference-based L2 norm as a basis for comparison, simple synthetic sensitivity tests using layered models are conducted to evaluate difference and cross-correlation based misfits of data in in various domains such as the (tau-p), (omega-p) and (omega-k) domains. Furthermore a singular value decomposition approach is also investigated as a way to obtain a misfit. The results of this study show that alternative misfits may allow to improve the well-posedness of the problem, and give promising perspectives for using robust FWI to image near-surface targets.

Investigating Elastic Anisotropy of the Leech River Complex, Vancouver Island using Finite Frequency Kernels

Gian Matharu[1], Michael Bostock[1], Nikolas I Christensen[1], Jeroen Tromp[2], Daniel Peter[3]

[1]University of British Columbia, Department of Earth, Ocean and Atmospheric Sciences, gmatharu@eos.ubc.ca
[2]Princeton University, Department of Geosciences
[3]ETH Zurich, Institute of Geophysics

The Leech River Complex (LRC) of southern Vancouver Island is a part of a once continuous belt of Cretaceous sandstone, mudstone and volcanics that formed an accretionary wedge along the northwestern margin of North America. Metamorphism at 50 Ma to prehnite-pumpellyite, greenschist, amphibiolite and blueschist faces produced pervasive foliations with strong phyllosilcate lattice preferred orientations.

In this study we seek to gain further understanding on the nature of anisotropy within the LRC using high signal to noise ratio low frequency earthquake (LFE) templates and 3-D simulations from the spectral element method (SEM). The LFE templates represent empirical Green's functions generated by thrust mechanism, point sources and lie along a surface between 27 and 37km depth that is inferred be the plate interface of the subducting oceanic crust, immediately underlying the LRC. The SEM modeling employs a regional mesh that incorporates realistic topography, bathymetry and a 3-D tomographic P-wave velocity model of southern Vancouver Island. It allows us to readily simulate wave propagation in general anisotropic media with up to 21 independent elastic constants.

In order to characterize anisotropy we use an observable known as the Chevrot splitting intensity. We adapt the approach of Siemenski et al (BSSA, 2008) that enables us to generate finite frequency kernels using adjoint methods and analyze the sensitivity of splitting intensity to perturbations in elastic parameters. An initial isotropic model is iteratively updated by minimizing the least squares misfit between observed and synthetic splitting intensities. By employing the finite frequency kernels and the anisotropic model we hope to constrain the orientation and distribution of anisotropy within the LRC.

Investigating faults using seismic interferometry

E. Matzel

Lawrence Livermore National Laboratory, matzel1@llnl.gov

Seismic interferometry has proven to be a powerful method for imaging the Earth's interior. To date, much of the work in seismic interferometry has used ambient noise correlation, which isolates the seismic energy between pairs of seismometers. This has resulted in sharp images of the crust and upper mantle, particularly in areas with dense seismic networks. Curtis et al. (2009) demonstrated that we can reverse the geometry of the problem to focus instead on the energy between pairs of earthquakes. The Virtual Seismometer method (VSM) involves correlating the coda of pairs of events recorded at individual stations and then stacking the results to obtain an estimate of the Green's function (EGF) between the two sources. By effectively replacing each earthquake with a "virtual seismometer" recording all the others, VSM isolates the portion of the data that is sensitive to the source region and significantly improves our ability to see into tectonically active features. VSM is proving to be a powerful method for studying individual earthquakes and the source region.

In this study, we focus on a region in Southern California which has thousands of precisely located earthquakes (Hauksson, et al. 2011). We use synthetic methods (SPECFEM and WPP) to develop and refine the methodology, particularly focusing on the effects of source geometry. We then apply VSM to explosions from the Salton Seismic Imaging Project. The exact size, location and timing of those explosions allows us to define the resolution of the method against real data. Finally we use data from well located earthquakes to investigate the Imperial Fault and Brawley Seismic Zone. When the two earthquakes are roughly in line with the path to the recording instruments, VSM obtains a good estimate of the Green's function along the path between them, modified by the source parameters. As the line between the events falls off the azimuth to the recorders, VSM diverges more from the true GF, but still provides a measure of the source region.

Using this technique, we are able to recover the EGF between pairs of earthquakes, relocate the earthquakes in time and space, measure the source-time function and source magnitude, and finally image the structure along the path between them.

Application of Seismic Array processing to Earthquake Early Warning

L. Meng[1*], R. Allen[1] and J-P. Ampuero[2]

[1]Berkeley Seismological Laboratory, U.C.Berkeley. meng@seismo.berkeley.edu
[2]Seismological Laboratory, California Institute of Technology.

Earthquake early warning (EEW) system is essential in mitigating seismic hazard by issuing warnings prior to the arrival of strong ground shaking during an earthquake. Many of the currently operating EEW systems work on the basis of magnitude-amplitude/frequency scaling for a point source, which saturates for large events such as the 2011 Tohoku-Oki earthquake. Here, we explore the concept of characterizing rupture dimensions in real time for EEW using clusters of dense seismic arrays located near an active fault. Back tracing the waveforms of earthquake recorded by such arrays allows the estimation of the rupture size, duration and directivity in real-time, which enables the early warning of M > 7 earthquakes. The concept is then demonstrated with the 2004 Parkfield earthquake recorded by the UPSAR array and the 2010 El Mayor-Cucapah earthquake recorded by the San Diego strong motion array. We proposed to deploy such small-scale arrays every 30km along the San Andreas Fault. The optimal aperture and geometry is also investigated by balancing the array waveform coherency and resolution limits. We also analyses the bias of rupture size estimation due to the effect of dipping structures beneath the array. The cost of such system can be significant reduced by using recently developed low-cost accelerometers.

Global finite-frequency surface-wave tomography

T D Mikesell[1], S Voronin[1], G Nolet[1], J Ritsema[1]

[1]Globalseis, Géoazur, Université de Nice Sophia-Antipolis, CNRS, IRD, Observatoire de la Côte d'Azur, dmikesell@geoazur.unice.fr, svoronin@geoazur.unice.fr, nolet@geoazur.unice.fr, jritsema@umich.edu

In recent years, seismic velocity models of the mantle have been created using combinations of long period surface-wave dispersion data, teleseismic body waveforms and travel times, and normal modes. Most models are based on ray-theoretical methods to minimize the computational burden. Although the large-scale features are robustly determined, finite-frequency theory is needed to constrain smaller structure at the Fresnel zone scale. It is our ultimate goal to incorporate finite-frequency theory into the tomographic solution for all data types. In this presentation we will focus on the influence of finite-frequency effects on the Rayleigh wave tomography. We use the updated van Heijst and Woodhouse (1999) Rayleigh wave phase-velocity dispersion data set which contains 20 million measurements of minor- and major-arc fundamental mode and higher-mode dispersion data. We compute isotropic shear wave velocity perturbations to the isotropic PREM reference model, using wavelets to compress the size of the tomographic problem. We show the differences in the tomographic solutions between models that do and do not account for phase conversion and mode coupling during scattering, which is known to occur at shorter periods. We show our wavelet approach and discuss the implications of our results on future finite-frequency tomographic problems based on combined data sets.

SHAKE-IT: realistic earthquakes scenario simulations in Northern Italy

I. Molinari[1], A. Morelli[1], A. Berbellini[1], A. Argnani[2], P. Basini[3], P. Danecek[1]

[1]Istituto Nazionale di Geofisica e Vulcanologia, molinari@ingv.it
[2] Istituto di Scienze Marine – Centro Nazionale delle Ricerche (CNR), Bologna, Italy
[3] University of Toronto, Department of Physics, Toronto, Canada.

Realistic calculation of seismic ground motion even in locally complex geologic structures is becoming a wide spread tool to contribute to hazard and risk assessments. Well-tested numerical techniques and current generations of numerical codes are easier to use — thanks to community resources such as SPECFEM — and high-performance computing infrastructures are becoming widely accessible. The limit to how well we can model real ground motion is clearly in the fidelity of the representation of the Earth structure. We apply numerical deterministic methodologies to the Po Plain in Northern Italy — a region with relatively rare earthquakes but having large property and industrial exposure. The destructive effects and high community cost of the M~6 events of May 20-29, 2012, showed the need and urgence to provide more accurate estimates of possible ground shaking in a region where known hazardous seismicity must be sought up to five or more centuries ago, or inferred on palaeo-seismological ground. The Po Plain is characterized by a deep sedimentary basin that covers a bedrock folded and fractured by compressional structures, imaged by the extensive surveys carried out for more than two decades for hydrocarbon exploration. Local amplification effects of the wavefield can be quite significant and need to be taken into account in detailed seismic hazard assessment. To provide a representation of this structure, appropriate for our target, we implement a new high-resolution, three-dimensional model, merging information coming from seismic tomographic studies, with high-resolution constraints deriving from exploration profiles, and geological information — applying geostatistical techniques. The model is then calibrated through test numerical simulations made for the ~20 moderate-magnitude events of the region, for which adequate instrumental records are available. Through comparison between simulated and recorded seismograms, model validation and tuning will allow to adjust the most significant parameters — such as extension of sedimentary basins, velocity profiles in sediments, Vp/Vs, attenuation model — to provide better fit (Kaeufl et al., 2013). This model 'tuning' stage will differ from classical gradient-based linearized inversions, that result in smoothed models even when done fitting the full waveform. We plan then to use the new model for calculation of seismic scenarios in the region.

AxiSEM: High-frequency global wavefields for forward and inverse modeling

T. Nissen-Meyer[1], M. v. Driel[1], S. Staehler[2], K. Hosseini[2], S. Hempel[3], A. Fournier[4]

[1] ETH Zurich, Institute of Geophysics, Switzerland, tarjen@earth.ox.ac.uk
[2] Ludwig-Maximilians-University Munich, Germany
[3] University of Muenster, Germany
[4] IPG Paris, France

We present a numerical method for 3D global seismic wave propagation (AxiSEM) and its diverse range of applications. The method assumes axi-symmetry and thereby collapses the computational domain to 2D while analytically evaluating the azimuthal dimension. This dimensional reduction allows for high-frequency simulations of 3D wavefields even on moderate clusters. The method includes anisotropy, attenuation, and finite sources of arbitrary radiation pattern. Various applications of forward modelling, especially at high frequencies, will be discussed such as once-and-for-all forward solutions, lowermost mantle structures or inner-core anisotropy. Resultant wavefields can also be used for time- and frequency-dependent waveform sensitivity kernels, i.e. a comprehensive and quantitative link between seismogram and Earth structure and the basis for global waveform tomography. The method furthermore serves as a foundation for scattering approaches, i.e. honouring 3D background structure honouring weak scattering such as required for Born/Rytov approximations. The presentation will cover the scientific motivation and basis for a hands-on tutorial based on the methodology.

Anti-waveguide effects in Pacific slab: evidence from high-frequency waveform analysis and numerical modeling

S.Padhy, T. Furumura and T. Maeda
Earthquake Research Institute, The University of Tokyo

There have been many studies on travel time seismic tomography to investigate the velocity structure of the subduction zones in the Pacific plate beneath the Japanese islands. Obayashi et al. (2009), based on teleseismic P-wave tomography, have shown the absence of slab-related velocity anomalies due to bending or tearing of the subducting Pacific slab at the junction between the Japan and Izu-Bonin arcs. On the other hand, Kennett and Furumura (2010), using seismic waveforms, have observed slab tear at the junction between Honshu and Kuril arcs. To corroborate the tomographic evidence for slab tear, we studied the detailed lateral structure of the subducting Pacific plate near Honshu by analyzing waveforms from deep earthquakes recorded at fore-arc Hi-net network and F-net broadband stations in Japan. Such waveforms explain the low-frequency ($f < 0.25$ Hz) precursors followed by high-frequency ($f > 2$ Hz) energies with long coda due to the multiple scattering and diffractions of seismic waves in the stochastic waveguide of the Pacific slab (Furumura and Kennett, 2005). However, recent analysis shows that for some particular source-receiver paths, the waveforms exhibit loss of high frequency energy in P-coda, high attenuation, loss of low-frequency precursor and presence of converted phases in P-coda for deep earthquakes occurring in the subducting Pacific plate. Such complexities in the observed waveforms are difficult to explain due to the radiation pattern of P- and S-waves and/or by anomalous propagation of seismic waves in existing plate model, indicating sudden lateral change in the wave guiding properties of the subducting slab, such as expected to be caused by the thinning or tearing the slab in deeper part representing anti-waveguide properties of the slabs.

To explain the observations, we employ two-dimensional finite-difference method (FDM) simulations of complete high-frequency P-SV wave propagation taking thinning of the Pacific slab into account. The model is represented by 5000 x 5000 grid points using a uniform grid size of 0.15 km. We use a parallel FDM simulation technique to conduct such large-scale 2-D simulations. The FDM simulation uses a staggered-grid 16^{th} order scheme in space and 2^{nd}-order accuracy in time. Random heterogeneity is introduced into the plate model through an anisotropic form of stochastic distribution described by a von Karman correlation function with elongated structures with a longer correlation length of 10 km in horizontal direction and much

shorter correlation length of 0.5 km in depth and standard deviation from background P- and S-wave velocities of 5% following the study of Furumura and Kennett (2007).

We expect that the observed guided wave energy must decouple from waveguide where the slab is deformed or thin. Low frequency energy leaks out of the slab and travels to the receivers along paths in the low-velocity and low-Q mantle surrounding the slab, while high frequency signal of shorter wavelength can travel through thin plate. The results of this study, along with the evidence for weak velocity anomaly as inferred from seismic tomography (Obayashi et al., 2009) and observations of slab tear in the Pacific plate (Kennett and Furumura, 2010) as mentioned earlier, we expect a local velocity anomaly or thinning in the oceanic lithosphere along the junction between Izu-Bonin and Honshu arc. It is necessary to examine these effects further with a 3D FDM simulation for different slab geometries and source depths, which is ongoing.

References

T. Furumura and B. L. N. Kennett, *J. Geophys. Res*. **110**, B10302, doi:10.1029/2004JB003486 (2005).

B. L. N. Kennett and T. Furumura, *Phys. Earth Planet Int.* **180**, 52-58 (2010).

M. Obayashi, J. Yoshimitsu, and Y. Fukao, *Science.* **324**, 1173-1175 (2009).

Rapid CAD and tetrahedral mesh generation for dynamic rupture problems

Christian Pelties[1], Cameron Smith[2], Gudmundur Heimisson[2], Stefan Wenk[1], Alice Gabriel[1]

[1]Dept.of Earth and Environmental Sciences, LMU Munich, Germany, pelties@geophysik.uni-muenchen.de
[2]Scientific Computation Research Center, Rensselaer Polytechnic Institute, NY, USA, smithc11@rpi.edu

The modeling of seismic wave propagation coupled to earthquake faulting will increases our understanding of earthquake source physics and enables realistic scenario simulations for seismic risk analysis and preparedness purposes. The accuracy and reliability of such simulations depend on the quality of the numerical approximation of the underlying physics and the geological model representation. Today, wave propagation can be modeled by many methods accurately and efficiently on large scale high-performance infrastructure, e.g. Dumbser et al. (2006), Cui et al. (2010), Peter et al. (2011) among others. Incorporating the co-seismic frictional sliding process is more challenging and necessitates either certain numerical properties of a solver, or the introduction of additional damping to suppress the generation of spurious oscillations. In particular, the rupture evolution is highly sensitive to the geometrical shape of the fault face, whereat rough, kinked or branching faults may radiate high frequency waves.

Thus, an accurate representation of the geological underground model, topography, bathymetry and fault planes are crucial for dynamic rupture simulations. Besides modern homogenization approaches (Capdeville et al. 2010) or a very fine sampling of the material background (possible e.g. with FD methods), numerical methods implemented on unstructured meshes are widely used in order to respect material interfaces and topography. However, for very complex geometries the mesh and preceding CAD model generation can be very time-consuming task and represent a bottleneck in the workflow: Assembling a satisfying CAD model that can be used to obtain a high quality mesh may require weeks to months of expert work.

Here, we will try to bring up new ideas for automated CAD model generation. The ultimate goal is to assemble a geological model including topography, faults and material interfaces from the raw data (e.g. point clouds from gocad, DEM data) with as less user interaction as possible. The final model must be 'watertight' in order to be discretized correctly. Faults, which potentially intersect geological layers, are usually not enclosing volumes naturally and can therefore be described as floating faces. Thus, an important feature for the CAD and mesh generation is the support of non-manifold geometries.

Although the CAD models could be used in principle by any meshing software, we will demonstrate a workflow using the mesh generator Simmodeler (by Simmetrix). Our Simmodeler version produces high quality tetrahedral meshes and is customized to the needs of SeisSol, a high-order accurate ADER-DG method (http://seissol.geophysik.uni-muenchen.de/). Additional to the CAD and mesh generation workflow linked to SeisSol, we will demonstrate that the ADER-DG algorithm is well suited for complex dynamic rupture simulations supported by latest benchmark results as well as scenario simulations based on the 1994 Northridge and 2011 Tohoku earthquakes.

References:

M. Dumbser and M. Käser. An arbitrary high order discontinuous Galerkin method for elastic waves on unstructured meshes II: The three-dimensional case. *Geophys. J. Int.*, 167(1):319–336, 2006.

Y Cui, K B Olsen, T H Jordan, K Lee, J Zhou, P Small, D Roten, and G Ely. Scalable Earthquake Simulation on Petascale Supercomputers. (November):1–20, 2010.

D. Peter, D. Komatitsch, Y. Luo, R. Martin, N. Le Goff, E. Casarotti, P. Le Loher, F. Magnoni, Q. Liu, C. Blitz, T. Nissen-Meyer, P. Basini, and J. Tromp. Forward and adjoint simulations of seismic wave propagation on fully unstructured hexahedral meshes. *Geophys. J. Int.*, 186(2):721–739, 2011.

Capdeville, Y**.** Guillot, L. and J. J. Marigo. 2D nonperiodic homogenization to upscale elastic media for P-SV waves. *Geophys. J. Int.*, Vol 182, pp 903-922, 2010.

Three Dimensional Simulation of Far-Field Ground Motion from Source Physics Experiment Using a Hydrodynamic-to-Elastic Coupling Technique

Arben Pitarka, Robert J. Mellors, Oleg Y. Vorobiev, Arthur J. Rodgers, William R. Walter, Tarabay Antoun, Anders Petersson, Bjorn Sjogreen, Eric Matzel and Jeff Wagoner

Lawrence Livermore National Laboratory, Livermore, CA 94551 USA

Monitoring of nuclear explosions typically relies on distant recordings where the effects of non-linear near-source processes are combined with path-specific propagation effects, such as complex scattering, causing difficulties in extracting source properties from available waveform data. Therefore understanding the effects of wave scattering in the source region where the material response is non-linear as well as in the far-field where the material response is linear is crucial for studying the excitation of seismic energy during underground explosions as well as developing empirical source models. Ground motion recorded during the Source Physics Experiment (SPE) at near-field and far-field stations provided an excellent opportunity for understanding the excitation and propagation of seismic waves from underground explosions. We used three–dimensional hydrodynamic simulations, including non-linear rheology of the near-source material, coupled with elastic wave propagation to model SPE ground motion recorded at far-field stations. The simulations were used to extract seismic source characteristics and investigate near-source wave propagation effects. Near-source motions were computed with GEODYN-L, a Lagrangian hydrodynamic code for modeling the response of a well-characterized granite to explosion loading. Explosion generated ground motions were passed to WPP, an anelastic finite-difference code, through a coupling approach using various three-dimensional velocity models with specified material heterogeneities. Our physics based modeling results were analyzed to separate complex non-linear effects near the source from various along path wave propagation scattering effects due to topography and material heterogeneity in the source region. In particular, we focused on the contribution of these effects to S-wave generation.

Adjoint Waveform Tomography of the Middle East

Christina Morency[1], Daniel Peter[2], Brian Covellone[3], Brian Savage[3], Arthur Rodgers[1], Jeroen Tromp[2]

[1] Lawrence Livermore National Laboratory, Livermore, CA 94551, USA

[2] Princeton University, and

[3] University of Rhode Island

The Middle East is a tectonically diverse and active region including strike-slip, continental collision and ocean spreading plate boundaries as well as stable continental and oceanic regions. In order to better characterize moderate-sized (M<5) seismic events at regional distances (<2000 km) using full waveform based techniques, there is a need for a three-dimensional (3D) wave speed model to accurately predict short period waveforms (2 to 30 s). Effects of 3D lithospheric structure, including, attenuation and anisotropy are critical at these periods. We are using adjoint waveform tomography to image 3D structure of the crust and upper mantle. Our study area covers Turkey and the Red Sea to the Hindu Kush and Indian subcontinent (west-to-east) and the Afar Triangle and Arabian Sea to the Kazakh Platform (south-to-north). The present model parameterization accounts for a transversely isotropic model with a vertical axis, which facilitates simultaneous fitting of Rayleigh and Love waves. Using an adjoint technique (following Tape et al., 2010 and Zhu et al., 2012) we effectively invert for four parameters - bulk sound wave speed, vertically and horizontally polarized shear wave speeds and a dimensionless parameter. Forward and adjoint calculations are performed using the spectral-element package SPECFEM3D_Globe developed and maintained by CIG. Currently we have performed 13 iterations using body-wave windows (14-30 s periods) and surface wave windows (24-120 s periods). Major tectonic features have been imaged, such as low wavespeeds beneath the Red Sea, Arabian Shield and Turkish-Iranian Plateau and high wavespeeds beneath the Arabian Platform and Zagros Mountains (consistent with continental collision). We expect to refine details as we add additional data and include more short-period energy into the inversions. Our ultimate goal is to improve the predictive capabilities of the current 3D wave speed model of the Middle East to 2 s, with a final model including 3D anelastic attenuation and anisotropy.

Data

Low velocities in the oceanic upper mantle and their relation to plumes: insights from SEM-based waveform tomography

B.Romanowicz[1,2,] Scott French[1], Ved Lekic[3]

[1]Berkeley Seismological Laboratory, U.C. Berkeley, barbara@seismo.berkeley.edu
[2]University of Southern Collège de France, Paris, France.
[3]Department of Geological Sciences, University of Maryland

The advent of 3D numerical seismic wavefield computations is beginning to bear fruits in seismic tomography, particularly as it enables better resolution of regions of lower than average velocity, which otherwise can be hidden by wavefront healing effects. Inspection of the oceanic part of our latest global tomographic model, SEMum2, developed using waveform inversion and the spectral element method, confirms the presence of a well marked shear wave low velocity zone beneath the lithosphere, with a velocity minimum which deepens progressively as a function of age of the plate, and reaches values that are lower than in previous tomographic global models and in agreement with local estimates where available. Interestingly, reaching below this "classical" low velocity zone, the model reveals a pattern of alternating lower and higher velocities organized into elongated bands in the direction of absolute plate motion (APM).

This fingerlike structure, strongest around 200-250 km and extending down to 350-400 km, is most prominent beneath the Pacific plate, but also present under the eastern Antarctic plate, in the south Atlantic and in parts of the Indian ocean. The wavelength of the fingers in the direction perpendicular to the APM, is on the order of 2000 km, consistent with the scaling predicted from laboratory experiments on Rayleigh Taylor instabilities. Below this depth, the low velocities appear organized into several vertically coherent "conduits", the most prominent under Hawaii and the Pacific superswell, where they appear to be rooted in the lower mantle. These conduits have complex shapes, in particular, the one associated with Hawaii undulates as it "rises", and is deflected towards the ridge as it reaches the bottom of the "fingering" layer. Individual hotspots do not lie immediately above the conduits but in their general vicinity. Nor are the fingers always associated with prominent hotspots.

This morphology in the top 400 km of the oceanic mantle suggests the presence of a complex dynamic interplay between secondary convection, return flow from the plate driven flow just below the lithosphere, and influx from the deep plume conduits.

Imaging with the Generalized Radon Transform: a review of the theory and applications

Stéphane Rondenay[1]

[1]University of Bergen, Department of Earth Science, rondenay@geo.uib.no

Over a decade ago we developed a new teleseismic migration approach to take full advantage of the densely sampled broadband seismic datasets starting to become available at the time. The approach considers the generation of scattered waves when 3-D teleseismic wavefields interact with 2-D lithospheric structure. The backprojection operator is cast as an inverse Generalized Radon Transform (GRT) that reconstructs scattering potentials from the forward- and back-scattered wavefields, with the backscattered wavefields arising from free-surface reflections of the incident wave. The inversion solves for material property perturbations (mainly Vs and Vp) relative to a smoothly varying background model. Since its inception, the 2-D GRT inversion has been applied successfully (and sometimes unsuccessfully) to many datasets spanning a range of tectonic environments. It appears particularly well suited to investigating the structure and dynamics of subduction zones, where sharp velocity contrasts associated with variations in composition and/or fluid content generate strong signals. In this presentation, I will give a review of the theory, applicability and resolving power of the 2-D GRT inversion. I will illustrate the strengths and weaknesses of the approach through a series of examples, and discuss the dynamical inferences that can be drawn from 2-D GRT images through applications to the Alaska subduction zone.

Full Wavefield Inversion's Impact on the Upstream Business

Partha Routh, David McAdow, Spyros Lazaratos, Jerry Krebs and Dave Hinkley

Upstream Research Company, ExxonMobil, Houston, USA

Full Wavefield Inversion (FWI) capabilities have advanced rapidly during the past few years, resulting in many applications of FWI to upstream exploration, development and production problems. Recent applications indicate the value of high-fidelity subsurface property information obtained using FWI. The high-resolution model of the subsurface obtained from FWI permits us to generate synthetic seismic data that match recorded seismic data with a high degree of accuracy. FWI is capable of incorporating the full physics of elastic wave propagation, including arbitrarily complicated anisotropy and attenuation. Key impediments to broadly employing FWI have been its high computational cost and technical challenges such as avoiding local minima, estimating multiple parameters and overcoming acquisition limitations . Advanced algorithms for wave-propagation simulation and optimization coupled with faster computer architecture are beginning to overcome many of these technical obstacles, and FWI is beginning to make an impact on the upstream business. We also demonstrate some of our pioneering technology developments that make it possible to apply FWI to large-scale practical problems. We discuss how diverse skill sets such as geophysics, geology, computational science and applied mathematics contribute to a large-scale, high-impact project such as FWI. Overall we provide an industrial flavor of such research program.

Fault Structures and Stress Orientations from Moderate Earthquake Sequences and Relocated Seismicity in the Mina Deflection, Western Nevada-Eastern California

C. Ruhl[1,2], T. Seaman[1,2], and K. Smith[2]

[1]University of Nevada, Reno, Department of Geological Sciences and Engineering; cruhl@unr.edu, tseaman@unr.edu
[2]University of Nevada, Reno, Nevada Seismological Laboratory; ken@seismo.unr.edu

Deformation within the Walker Lane (WL) of Nevada and California, which accommodates 20-25% of relative Pacific-North American plate motion, includes normal faulting along the Sierran Range front; primarily dextral slip within the Eastern California Shear Zone, Central WL, and Northern WL; and sinistral and normal faulting within the Mina Deflection (MD). The MD, an ~50 km wide, ~100 km long zone of complex deformation is composed of numerous NE-ENE trending normal and sinistral faults that link the dominantly NW trending dextral faults of the Central and Southern WL. It functions as a right-stepping relay zone within a broader dextral shear zone, accommodating ~100 km of dextral offset, and has generated several M5+ earthquakes and extensive aftershock sequences. The mechanism by which dextral slip is transferred through the MD is complex; among proposed processes are transtensional block rotations, displacement transfer through closely spaced normal faults, and clockwise block rotations accommodating sinistral faulting. To understand the seismological aspects of the MD, we have relocated earthquakes from 1984 to present to identify active structures within the complex fault geometry. Small faults are active within the MD that do not correspond with mapped structures and seismicity tends to follow structural transitions that possibly represent stress concentrations. Notably, a dominant trend of seismicity appears to follow an important change in orientation of closely spaced faults between Mono Lake and the Queens Valley. We have compiled over 300 published and computed earthquake focal mechanisms including moment tensors from M > ~3.5 events and inverted these for principle stress orientations. Results show a consistent ENE striking extensional stress direction, smoothly evolving to a more E-W orientation westward, approaching the Sierran range front. Compressional axes vary widely in trend and plunge reflecting the overall transtensional environment. Inversion of USGS Quaternary fault data results in a more consistent E-W extensional stress axes orientation, while the principal strain axes from GPS (Corné Kreemer, personal communication) show more variability in both extensional and compressional axes orientations, including suggested compression in some areas. This may be a reflection of strain partitioning processes that characterize the MD. Crustal thicknesses are fairly well constrained within the MD. Fault orientations along with the stress and strain results provide additional constraints for modeling crustal deformation in this structural transition zone. We are interested in experimenting with codes that allow us to model various deformation and slip transfer mechanisms that may arise from this right-step within the broader WL dextral shear zone as well as flexural models of Sierran uplift and evolution of normal faulting along the eastern Sierra, which are other interesting structural transition zones in the WL.

Global Seismic Tomography Based on a Sensitivity Kernel Database

E. Sales de Andrade[1] and Q. Liu[2].

[1]University of Toronto, Department of Physics, esalesde@physics.utoronto.ca
[2]University of Toronto, Department of Physics, liuqy@physics.utoronto.ca

Seismic tomography is instrumental in determining 3D velocity structures of the Earth's interior based on measurements of travel-time anomalies and waveform differences. The computation of sensitivity kernels that link velocity anomalies to measurements made between data and synthetics is crucial in forming consistent global tomography problems. Although both ray theory and other asymptotic methods have been successfully employed in global tomography, they are less accurate for long-period waves or steep velocity gradients, and lack the ability to predict "non-geometrical" effects such as core diffracted phases (P_{diff}, S_{diff}) that are crucial for mapping heterogeneities in the lower-most mantle (D" layer). On the other hand, sensitivity kernels can be accurately calculated with no approximation by interactions of forward and adjoint wavefields, both numerically simulated by spectral element methods (SEM), which can be applied to full 3D background models. However, the formulation of the design matrix used in classical traveltime tomography is generally computationally unrealistic, as two simulations are required for each kernel between a source-receiver pair.

As global tomographic models exhibit perturbations under 10% in most regions, 1D reference models may still be used. In this study, by taking advantage of the symmetry of 1D reference models, we efficiently construct sensitivity kernels of both pressure and shear waves based on the storage of forward and adjoint strain fields for a few SEM simulations of selected source and receiver geometry. The symmetry enables us to reduce the storage of the full strain wavefield to just the equatorial plane (tens of MiB for kernels and a few GiB for strain fields of 20-s accuracy). This technique has been used to create a database of strain fields as well as sensitivity kernels for phases typically used in global inversions, including *P*, *S*, *PP*, *SS*, *pP*, *PcP*, *ScS*, P_{diff}, S_{diff}, surface waves, as well as boundary kernels for discontinuity-reflected phases such as *S660S*. Creating such a database enables fast and accurate interpretation of global seismic phases and will be applied to global tomographic inversions in the near future.

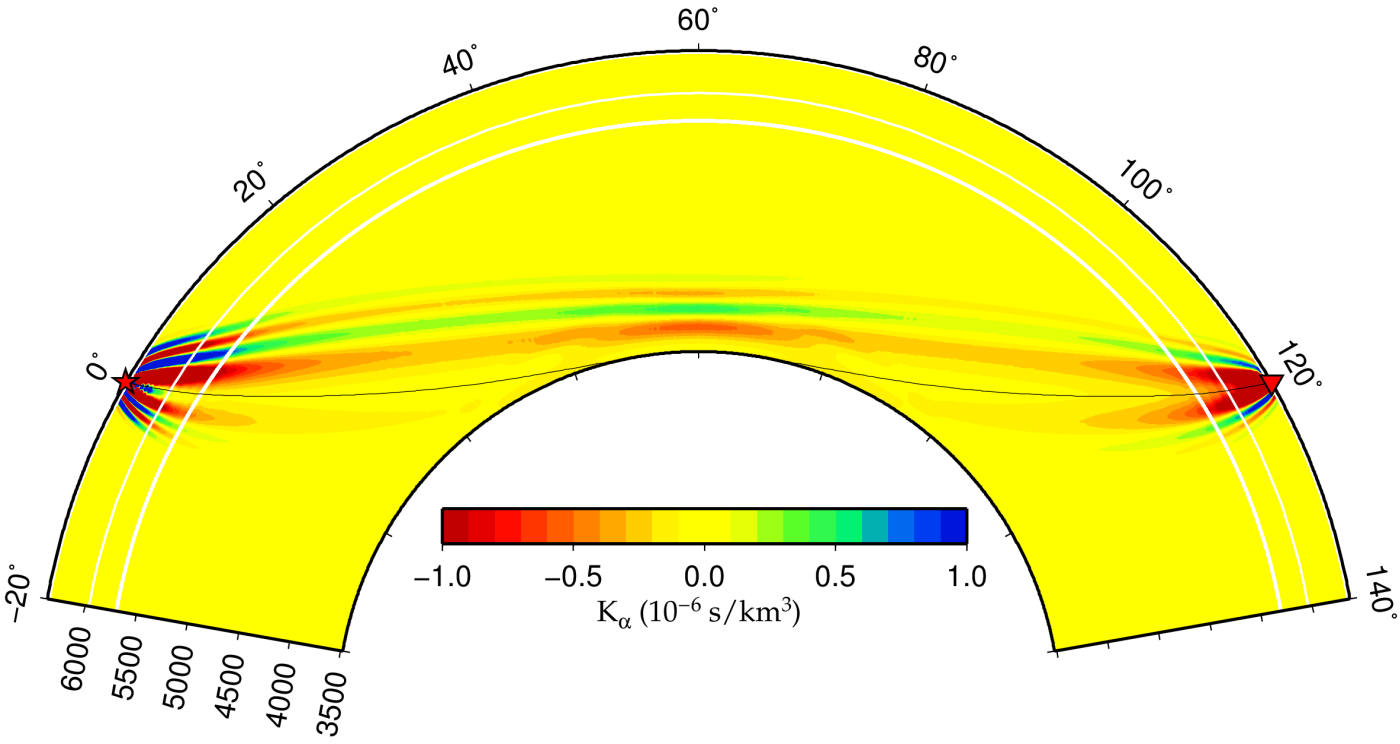

FIGURE: Example diffracted K_α travel-time kernel for an epicentral distance of 120º calculated using our method. Note the wide sensitivity as compared to the ray theory path, especially above the diffracted region.

Lithosphere Temperatures within the western United States

D. L. Schutt[1], A. R. Lowry[2], J. S. Buehler[3], and D. D. Blackwell[4]

[1]Colorado State University, Department of Earth Sciences, derek.schutt@colostate.edu
[2]University State University, Department of Earth Sciences, Tony.Lowry@usu.edu
[3]University of San Diego, Scripps Institution of Oceanography, buehlej@gmail.com
[4]Southern Methodist University, Huffington Department of Earth Sciences, blackwell@smu.edu

The evolution, deformation, and dynamics of the U.S. lithosphere are fundamentally connected to its temperature. This property ties surface processes to deep forces, affects the stability of cratonic lithosphere, and modulates the forces and strengths of deforming lithosphere (among many other things). Estimates of lithospheric temperature are challenging, however. Using heatflow to estimate geotherms is limited by uncertainty in the distribution of crustal heat production. Using upper mantle seismic velocity measurements is also challenging, because of uncertainty in the mapping between temperature and velocity--especially above roughly 900C, at which still poorly understood anelastic effects start to occur. A particularly useful measurement is Pn velocity, for two reasons. The first is that the depth at which the velocity is measured is well-constrained, compared to surface wave velocities. The second is that the temperature at the Moho is often below 900C, allowing one to use relatively well-known anharmonic velocity-temperature scalings. Using Pn-derived temperatures plus newly revised estimates of heatflow and shallow subsurface temperatures allows one to "pin" lithospheric geotherms at the near-surface and just below the Moho. In conjunction with a grid-search method that makes only very limited assumptions about the distribution of heat producing elements, we are able to place tight constraints on lithospheric geotherms in much of the western U.S. Where Pn velocities and surface heatflow mismatch, this suggests transient or horizontally-advective thermal processes, or compositionally modulated Pn velocity variations.

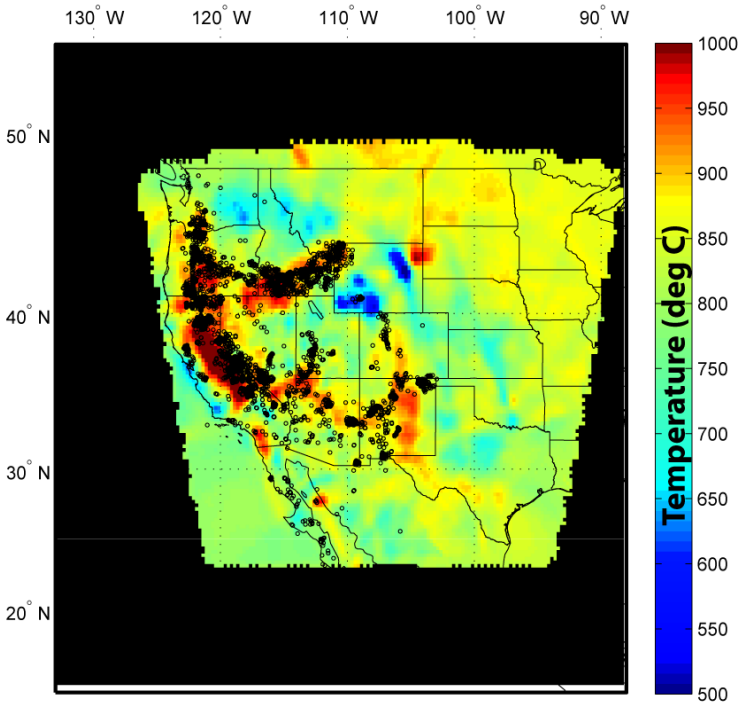

Preliminary map of temperatures at the base of the Moho calculated from Pn velocities (*Buehler and Shearer*, 2010 and subsequent work). Black circles indicate volcanism in the last 10 M.y., from the NAVDAT database.

Seismic moment tensor inversion: Sampling the posterior probability distribution

Vipul Silwal and Carl Tape

Geophysical Institute and Department of Geology & Geophysics, University of Alaska, Fairbanks
silwal@gi.alaska.edu, carltape@gi.alaska.edu

We perform a grid search to estimate moment tensors—with uncertainties—for earthquakes in southern Alaska, $M_w > 4$. The earthquakes are parameterized as double couple mechanisms, such that our five inversion parameters are four for the moment tensor (strike, dip, rake, M_w) and one for depth. Our inversion algorithm is based on the cut-and-paste method of Zhu and Helmberger (1996), which attempts to fit synthetic and observed waveforms for body wave and surface wave components separately by using different bandpass filters and allowing for different time shifts for effects of unmodeled three-dimensional (3D) structure. This misfit function is an unnormalized weighted L2 norm. The misfit function is completely evaluated within the 5-dimensional model space. For most earthquakes, the misfit function in this space is quite smooth, which causes challenges for quantifying the uncertainity and for generating moment tensor samples of the posterior probability density. We establish a scaling of the misfit function that generates 'reasonable' posterior samples, by which we mean that 95% of the posterior samples adequately fit the observations, while 5% do not. Figure 1 shows 20 posterior samples for one earthquake. Based on our posterior samples, we can express other statistical quantities, such as the variation in strike, dip, or rake. Our uncertainty estimates are considerably larger than those reported in the literature for the same technique. We have examined 20 earthquakes in detail and expect to complete a moment tensor catalog of 100 earthquakes in southern Alaska.

Future work will involve developing a 3D seismic velocity model for Alaska, which will then be used for simulation-based moment tensor inversions using 3D Green's functions. By reducing the time shifts that are applied during the moment tensor inversions, the 3D velocity model will reduce the occurrence of misaligned waveforms from data and synthetics.

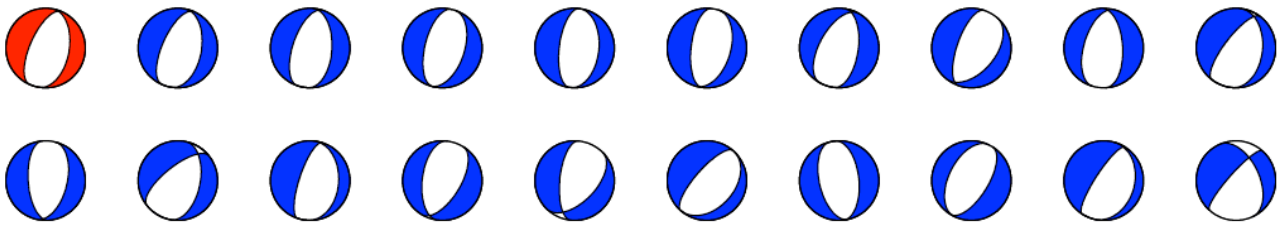

Figure 1. Twenty samples of the posterior probability distribution, sorted in order of decreasing misfit value. The sample in red is the best solution, the sample at the lower right is the worst solution, and the other samples show the range of permissible solutions. This is a M_w 4.5 earthquake near Anchorage, Alaska (eid 20090407201255).

The 2011 M9.0 Tohoku-Oki earthquake: a new challenge for multi-data finite-fault slip inversions.

A.Sladen[1], Q.Blétery[1], B.Delouis[1]

[1]Geoazur, University of Nice, France sladen@geoazur.unice.fr

The diversity and quality of data collected in the aftermath of 2011 M9.0 Tohoku-Oki earthquake offers a unique opportunity to investigate the details of its coseismic rupture. Many studies have taken advantage of the very dense on land strong-motion, broad-band and high-rate GPS networks. But resolution tests and the variability in the proposed solutions has highlighted the difficulty to uniquely resolve the slip distribution from networks with limited azimuthal coverage. This limitation is even more prononced in the case of Tohoku-oki earthquake with several measurements indicating very large motions at the distant trench (>200km away from the coast). But for the first time, tsunami data offer an almost complete azimuthal coverage of a large earthquake, and might alone provide a robust description of the source even at the trench.

In this study we present a serie of finite-fault slip inversions of the different aforementioned dataset (strong-motion, teleseismic, static GPS, continuous GPS and tsunami) to discuss their relative contribution. These inversions are performed using a 3D fault geometry allowing to take into account the extra level of complexity of the shallow portion of the megathrust. We show that this level of refinement is required to properly model both the sea-bottom deformation and the contribution of the bathymetry to the tsunami excitation. Our preferred slip model shows that almost the entire slip distribution occurred updip of the epicenter with a maximum of 65 m of slip decreasing to values of 30-50m at the trench. This model implies that the largest slip was not at the trench.

An Adapatable Seismic Data Format for High-Performance Computing

J. Smith[1], E. Bozdag[1], M. Lefebvre[1], J. Tromp[1]

[1]Princeton University, Department of Geosciences

The challenge of imaging the Earth's interior at the scale of the globe is closely linked to the challenge of handling large data sets. High-performance computing facilitates more accurate simulations of seismic wave propagation aimed at stronger constraints Earth structure. Generating higher resolution Earth models requires a vast amount of data that is beyond the capabilities of currently used techniques. In order to implement the workflow for global adjoint tomography on modern HPC systems, a new data format is being developed. ASDF, or adaptable seismic data format, is designed to replace currently used data formats with a more flexible format that allows for parallel IO. The metadata has been divided into abstract categories, such as event, receiver, simulation, and time-series data so that it is not tied to one specific format. The ADIOS library is used as an application programming interface (API) because it has demonstrated superior performance and scalability as compared to parallel NetCDF and parallel HDF5. The interfacing of ASDF with embarrassingly parallel processing scripts allows for an automated, efficient project workflow for global adjoint tomography.

High-resolution Data in Seismic Source Imaging

S. N. Somala[1]

[1]California Institute of Technology (Caltech), snsomala@gmail.com

Seismic source imaging is known to show significant disagreement across source inversion modelling groups both for real earthquakes as well as synthetic cases. The five published slip models for 1999 Izmit earthquake in Turkey had little resemblance with each other (Beresnev, 2003). The SPICE BlindTest exposed that even the source models no different from a random model can fit data quite well (Mai et al., 2007). Both these cases had scattered set of data spaced tens of km apart. Source inversion with such sparse datasets is severely non-unique and the subjective assumptions made to constrain this problem limits the extent of earthquake physics to be discovered from seismological data.

Unconventional earthquake observation systems are about to provide much finer spatial sampling (100's of meters) than the traditional seismometers. One such feasible system is a Geostationary Seismic Imager (GSI) that works on the principles of optical imaging (Michel et al., 2012). The low-cost MEMS-based sensors to be deployed as part of Community Seismic Network (CSN) can provide similar high-resolution data in urban areas (Clayton et al., 2012). In principle, such high-resolution data could enable source inversions with minimal or no assumptions, allowing the data to dictate how the rupture evolved. To demonstrate how the GSI measurements can revolutionize our understanding of earthquake sources, realistic earthquake scenarios are simulated. Physics-based models of earthquakes show complex features that may be resolved only using dense datasets. We investigate several such scenarios to determine what can be learned with feasible GSI designs. The scenarios address open questions in earthquake dynamics and recent intriguing seismological observations, and are also inspired by dynamic rupture simulations and laboratory observations. They include complexities such as multiple rupture fronts, apparent intersonic fronts and back-propagating fronts. It would be challenging for the current source inversion codes to handle the enormous amount of data dealt with in this study.

Probabilistic Seismic Source Inversion from teleseismic Body-waves

S. C. Stähler[1], K. Sigloch, R. Zhang[2], K. Hosseini-zad[1], H. Igel[1]

[1]LMU München, Geophysics, Earth and Environmental Sciences, München, Germany
staehler@geophysik.uni-muenchen.de
[2]Center for Mathematical Sciences, Technische Universität München, Germany

Large earthquakes and those in densely instrumented areas are now being studied in great detail and in extended-source frameworks like finite-fault or back-projection. However, smaller earthquakes (below M_W 7.5) and especially remote ones with sparse data coverage are still approximated best by a point source. For earthquakes larger M_W 5.5 it is generally possible to invert for the temporal evolution and describe it in the form of a moment rate or Source Time Function (STF).

A reliable STF is crucial for broadband waveform tomography. Its uncertainty is hard to quantify, especially since it is correlated with the estimated source depth, e.g. when surface-reflected phases are mapped into the STF. While the inversion for the STF and the moment tensor is linear, the depth inversion is inherently non-linear. Experience shows that data from shallow earthquakes can often be fitted well by several distinct depths. Therefore it is hard to linearise the inversion for the depth. We therefore propose a fully probabilistic inversion scheme for the Source Time Function, depth and moment tensor as follows:

1. To reduce the size of the model space, the STF is parametrized in empirical orthogonal functions. Those wavelets are derived from the results of a catalogue of deterministic source inversions. The STF can be described by 10 weighting factors of these wavelets.
2. As a misfit criterion we use the waveform coherence in the P- and SH-window. While it is not possible to derive an Likelihood distribution for this measure analytically, we use a large number of synthetic waveforms calculated with catalogue source solutions to find such a Likelihood function empirically.
3. Inter-station covariances are also estimated from the results of the deterministic catalogue.
4. The parameter space then has 16 dimensions, and is sampled with the Neighbourhood Algorithm, where synthetic waveforms are precomputed using a reflectivity code on the IASP91 mantle with local crust models from CRUST2.0. One forward solution takes around 0.1 CPU-seconds.

Exhaustive sampling of the model space requires around 10^5 forward solutions to be calculated, which takes less than one hour on a modern multi-core computer. The resulting ensemble offers more than just a best solution, but rather probability density functions for all parameters.

From those, pdfs of derived parameters like finite-frequency observables can be calculated, to correctly account for source uncertainties in a structural inversion.

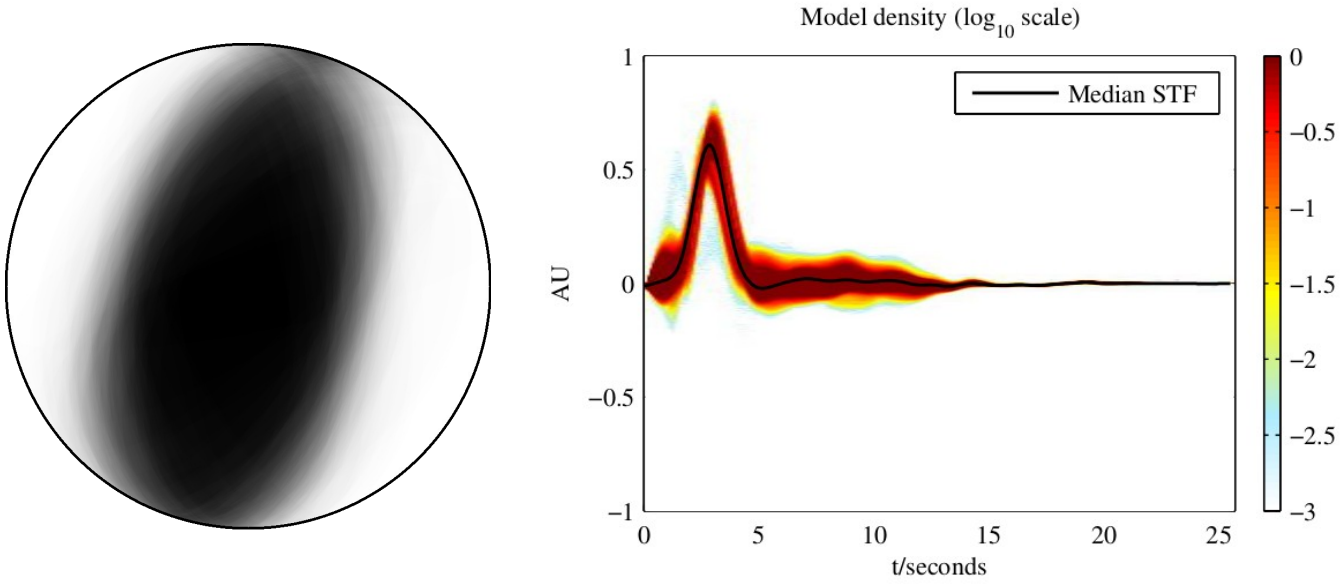

Fig. 1: Density of solutions for the focal mechanism (left) and the source time functions of the 23/08/2011 Virginia earthquake.

Comparative validation of a set of physics-based simulations of the 2008 Chino Hills earthquake using different velocity models

R. Taborda[1] and J. Bielak[2]

[1]Carnegie Mellon University, Department of Civil and Environmental Engineering, rtaborda@cmu.edu
[2]Carnegie Mellon University, Department of Civil and Environmental Engineering, jbielak@cmu.edu

We present a comparative validation of a set of simulations of the Mw 5.4 2008 Chino Hills earthquake that use different velocity models available for Southern California. The simulation models are tailored for a maximum frequency and a minimum shear wave velocity equal to 4 Hz and 200 m/s, respectively. We validate the ground motion synthetics from each simulation with data obtained from seismic networks on more than 300 recording stations, and compare the synthetic results from the models with each other and with observations in order to draw insights about each model's description of the crustal structure and geotechnical layers. The simulations are done using Hercules, the parallel octree-based finite-element earthquake simulator developed by the Quake Group at Carnegie Mellon University. The source model corresponds to that of an independent inversion study and it remains fixed for all simulations. The seismic velocity models used are the community velocity models developed by the Southern California Earthquake Center (CVM-S) and by SCEC's partners at Harvard University (CVM-H). In the case of CVM-H, we performed simulations for the two alternatives available with this model, namely with and without considering the Vs30-rule based geotechnical layers (GTL). Our results show significant dependency on the velocity models, with differences present at both low and high frequencies. The differences at the lower frequencies indicate that there exist distinctions in the way each model represents the crustal structures in the region, suggesting that the models need to be cross-referenced in the future. On the other hand, the differences at the higher frequencies suggest a strong sensitivity to the description of the shallower sedimentary deposits. The validation is done qualitatively and quantitatively. For the quantitative validation, we use a goodness-of-fit criteria (GOF) to characterize the quality of the match between synthetics and data. GOF results show the areas where each model leads to better results. In general, CVM-S results yield a better match than CVM-H, but in some areas, the results of CVM-H can improve significantly when considering the GTL option. Overall, our results indicate that, from a regional perspective, the simulation starts to deviate from the data at frequencies above 1 and 2 Hz. However, at some particular locations, the synthetics can still yield very good results at frequencies between 2 and 4 Hz. The best results are obtained with CVM-S between 0.1 and 0.25 Hz over the entire region, and up to 1 Hz with CVM-S and CVM-H+GTL within the major basins. While we understand that our results are particular to the event considered here, future similar studies may help guide the improvement of both seismic velocity and source models. This type of simulations also suggests that extending the maximum frequency of deterministic earthquake simulations is an effort worth pursuing.

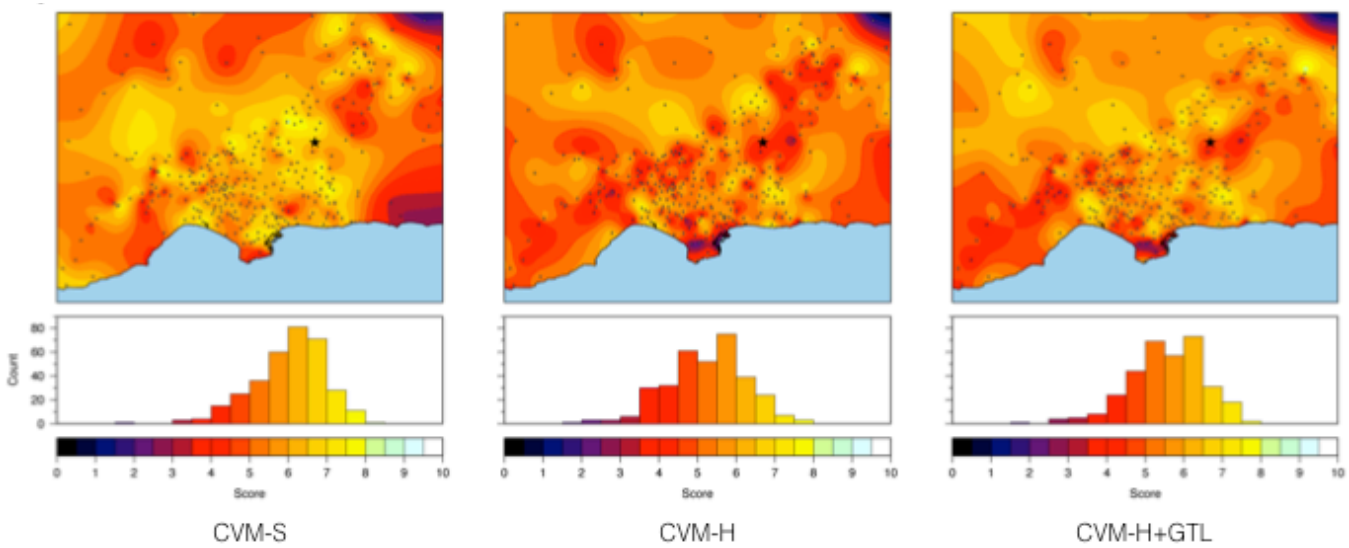

Comparison of the spatial distribution and histograms of the GOF scores obtained for the three simulation models up to 2 Hz.

A three-dimensional seismic velocity reference model for Alaska

Carl Tape

Geophysical Institute and Department of Geology & Geophysics, University of Alaska, Fairbanks
carltape@gi.alaska.edu

We assemble a catalog of moment tensors and a three-dimensional seismic velocity model for Alaska, in preparation for an iterative tomographic inversion using spectral-element and adjoint methods. The primary geometrical interfaces in the model are the Moho surface, the basement surface of major sedimentary basins, and the topographic surface. The Moho is constructed from existing data, including receiver functions, active source surveys, and gravity measurements. The crustal and upper mantle tomographic model is from Eberhart-Phillips et al. (2006), but modified by removing the uppermost slow layer, then embedding models for two major sedimentary basins. We compute 3D synthetic seismograms using the spectral-element method. We demonstrate the accuracy of the initial three-dimensional reference model by comparing 3D synthetics with observed data for several earthquakes originating in the crust and underlying subducting slab. Full waveform similarity between data and synthetics over the period range 4 s to 30 s provides a solid basis for an iterative inversion. The target resolution of the crustal structure is 4 km vertically and 16 km laterally. We use surface wave and body wave measurements from local earthquakes to obtain moment tensors that will be used within our tomographic inversion. Local slab events down to 180 km depth, in additional to pervasive crustal seismicity, should enhance resolution.

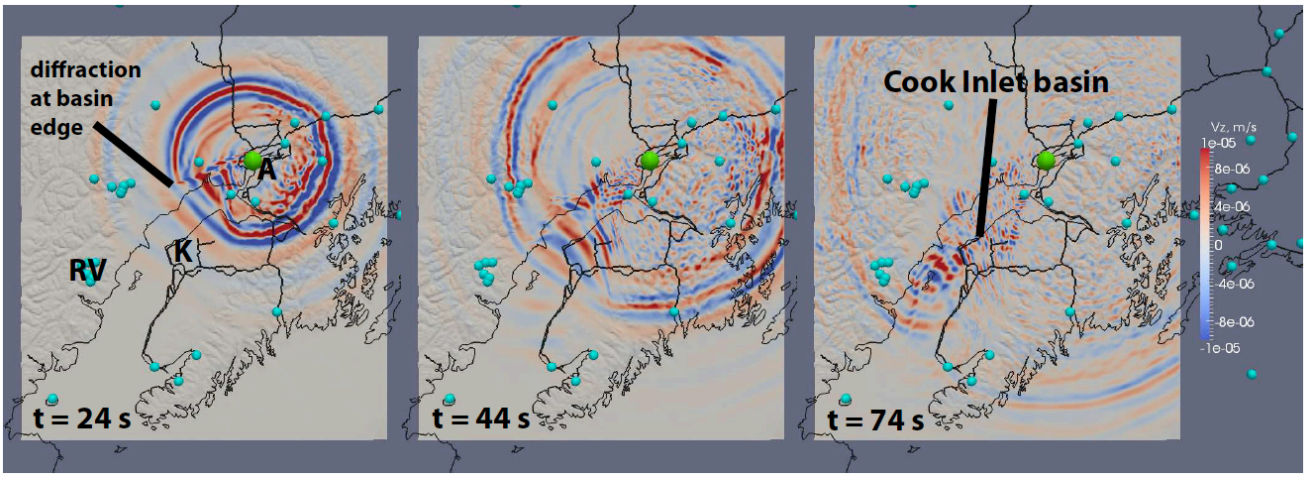

Figure 1: Snapshots of a 3D wavefield simulation, showing the strong influence of the Cook Inlet basin on the wavefield. Blue circles denote permanent broadband stations. A = Anchorage, K = Kenai, RV = Redoubt volcano.

Earthquake nucleation and triggering on an optimally oriented fault (Sumatra to Alaska)

Carl Tape, Michael West, Vipul Silwal, Natasha Ruppert

Geophysical Institute, University of Alaska, Fairbanks
carltape@gi.alaska.edu, mewest@alaska.edu, vsilwal@gi.alaska.edu, natasha@gi.alaska.edu

Seismic surface waves from large, distant earthquakes commonly trigger smaller earthquakes. However, delay times of hours to days between the surface waves and the triggered earthquakes weaken the causal connection. Furthermore, when there is no delay, the triggered earthquakes are typically too small or too obscured to obtain reliable source mechanisms. We present observations of instantaneous triggering of a strike-slip earthquake in central Alaska. Shear strain from the optimally aligned teleseismic Love wave induced a 24 s exponential foreshock signal leading to the triggered earthquake. This nucleation phase, and the alignment of the triggered earthquake source mechanism with the teleseismic stress field, reveal the behavior of an existing fault under well-calibrated strain conditions. The Alaska earthquake provides the first observation of combined nucleation and triggering, and it suggests that transient stresses during nucleation may influence the subsequent earthquake rupture. Laboratory and theoretical studies of nucleation and triggering may help discriminate between different interpretations for the Alaska earthquake.

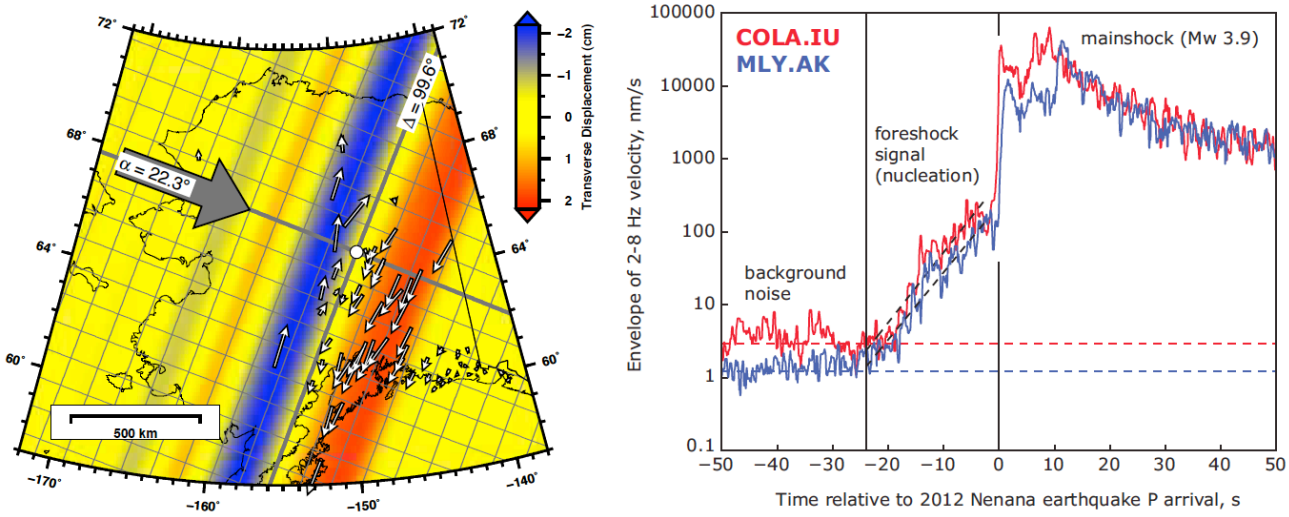

Figure 1: Nucleating and triggering a M_w 3.9 earthquake in central Alaska from Love waves of the April 11, 2012 M_w 8.6 Sumatra earthquake. (a) Horizontal displacement field in Alaska at the origin time of the M_w 3.9 Nenana earthquake in central Alaska. The epicenter of this event is marked by the white dot at the center of the thick gray lines. The large gray arrow denotes the wave propagation direction from Sumatra. The grid lines represent increments of 1° in α and 1° in Δ from the Nenana epicenter. (b) Envelope of velocity seismograms for two representative stations. The amplitudes are plotted on a log scale so that the noise level, foreshock signal, and mainshock are all visible. The linear slope of the foreshock signal represents an exponential growth in amplitude.

High-resolution seismic array imaging based on SEM-FK hybrid methods

P. Tong[1], C.W. Chen[2], P. Basini[1], Q. Liu[1]

[1]Department of Physics, University of Toronto, Toronto M5S1A7, Canada, tongping85@gmail.com
[2]Institute of Oceanography, National Taiwan University, Taiwan

Seismic coda waves (including converted and scattered waves) have been used extensively to image detailed structures beneath seismic arrays, based on methods such as receiver functions, Kirchhoff migration and generalized Radon transform (GRT). Utilizing the same coda waves, we show the feasibility of high-resolution seismic array imaging utilizing full numerical wave simulations. A hybrid method that interfaces frequency-wavenumber (FK) calculations, which provide semi-analytical solutions to 1D layered models, with a spectral-element (SEM) numerical solver, is developed to calculate synthetic responses of local media to plane-wave incidence. This hybrid method accurately deals with local heterogeneities and discontinuity undulations, and presents an efficient tool for the forward modelling of teleseismic coda waves. The accuracy of the SEM-FK hybrid method is benchmarked against FK solutions for 1D media. Sensitivity kernels for teleseismic coda waves are then computed by interacting the forward teleseismic waves with an adjoint wavefield, produced by injecting coda waves as adjoint sources, based on adjoint techniques. These sensitivity kernels provide the basis for mapping variations in subsurface discontinuities, density and velocity perturbations through non-linear conjugate-gradient methods. We illustrate various synthetic tests, designed for discontinuity characterization and volumetric structural inversion in the crust or in subduction zones. Synthetic tests show that using preconditioners based upon the scaled product of sensitivity kernels for different phases, combining finite-frequency traveltime inversion and waveform inversion, or adopting hierarchical inversions from long- to short-period waveforms can reduce the non-linearity of seismic inversion and speed up the convergence. The final results of these synthetic examples suggest that inversion of teleseismic coda phases based on SEM-FK hybrid methods and adjoint techniques may be a promising tool for structural imaging beneath dense seismic array.

Imaging Earth's Interior based on Spectral-Element and Adjoint Methods

Jeroen Tromp[1,2], Ebru Bozdag[1], Matthieu Lefebvre[1], Wenjie Lei[1], James Smith[1], Hejun Zhu[1]

[1]Department of Geosciences, Princeton University, jtromp@princeton.edu
[2]Program in Applied & Computational Mathematics, Princeton University

Harnessing high-performance computers and accurate numerical methods to better constrain physical properties of Earth's interior is rapidly becoming one of the most important research topics in exploration and global seismology. We use spectral-element and adjoint methods to iteratively improve 3D subsurface images ranging from exploration to global scales. The spectral-element method, a high-order finite-element method with the advantage of a diagonal mass matrix, is used to accurately calculate three-component synthetic seismograms in complex 3D Earth models. An adjoint method is used to numerically compute Frechet derivatives of a misfit function based on the interaction between the wavefield for a reference Earth model and a wavefield obtained by using time-reversed differences between data and synthetics at all receivers as simultaneous sources. In combination with gradient-based optimization methods, such as the L-BFGS method, we are able to iteratively improve 3D images of Earth's interior and gradually minimize discrepancies between observed and simulated seismograms. Various misfit functions may be chosen to quantify these discrepancies, such as cross-correlation traveltime differences, frequency-dependent phase and amplitude anomalies as well as full-waveform differences. Various physical properties of the Earth are constrained based on this method, such as elastic wavespeeds, radial anisotropy, azimuthal anisotropy, shear attenuation and impedance contrasts. We apply this method to study seismic inverse problems at various scales, from exploration-scale full-waveform inversion to global- and regional-scale seismic tomography.

The Virtual Earthquake and Seismology Research e-science Community in Europe: lessons and some identified challenges

Jean-Pierre Vilotte[1]

[1]IPG Paris & CNRS-INSU

The nature of science in seismology is changing – new discoveries will emerge from statistical analysis and modelling (inversion, assimilation) of the large amounts of complex data generated from dense observation networks and large-scale wave propagation simulations.

VERCE is a four years FP7-INFRASTRUCTURE project that started October 2011 with a consortium of ten partners. It is a contribution to the e-science infrastructure of the European Plate Observatory System (EPOS), the ESFRI initiative of the solid Earth community in Europe.

The aim of VERCE is to provide an e-science environment - enabling innovative data-intensive statistical analysis and modelling methods - built upon a service-oriented architecture and a platform of tools and services integrating European HPC and Grid infrastructures, private resources together with the seismology data archives.

We report here progress and experience of VERCE - after almost 2 years - focussing on selected data-intensive analysis and modelling use cases. We discuss lessons learned so far and some identified challenges.

Full waveform inversion: challenges

Amir Asnaashari∗ , Romain Brossier∗ , Michel Dietrich*, Stéphane Garambois∗ , Ludovic Métivier‡ , Stéphane Operto† , Alessandra Ribodetti† , Jean Virieux∗§

∗ ISTerre, Université Joseph Fourier Grenoble I & CNRS, France
† Géoazur, Université Nice-Sophia Antipolis, CNRS, IRD, Observatoire de la Côte d'Azur, France
‡ LJK & ISTerre, Université Joseph Fourier Grenoble I & CNRS, France

The dramatic increase of the seismic data both at the industrial and at the academic levels using thousands of sensors with an increasing illumination allows one to better image the Earth structure at all scales. Heterogeneities inside the Earth, especially for crustal structures, make the imaging challenging as we face difficulties at different levels.
Since the seminal article of Woodhouse & Dziewonski (1984) of waveform inversion (WI) for mantle imaging, full waveform inversion (FWI) has been introduced by Lailly (1983); Tarantola (1984) in the time domain for crustal targets and investigated by Pratt and Worthington (1990); Pratt (1990) in the frequency domain: it has demonstrated its capacity of recovering high-resolution seismic imaging in various geological contexts with the dramatic improvement of data acquisition systems. From the beginning, difficulties have been identified for converging to the expected solution as this non-linear optimization suffers from cycle-skipping problems (Choi and Alkhalifah, 2011). These problems could arise for various reasons related to the optimization itself, to the seismic data we consider and to the model structure we are looking for. Which data should we consider? How could we compawoodhousere observed and synthetic data? How to sample the model space through local versus global descriptions and/or through multi-scales? How precise should be the physics for estimating synthetics? What is the relative importance of the different model parameters in relation with the physics behind? Could we provide posterior uncertainty estimation on these recovered parameters? Many questions appear as the technique gains in maturity (Plessix, 2012).
The description of the investigated medium and of the prior information impacts drastically the optimization and the forward problem engine. Introducing progressively the complexity of the seismic data will avoid to be trapped into local solutions. At the end of the imaging procedure, we may question what is the meaning of the "full" prediction of the observed data.
Through few synthetic examples, we shall consider these different aspects of the seismic imaging procedure: the data and synthetics issue, the model issue and the optimization issue. A 2D section of the already complex elastic SEG overthrust model illustrated the difficulties when considering elastic propagations. A simple time-lapse target tracking will show the importance of the prior information (figure 1) while the BP model will illustrate the importance of Hessian estimation for improving convergence.

Figure 1: Time-lapse reconstruction (top panel) on a synthetic example using only smooth regularization making difference between images (left) or difference between data (right) for detecting two small reservoirs as shown in the middle panel (two left figures) while the last panel shows reconstruction using prior information as displayed on the right of the middle panel.

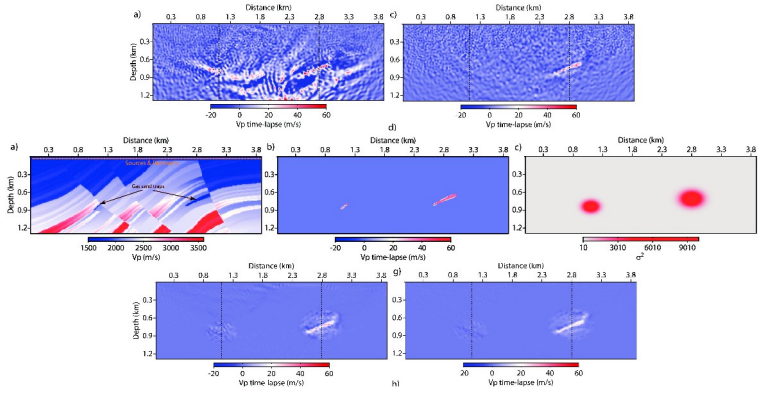

Application of the ADER-DG method to simulate Love waves in the ocean generated noise wave field

S. Wenk[1], C. Hadziioannou[2], C. Pelties[2], and H. Igel[2]

[1]Department of Astronomy, Geophysics, and Meteorology, Comenius University Bratislava
[2]Department of Earth and Environmental Sciences, Ludwig-Maximilians-Universität Munich

Noise correlations allow us to exploit the vast amounts of background noise recorded continuously around the world. The resulting high-resolution tomographic images of the past decade provides us with better event locations, better strong motion predictions and a deeper understanding of crustal dynamics. However, the potential of noise correlation techniques is not yet exhausted and could be further enhanced by an improved understanding of noise sources and their behaviour. While sources of the vertical component motion in microseismic Rayleigh waves are already widely studied, those for the horizontal shear motions in Love waves remain relatively unexplored. We will try to characterize and understand Love waves in ambient seismic noise, and their contribution to noise correlation methods.

In the so-called secondary microseismic band ambient noise is generated by a vertical excitation of pressure fluctuations in the water layer acting on the seafloor. On a plane fluid-solid interface this would only generate Rayleigh waves. Therefore, we want to focus in particular on possible mechanisms of Love wave generation.

To test different approaches, we employ realistic 3D noise simulations considering complex topography information, the fluid-solid contrast and an arbitrary number of noise sources using variable mechanisms and temporal evolutions. To this end, we apply the high-order ADER-DG method to produce reliable solutions of 3D wave propagation over long propagation distances. We will show first results of Love to Rayleigh wave energy distributions for 3D random material perturbations on top of a 1D background model of the oceanic crust. Furthermore, the difficulties in generating complex 3D modeling domains will be discussed.

Compressive sensing of great earthquake ruptures

Huajian Yao[1], Peter Shearer[2], Peter Gerstoft[2], Jiuxun Yin[1]

[1]University of Science and Technology of China, Laboratory of Seismology and Physics of Earth's Interior, hjyao@ustc.edu.cn
[2]University of California, San Diego, Scripps Institution of Oceanography

Investigations of rupture characteristics of great earthquakes from seismic and/or other geophysical data are important to understand the earthquake physics and for earthquake early warning. We use the compressive sensing (CS) technique (Yao et al., 2011) to systematically analyze the frequency-dependent along-dip and along-strike seismic radiation from recent great earthquakes. CS is a sparse-source inversion method with higher resolution than the conventional beamforming and back-projection approaches or super-resolution beamforming methods (e.g., MUSIC) in resolving two or multiple sources, in particular for transient earthquake signals.

For the subduction zone megathrust earthquakes, we resolve generally low-frequency radiation closer to the trench at shallower depths and high-frequency radiation farther from the trench at greater depths (Yao et al., 2013). The pattern of the along-strike seismic radiation is generally more complicated, reflecting substantial variability in the along-strike distribution of asperities and barriers on the fault plane. We also compare the frequency-dependent energy radiation to the spatial distribution of major co-seismic slip and the early aftershocks to infer the depth-varying frictional properties of subduction zone slab interfaces. Our results infer that the shallower portion of the slab interface (above ~15 km), which is frictionally stable or conditionally stable, is the source region for tsunami earthquakes with large coseismic slip, deficient high-frequency radiation, and few early aftershocks. The slab interface at intermediate depths (~15–35 km), which is the main unstable seismogenic zone for the nucleation of megathrust quakes, typically has large coseismic slip, abundant early aftershocks, and intermediate- to high-frequency radiation during megathrust rupture. The deeper portion of the slab interface (~35–45 km) is seismically unstable, however with small coseismic slip, dominant high-frequency radiation, and relatively fewer aftershocks.

For the 2012 Mw 8.6 Sumatra strike-slip earthquake, our CS results resolve four different rupture stages with complicated frequency-dependent along-strike seismic radiation patterns. This earthquake also exhibits super shear rupture behaviour, similar to the 2002 Mw 7.9 Denali earthquake in Alaska. However, the Mw 8.2 aftershock of this Sumatra earthquake shows much simpler bilateral rupture behaviour.

Reference

Yao, H., Shearer, P., Gerstoft, P., 2013. Compressive sensing of frequency-dependent seismic radiation from subduction zone megathrust ruptures. *Proceedings of National Academy of Sciences (PNAS),* 110(12), 4512-4517, doi: 10.1073/pnas.1212790110

Yao, H., Gerstoft, P., Shearer, P., Mecklenbrauker, C., 2011. Compressive sensing of the Tohoku-Oki Mw 9.0 Earthquake: Frequency-dependent rupture modes, *Geophys. Res. Lett.*, doi:10.1029/2011GL049223

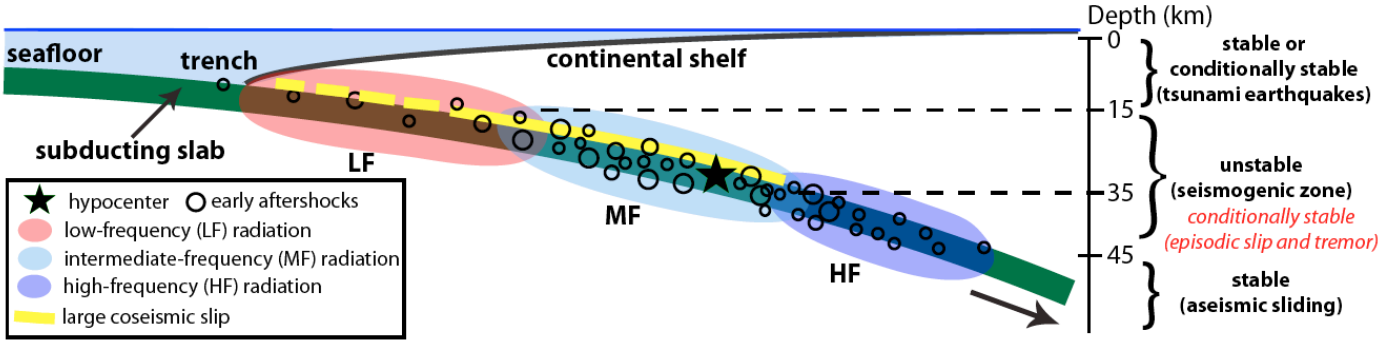

Figure 1. Seismic observations of subduction zone megathrust earthquakes and frictional stability regimes of the subducting plate interface. The yellow dashed line suggests possible large coseismic slip in the shallow portion of the slab interface in the case of tsunami earthquakes (Yao et al., 2013).

Rupture Processes and Seismic Radiation Characteristics for Large Earthquakes

Lingling Ye[a] and Thorne Lay

University of California Santa Cruz, Santa Cruz, California, 95064 USA. [a] lye2@ucsc.edu

Teleseismic and regional recordings from broadband and strong-motion sensors have been used to examine systematic variations due to source depth and location along the megathrust for regions that have very strong seismic coupling (Tohoku region of Japan megathrust), very weak seismic coupling (Sanriku low-seismicity region down-dip of the 1896 tsunami earthquake), and intermediate seismic coupling (Middle American subduction zone). Differences between interplate and intraplate faulting have been examined along with stress transfer and interactions between large megathrust and slab events, like August 31, 2012 Philippine outer-trench compressional earthquake (M_w 7.6), October 28, 2012 Haida Gwaii thrusting earthquake (M_w 7.8), December 7, 2012 Japan earthquake doublet (M_w 7.2, 7.1), and February 6, 2013 Santa Cruz Islands earthquake (M_w 8.0). The primary approaches that I have used include determination of the source spectra and radiated energy for large events, along with constraining overall rupture attributes using teleseismic finite-fault inversions and waveform analyses of aftershock sequences, accompanied by static stress change calculations.

Multiscale adjoint waveform-difference tomography using wavelets

Yanhua Yuan[1], Frederik J. Simons[2]

[1]Princeton University, Department of Geosciences, yanhuay@princeton.edu
[2]Princeton University, Department of Geosciences, fjsimons@princeton.edu

We present a wavelet-based multi-scale strategy in full waveform inversion. Thanks to the accuracy and flexibility of spectral element method, we are able to obtain full wave solutions for Earth-like complex models. The motivation of explaining all available seismic data to constrain wave-speed structures are challenged due to an increasing nonlinearity of full waveform inversion problems. Since wave-speed perturbations are more linearly dependent on misfits of long-wavelengths, we applied a multi-scale strategy in which coarse level seismograms are first used to constrain large structures, then step by step more oscillatory seismic arrivals are explained. Wavelet transform is taken advantage of in the multi-scale approach due to the freedom of choices of wavelets and non-overlapping features in scales. Optimal wavelet family is selected based on predicted and true seismograms under considerations, as well as computational costs in analysis and synthesis. Starting scale level is determined to guarantee an easy starting point based on the frequency contents involved in seismic data. We used a toy model and the Marmousi industry standard to test the robustness and efficiency of the proposed approach.

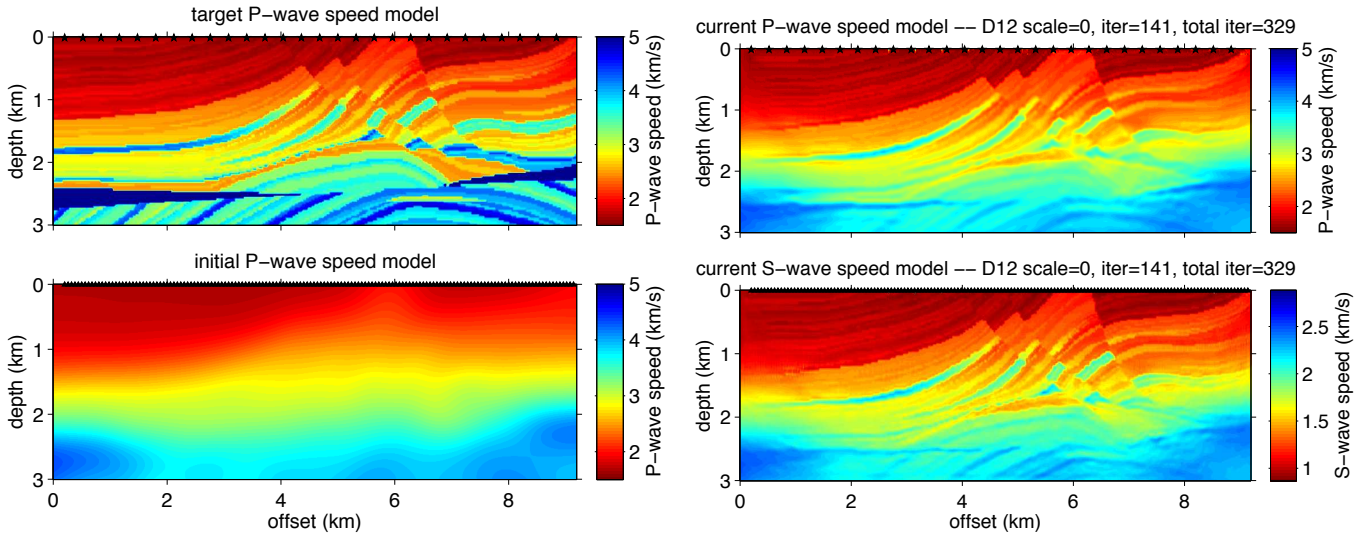

(a) (b)

(a) top: the Marmousi model with 112 shots (stars) and 300 receivers (triangles); bottom is smoothed version of the target model served as our starting model. The target and initial Marmousi models are modified to be elastic models in which shear wavespeed model is derived from the compressional model assuming the material to be Poisson solid. In this numerical setting, 112 shots at depth 10 m with 80 horizontal interval and 300 two-component receivers at depth 5m with 25 horizontal spacing are used to excite and record full elastic body wavefields. By taking advantage of coarse-to-fine wavelet-based multi-scale strategy together with spectral-element-method for elastic solutions as well as adjoint method for misfit gradients, we proceed from scale 9, up to 8, 7, 6, then to the full-resolution data space, and after 329 total iterations, current result in (b) captures both big and detailed structures shown in the target. The deep features near the bottom is not well resolved due to the sparse sampling of seismic rays.